INSTITUTO POTOSINO DE INVESTIGACIÓN CIENTÍFICA Y TECNOLÓGICA, A.C.

POSGRADO EN CIENCIAS EN BIOLOGIA MOLECULAR

Estrategias moleculares y de bioprocesos para la producción de hidrógeno, etanol y 2,3-butanodiol utilizando residuos agro-industriales como sustrato

Tesis que presenta

Cecilia Lizeth Alvarez Guzmán

Para obtener el grado de

Doctora en Ciencias en Biología Molecular

Director de la Tesis:

Dr. Antonio De León Rodríguez

San Luis Potosí, S.L.P., julio 2020

Constancia de aprobación de la tesis

La tesis "**Estrategias moleculares y de bioprocesos para la producción de hidrógeno, etanol y 2,3-butanodiol utilizando residuos agro-industriales como sustrato**" presentada para obtener el Grado de Doctora en Ciencias en Biología Molecular fue elaborada por **Cecilia Lizeth Alvarez Guzmán** y aprobada el **26 de junio de 2020** por los suscritos, designados por el Colegio de Profesores de la División de Biología Molecular del Instituto Potosino de Investigación Científica y Tecnológica, A.C.

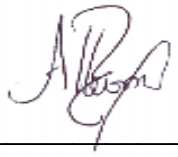

Dr. Antonio De León Rodríguez

Director de la tesis

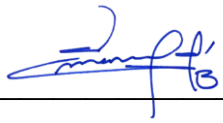

Dr. Victor Emmanuel Balderas Hernández

Miembro del Comité Tutoral

Dr. Luis Manuel Rosales Colunga

Miembro del Comité Tutoral

Dr. Raúl González García

Miembro del Comité Tutoral

Créditos Institucionales

Esta tesis fue elaborada en el Laboratorio de Bioingeniería y Biotecnología molecular de la División de Biología Molecular del Instituto Potosino de Investigación Científica y Tecnológica, A.C., bajo la dirección del Dr. Antonio De León Rodríguez.

Durante la realización del trabajo se contó con el apoyo del CONACyT a través de los proyectos CONACyT-Básicas 281700, CONACyT-Pro Nal 247498 y SENER CONACyT- 249564. La autora recibió una beca académica del Consejo Nacional de Ciencia y Tecnología 330870.

Instituto Potosino de Investigación Científica y Tecnológica, A.C.

Acta de Examen de Grado

El Secretario Académico del Instituto Potosino de Investigación Científica y Tecnológica, A.C., certifica que en el Acta 110 del Libro Segundo de Actas de Exámenes de Grado del Programa de Doctorado en Ciencias en Biología Molecular está asentado lo siguiente:

En la ciudad de San Luis Potosí a los 15 días del mes de julio del año 2020, se reunió a las 09:00 horas en las instalaciones del Instituto Potosino de Investigación Científica y Tecnológica, A.C., el Jurado integrado por:

Dr. Luis Manuel Rosales Colunga	**Presidente**	**UASLP**
Dr. Victor Emmanuel Balderas Hernández	**Secretario**	**IPICYT**
Dr. Antonio De León Rodríguez	**Sinodal**	**IPICYT**
Dr. Raúl González García	**Sinodal externo**	**UASLP**

a fin de efectuar el examen, que para obtener el Grado de:

DOCTORA EN CIENCIAS EN BIOLOGÍA MOLECULAR

sustentó la C.

Cecilia Lizeth Alvarez Guzmán

sobre la Tesis intitulada:

Molecular and bioprocess strategies for the production of hydrogen, ethanol and 2,3-butanediol using agro-industrial residues as substrate

que se desarrolló bajo la dirección de

Dr. Antonio De León Rodríguez

El Jurado, después de deliberar, determinó

APROBARLA

Dándose por terminado el acto a las 11:40 horas, procediendo a la firma del Acta los integrantes del Jurado. Dando fe el Secretario Académico del Instituto.

A petición de la interesada y para los fines que a la misma convengan, se extiende el presente documento en la ciudad de San Luis Potosí, S.L.P., México, a los 15 días del mes de julio de 2020.

Dr. Marcial Bonilla Marín
Secretario Académico

Mtra. Ivonne Lizette Cuevas Vélez
Jefa del Departamento del Posgrado

INSTITUTO POTOSINO DE INVESTIGACIÓN CIENTÍFICA Y TECNOLÓGICA, A.C.
IPICYT
SECRETARÍA ACADÉMICA

Dedicatorias

Este trabajo y todo lo que representa para mí, está dedicado enteramente a mi familia:

A mis padres Pedro Alvarez Gallegos y Patricia Guzmán Lerma.

A mi hermana Oralia Alvarez Guzmán.

A mi papá Martín Guzmán Lerma, a mi abuelita Bety Guzmán Lerma y a Cuquis Guzmán Lerma.

Gracias por ser mi inspiración, los amo con todo mi corazón.

Agradecimientos

Agradezco al Dr. Antonio De León Rodríguez por darme la oportunidad de realizar mi trabajo de doctorado en su laboratorio. Agradezco también la oportunidad y la confianza que me brindó desde la licenciatura, gracias porque el trabajar en su grupo de investigación me permitió crecer personal y académicamente y reafirmó mi interés por la investigación.

Agradezco al Dr. Victor E. Balderas Hernández por siempre brindarme su apoyo incondicional desde la maestría hasta el doctorado. Gracias Dr. por siempre tomarse el tiempo de asesorarme y por siempre motivarme a seguir adelante, gracias por confiar siempre en mí y recordarme que soy capaz de hacer lo que me proponga.

Al Dr. Luis Manuel Rosales Colunga por la asesoría, los valiosos comentarios y las recomendaciones que ayudaron a enriquecer este trabajo.

Al Dr. Raúl González García gracias por sus comentarios en cada seminario, por sus consejos y por asesorarme en los temas estadísticos.

Al Consejo Nacional de Ciencia y Tecnología (CONACyT) por el otorgamiento de la beca No. 330870 y a los proyectos CONACyT-Básicas 281700, CONACyT-Pro Nal 247498 y 247498 y SENER CONACyT- 249564, los cuales financiaron los trabajos presentados en esta tesis.

Agradezco a mis amigos del laboratorio de Biotecnología y bioingeniería molecular, a Karen, Marquito, Arlette, Mariana, Dani y Vic quienes además de ser mis amigos son mi segunda familia. Gracias por siempre apoyarme y escucharme en los momentos más difíciles, gracias por siempre hacerme sentir el laboratorio como mi segunda casa, ustedes saben lo mucho que significan para mí.

A Karen, por ser una gran amiga, gran roomie, gran compañera de lab, gracias por escucharme siempre, tenerme paciencia y nunca dejarme sola. Gracias por apoyarme incondicionalmente.

Finalmente, y de forma muy especial quiero agradecer a mis padres Patricia Guzmán Lerma y Pedro Alvarez Gallegos porque si llegue hasta aquí es gracias a todo su sacrificio, su amor y su apoyo incondicional, ustedes son y siempre serán mi más grande motivación y lo más grande en mi vida. Ojalá algún día pueda regresarles, aunque sea un poquito de lo mucho que ustedes me han dado. Gracias a mi hermana Oralia Alvarez Guzmán por siempre confiar en mí, apoyarme y motivarme a seguir adelante, te amo hermanita. También quiero agradecer a mi papá Martín Guzmán, soy muy afortunada al tenerlo, gracias por todo su amor y por siempre creer en mí y ayudarme a alcanzar mis sueños. Por último, gracias a mi abuelita Bety Guzmán y a Cuquis Guzmán que, aunque el día de hoy ya no estén físicamente conmigo, sé que siempre me acompañan a donde quiera que voy. Gracias por compartir mis sueños y por su amor incondicional.

Contenido

Lista de tablas

Lista de figuras

Resumen

“Estrategias moleculares y de bioprocesos para la producción de hidrógeno, etanol y 2,3-butanodiol usando residuos agro-industriales”

La generación de biocombustibles ofrece prometedoras ventajas sobre los combustibles fósiles, ya que estos son producidos bajo condiciones de presión y temperatura ambiente. De entre los procesos biológicos de producción de biocombustibles, la fermentación oscura presenta altas velocidades de producción, requiere de tecnologías sencillas y es posible utilizar una gran variedad de sustratos de bajo costo que no compiten con la alimentación humana. Además, es posible producir de forma simultánea diferentes biocombustibles gaseosos y líquidos con alto contenido energético, tales como el hidrógeno (122 kJ g^{-1}), etanol (29.01 kJ g^{-1}) y 2,3-butanodiol (27.2 kJ g^{-1}). Por lo tanto, en este trabajo se evaluaron diferentes estrategias para mejorar la producción de estos biocombustibles utilizando bacterias psicrófilas y mesófilas. En el primer capítulo se muestra la optimización de las condiciones operacionales y de la composición del medio de producción de hidrógeno por la bacteria antárctica N92, usando glucosa como sustrato. Los resultados mostraron que las condiciones óptimas para el máximo rendimiento de hidrógeno de 1.7 mol mol^{-1} glucosa fueron 29°C, pH inicial 6.86 y 28.4 g dm^{-3} glucosa, así como también una concentración inicial de $(NH_4)_2SO_4$, $FeSO_4$ y $NaHCO_3$ de 1.55, 0.53 y 1.64 g dm^{-3}, respectivamente. En el segundo capítulo se presenta la producción simultánea de hidrógeno, etanol y 2,3-butanodiol por la bacteria antárctica GA0F utilizando diferentes sustratos agroindustriales tales como el suero de leche en polvo (CWP), hidrolizado de paja de trigo (HWS) y melaza de caña de azúcar (SCM). De los sustratos evaluados se concluyó que el mayor rendimiento de hidrógeno (73.5 ± 10 cm^3 g^{-1}), etanol (0.24 ± 0.03 g g^{-1}) y 2,3-butanodiol (0.42 ± 0.04 g g^{-1}) se presentó utilizando CWP como fuente de carbono a 25°C seguido por el uso de SCM y WSH. Por otro lado, en el tercer capítulo presenta la expresión de una α-amilasa de *Bacillus megaterium* en la superficie celular de las cepas sobreproductoras de hidrógeno de *E. coli* utilizando el sistema de autotransporte AIDA para la conversión de almidón en hidrógeno, etanol y ácido succínico. Por último, en el cuarto capítulo se muestra la optimización de la producción de hidrógeno por *E. asburiae* utilizando CWP como sustrato, así como también un estudio quimiométrico de los metabolitos solubles producidos las condiciones experimentales. Las condiciones óptimas fueron 25.6°C, pH inicial 7.1 y 22.8 g dm^{-3} CWP para obtener un rendimiento y velocidad de producción de 1.2 mol mol^{-1} lactosa y 9.34 cm^3 dm^{-3} h^{-1}, respectivamente. El análisis quimiométrico permitió identificar que la producción de ácido acético, ácido fórmico y etanol fue estimulada principalmente a una baja temperatura de 15°C, mientras que la producción de ácido succínico, ácido láctico y 2,3-butanodiol fue favorecida por las condiciones de 30°C, pH inicial 6.8 y CWP ≥ 30 g dm^{-3}.

PALABRAS CLAVE: Fermentación oscura, Biocombustibles, Bacterias psicrófilas, Bacterias mesófilas.

Abstract

"Molecular and bioprocess strategies for the production of hydrogen, ethanol and 2,3-butanediol from agro-industrial residues as substrate"

Biofuel generation offers promising advantages over fossil fuels since these are produced under ambient pressure and temperature conditions. Among the different biological methods for the biofuel production, dark fermentation offers high production rates, requires simple technology and it is possible to use a wide variety of substrates which do not compete with human feed. Also, it is possible to produce simultaneously different gaseous and liquid biofuels with high heating value, such as hydrogen (122 kJ g^{-1}), ethanol (29.01 kJ g^{-1}) and 2,3-butanediol (27.2 kJ g^{-1}). Therefore, in this work, different strategies were evaluated to improve the production of these biofuels using psychrophilic and mesophilic bacteria. The first chapter shows the optimization of the operating conditions as well as the composition of the hydrogen production medium for the antarctic N92 bacterium using glucose as substrate. The results showed that optimum conditions for the maximum hydrogen yield of de 1.7 mol mol^{-1} glucose were 29°C, initial pH 6.86 and 28.4 g dm^{-3} glucose, along with an initial concentration of $(NH_4)_2SO_4$, $FeSO_4$ and $NaHCO_3$ of 1.55, 0.53 and 1.64 g dm^{-3} respectively. The second chapter shows the simultaneous production of hydrogen, ethanol and 2,3-butanediol by the antarctic GA0F bacterium using different agro-industrial residues such as cheese whey powder (CWP), wheat straw hydrolysate (WSH) and sugarcane molasses (SCM). From the evaluated substrates it was concluded that the highest hydrogen (73.5 ± 10 cm^3 g^{-1}), ethanol (0.24 ± 0.03 g g^{-1}) and 2,3-butanediol (0.42 ± 0.04 g g^{-1}) yield was achieved using CWP as carbon source at 25°C followed by the use of SCM and WSH. On the other hand, the third chapter shows the expression of an α-amylase from *Bacillus megaterium* on the cellular surface of *E. coli* by the autotransport system AIDA with the aim to achieve the starch conversion into hydrogen, ethanol and succinic acid. Finally, the fourth chapter shows the optimization of the operating conditions for hydrogen production by *Enterobacter asburiae* using CWP as substrate, as well as the chemometric study of the soluble metabolites produced in the different experimental conditions. The optimum conditions were 25.6°C, initial pH 7.2 and 23 g dm^{-3} CWP for the highest hydrogen yield and production rate of 1.2 mol mol^{-1} lactose and 9.34 cm^3 dm^{-3} h^{-1}, respectively. The chemometric analysis allowed to identify that the acetic acid, formic acid and ethanol production was stimulated by the low temperature of 15°C, while the synthesis of succinic acid, lactic acid and 2,3-butanediol was favored by the conditions of 30°C, initial pH 6.8 and CWP ≥ 30 g dm^{-3}.

KEYWORDS: Dark Fermentation, Biofuels, Psychrophilic bacteria, Mesophilic bacteria.

Chapter 1

Optimization of biohydrogen production by the novel psychrophilic strain N92 collected from the Antarctica

Abstract

In this study, the response surface methodology (RSM) with central composite design (CCD) was employed to improve the hydrogen production by the psychrophilic N92 strain (EU636058) isolated from Antarctica, which is closely related to *Pseudorhodobacter* sp. (KT163920). The influence of operational conditions such as temperature (4.7-55.2°C), initial pH (3.44-10.16), and initial glucose concentration (4.7-55.23 g dm^{-3}), as well as the initial concentrations of $(NH_4)_2SO_4$ (0.05-3.98 g dm^{-3}), $FeSO_4$ (0.02-1.33 g dm^{-3}) and $NaHCO_3$ (0.02-3.95 g dm^{-3}) was evaluated. The linear effect of glucose concentration, along with the quadratic effect of all the six factors were the most significant terms affecting the biohydrogen yield by N92 strain. The optimum conditions for the maximum hydrogen yield of 1.7 mol mol^{-1} glucose were initial pH of 6.86, glucose concentration of 28.4 g dm^{-3}, temperature 29°C and initial concentration of $(NH_4)_2SO_4$, $FeSO_4$ and $NaHCO_3$ of 0.53, 1.55 and 1.64 g dm^{-3} respectively. Analysis of the metabolites produced under the optimum conditions showed that the most abundant were acetic acid (0.8 g dm^{-3}), butyric acid (0.7 g dm^{-3}) and ethanol (2.1 g dm^{-3}). We suggest that the bioprocess established in this study using the strain N92 could be an alternative for hydrogen production with the advantages of constituting low energy costs in fermentation.

Keywords: Biohydrogen; Central composite design; Dark fermentation; Psychrophilic bacteria; Response Surface Methodology.

Cisneros de la Cueva S, Alvarez Guzmán CL, Balderas Hernández VE, De León Rodríguez A. Optimization of biohydrogen production by the novel psychrophilic strain N92 collected from the Antarctica. Int J Hydrogen Energy 2018;43:13798–809. https://doi.org/10.1016/j.ijhydene.2017.11.164.

1. Introduction

Hydrogen is considered as an attractive future energy carrier and it is preferred over biogas or methane because hydrogen is not chemically bound to carbon, and therefore, its burning does not contribute to greenhouse gases or acid rain [1]. There are several approaches to produce hydrogen such as steam reforming of natural gas, coal gasification and water electrolysis, as well as novel chemical processes like the hydrolysis of hydrides with steam, which combines both hydrogen production and storage in one step [2-9]. On the other hand, there are the biological methods which mostly operate at ambient temperatures and pressures [8, 10]. These approaches mainly include photosynthetic and dark fermentative hydrogen production. However, dark fermentation has advantages over other processes because of its ability to continuously produce hydrogen from a number of renewable feedstocks [11]. During the dark fermentative process, when glucose is used as model substrate under anoxic conditions, bacteria convert glucose to pyruvate through glycolytic pathways producing adenosine triphosphate (ATP) from adenosine diphosphate (ADP) and the reduced form of nicotinamide adenine dinucleotide (NADH). Pyruvate is further oxidized to acetyl coenzyme A (acetyl-CoA), carbon dioxide (CO_2) and H_2 by pyruvate ferredoxin oxidoreductase and hydrogenase. Depending on the type of microorganism and environmental conditions, pyruvate may also be converted to acetyl-CoA and formate, which may be further converted into H_2 and CO_2. Also, acetyl-CoA might be converted to acetate and ethanol [12]. This process is complex and influenced by many factors such as inoculum, substrate, nitrogen, phosphate, metal ion, temperature and pH [13]. The effect of these factors has been widely studied, however, most of the fermentative hydrogen production processes are focused on the use of mesophilic and thermophilic microorganisms and there are few reports available addressing psychrophilic bacteria [14-16]. The use of psychrophilic hydrogen producing microorganisms could be an economical advantage due to its operation temperatures. These microorganisms have high enzymatic activities and catalytic efficiencies in the 0-20°C temperature range in which homologous mesophilic enzymes are less active, and allow to renounce on expensive heating/cooling

systems, thus constituting a considerable progress towards the saving of energy [17]. Therefore, the aim of this experimental work was the production of hydrogen using a newly psychrophilic N92 strain isolated from Antarctica [18]. Since there is insufficient information about the operational conditions for psychrophilic hydrogen production, we have applied the response surface methodology to set the optimum operation conditions and media composition to reach the maximum hydrogen production. In this context, temperature, pH and substrate concentration are important factors influencing the activity of bacteria towards hydrogen production. Moreover, temperature is a key factor since it might alter process efficiency, hydrogen production activity, and liquid product distribution by influencing the bacterial enzymatic activity. Kumari and Das [19] reported that an initial pH in an inadequate range affects the activity of the hydrogenase enzymes as well as an inadequate initial substrate concentration affects metabolic pathways decreasing the production of biohydrogen. On the other hand, at the cellular level, some elements have certain effects on the activity of hydrogen-producing bacteria, particularly the concentrations of nitrogen and iron, essential nutrients for hydrogen production, as well as buffer supplementation [13]. Iron is an essential component of ferredoxin and hydrogenase that catalyzes the reduction of H^+ to H_2. The Fe-S bindings are responsible for the transport of electrons in specific proteins that participate on the pyruvate oxidation to acetyl-CoA, CO_2 and H_2. It has been reported that the *in vivo* activity of the hydrogenase decreases with iron depletion, suggesting that the presence of iron in the fermentation medium is required to preserve the bacteria and prevent the loss of its characteristics. Moreover, nitrogen is one of the essential nutrients needed for the growth of hydrogen-producing bacteria. A source of nitrogen is demanded for the syntheses of proteins, nucleic acids, and enzymes. Among the sources of nitrogen, ammonia has been applied in hydrogen production by dark fermentation, it is a cheap inorganic nitrogen source compared to other organic nitrogen sources and it has been shown that in an appropriate concentration range, ammonia nitrogen is beneficial to fermentative hydrogen production, while at a much higher concentration could have an inhibitory effect for it may change the intracellular pH of hydrogen-producing bacteria,

increase the maintenance energy requirement or inhibit specific enzymes related to fermentative hydrogen production [20]. Low or high concentration of these nutrients may cause low hydrogen yields. Therefore, in this work the effects of these operational factors (temperature, pH and substrate concentration) and mineral nutrient concentration (ammonia, carbonate and ferrous ion) on hydrogen production were studied using two central composite designs to obtain optimum hydrogen production conditions by the psychrophilic N92 strain.

2. Materials and methods

2.1. Microorganism and growth media

In this work, the strain N92 (EU636058) highly related to *Pseudorhodobacter* sp. (KT163920) according to NCBI blast was used. It was isolated from samples of glacier sediment from Antarctica [18]. The strain was grown in YPG agar plates in g dm^{-3} (2.75 of Bacto-tryptone, 0.25 of yeast extract, 25 of glucose and 15 of Bacto-agar) and maintained at 4°C [15].

2.2. Experiment designs

The first central composite design with two center points was implemented to optimize the temperature, initial pH and initial glucose concentration to maximize biohydrogen yield by batch cultures fermentations of N92 strain (Table 1) [21].

Table 1. Independent variables and levels used in the experimental design to optimize the operational factors.

Independent variables	**Levels**		
	-1	**0**	**1**
***X_1*-Temperature (°C)**	15	30	45
***X_2*-pH**	4.8	6.8	8.8
***X_3*-Glucose concentration (g dm^{-3})**	15	30	45

A second order polynomial mathematical model (Equation 1) was proposed to describe the effects of several factors on the response based on experimental results.

$$Y_i = \beta_0 + \sum_i^{\beta} x_i + \sum_{ii}^{\beta} x_i^2 + \sum_{ij}^{\beta} x_i x_j \quad \text{Eq. 1}$$

Where Y_i is the corresponding response, x_i and x_j are the independent variables, β_0 is the model intercept, β_i are the linear coefficients, β_{ii} are the squared coefficients and β_{ij} are the interaction coefficients [13]. In addition, the analysis of variance (ANOVA) was used to obtain the relationship between independent variables and the response, as well as to describe the effects of several factors on the response based on the experimental results by using a second order polynomial model. The statistical software, Design-Expert 7.0.0 version (Stat-Ease, Inc., Minneapolis, MN, USA) was used to performance the regression analysis and the response surface analysis [22].

Furthermore, a second central composite design with two center points was used to optimize the culture medium with the objective of increasing the biohydrogen production by dark fermentation using N92 strain (Table 2). ANOVA was used to obtain the relationship between independent variables and to describe the effects of various factors on the response based on experimental results of a second order polynomial model (Eq. 1) [23-25].

Table 2. Independent variables and levels used in the experimental design to optimize the medium composition.

Independent variables	Levels		
	-1	**0**	**1**
X_4-$FeSO_4$ (g dm^{-3})	0.02	0.51	1
X_5-$(NH_4)_2SO_4$ (g dm^{-3})	0.05	1.515	2.98
X_6-$NaHCO_3$ (g dm^{-3})	0.02	1.485	2.95

2.3. Batch Fermentations Experiments

The batch fermentations were carried out in 0.120 dm^{-3} serum bottles. Silicone rubber stoppers were used to avoid gas leakage from the bottles [14]. The mineral medium used in the first experimental design to evaluate the influence of initial pH, temperature and initial glucose concentration consisted of the following composition in g dm^{-3}: 3 of KH_2PO_4, 7 of K_2HPO_4, 1 of $MgSO_4$, 0.39 of $FeSO_4$ $7H_2O$, 3 of yeast extract and 0.5 of Bacto-tryptone [25].

In the second experimental stage, in order to evaluate the effect of the concentration of $FeSO_4 \cdot 7H_2O$, $(NH_4)_2SO_4$ and $NaHCO_3$, the medium used for hydrogen production experiments was the same as the one used in the first experimental design without the addition of $FeSO_4 \cdot 7H_2O$, since this was tested in the experimental design. All bottles in both experimental designs were inoculated with 0.5 OD_{600nm} of N92 strain [23, 26].

2.4. Analytical methods

The biogas produced was determined at room temperature (25°C) by displacement of acid water (pH < 2) [27]. The percentage of hydrogen in the biogas accumulated in the headspace of serum bottles was measured by Gas Chromatography as described elsewhere [27]. The pH value was obtained by Thermo Orion 8103BN, Waltham, MA. Remaining glucose and fermentation end products (succinic acid, lactic acid and acetic acid) were analyzed by High Performance Liquid Chromatography (HPLC, Infinity LC 1220 Agilent Technologies, Santa Clara, CA, USA) using a column Phenomenex Rezex ROA (Phenomenex, Torrance, CA, USA) at 60°C and using 0.0025 M H_2SO_4 as mobile phase at 0.55 cm^3 min^{-1}. ethanol, acetoin, propionic acid and butyric acid were analyzed in a Gas Chromatograph 6890N (Agilent Technologies, Wilmington, DE, USA) using a capillary column HP-Innowax with the following dimensions (30 m X 0.25 mm i.d. X 0.25 m film thickness; Agilent Technologies, Wilmington, DE, USA). Temperatures of the injector and flame ionization detector (FID) were 220 and 250°C respectively. Helium was used as carrier gas at a flow rate of 25 cm^3 min^{-1}. The analyses were performed with a split ratio of 5:1 and a temperature program of

25°C for 10 min to 280°C, and was maintained at this temperature for a final time of 10 min [14].

3. Results and discussion

3.1. Optimization of operational conditions

Response surface methodology was adopted to investigate and optimize the effect of process variables on biohydrogen production yield. Applying multiple regression analysis to the experimental data, the following mathematical second order model was established to explain the biohydrogen yield as a function of the independent variables within the region under investigation, expressed by the equation 2.

$$Y = 0.66 - 0.020X_1 + 8.515e^{-3}X_2 - 0.049X_3 - 0.011X_1X_2 + 0.017X_1X_3 - 4.374e^{-3}X_2X_3 - 0.23X_1^2 - 0.23X_2^2 - 0.17X_3^2 \quad \text{Eq. 2}$$

The code of the variables of model equation corresponds to temperature (X_1), initial pH (X_2), and initial glucose concentration (X_3) along with the experimental values of the biohydrogen yield. In Table 3 is shown the ANOVA conducted to test the significance of the fitting model along with the linear, quadratic, and interactive effects of the variables.

Table 3. ANOVA of the fitting model of the experimental response at various levels of temperature, pH and glucose concentration.

Source	Sum of squares	df	Mean Square	*F* value	*p*-value
Model	0.75	9	0.083	18.1	0.0011
X_1-Temperature	5.25E-03	1	5.25E-03	1.14	0.3263
X_2-pH	9.90E-04	1	9.90E-04	0.22	0.6589
X_3-Glucose concentration	0.033	1	0.033	7.15	0.0368
X_1X_2	1.05E-03	1	1.05E-03	0.23	0.6495
X_1X_3	2.20E-03	1	2.20E-03	0.48	0.5152
X_2X_3	1.53E-04	1	1.53E-04	0.033	0.8612
X_1^2	0.49	1	0.49	106.62	< 0.0001

X_2^2	0.49	1	0.49	106.62	< 0.0001
X_3^2	0.28	1	0.28	60.05	0.0002
Residual	0.028	6	4.60E-03		
Lack of Fit	0.028	5	5.51E-03	634.15	0.0301
Pure Error	8.69E-06	1	8.69E-06		
Total	0.78	15			

The *p*-values were used to check the significance of each variable, also to indicate the strength of the interaction between each independent variable. The *p* values (probability > F) lower than 0.05 indicate that model terms are significant, while *p* values greater than 0.05 indicate that the model terms are insignificant. The model *p* value of 0.0011 implies that the model was significant. Table 3 shows the model F value of 18.1, which indicates an adequate description of the variation about its mean. The coefficient of determination R^2 was 0.9645, indicating that the model could explain 96.45% variability of the response variable and that the mathematical model is reliable to estimate the predicted values.

Figure 1 shows 3D response surface plots and 2D contour plots depicting the interactions between pairs of variables keeping the third variable at its optimum level for biohydrogen yield. The shape of the contour plot explicitly demonstrates the mutual or combined effect of the independent variables on the response. A clear peak point can be found in each response surface plot, which indicates that the maximum biohydrogen yield could be achieved inside the design boundary of all three variables.

The effect of temperature in dark fermentation on the production of biohydrogen was analyzed according to the ANOVA, showing that only in the quadratic terms of the polynomial mathematical model showed significant effect with a lower *p* value of 0.05 (Table 3). In the figures 1b and 1d the contour plots of temperature with respect to the initial pH and initial glucose concentration showed that the temperature in both variables has an interactive effect on the biohydrogen yield due to the circular shape that is shown in the plots. The response surface plots of the figures 1a and 1c show that at low temperatures of 15°C both variables have a negative effect on the anaerobic fermentation using the strain N92, showing the lowest yield of biohydrogen.

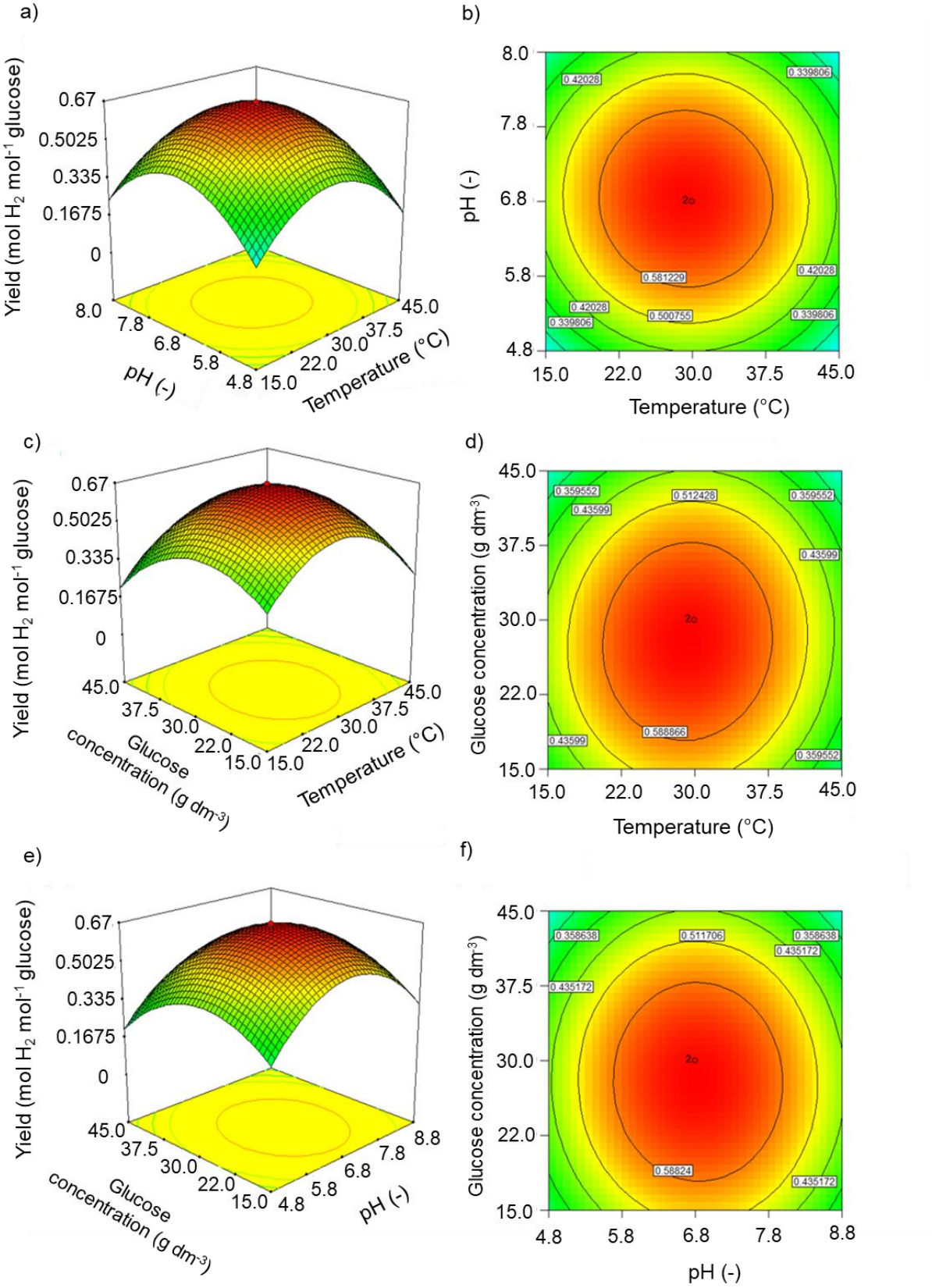

Figure 1. Response surface plots and contour plots showing the interactive effect of operational conditions on biohydrogen yield.

The gradual increase of the temperature in a range from 15 to 30°C resulted with gradual increase in the production of biohydrogen reaching the maximum production of biohydrogen at a temperature of 29.3°C, from this value the gradual increase in temperature caused a gradual decrease in the biohydrogen yield having the lowest of value at 45°C. This behavior exhibited by the N92 strain can be attributed to psychrophilic nature of bacteria which has the ability to ferment sugars at low temperatures and produce biohydrogen, however the biohydrogen production is low, this is due to the fact that it has been shown that incubation temperature dramatically affects the growth rate of bacteria, since it affects the rates of all cellular reactions, the metabolic patterns, the nutritional requirements and the composition of bacterial cells [28]. The increase in biohydrogen yield corresponds to the increase in temperature, which can be explained as a positive effect on the hydrolysis of the complex particles. It has also been demonstrated that an increase in temperature produces an increase in the hydrogen production because the increment of temperature doubles the enzymatic activity every 10°C until reaching the optimum temperature [28]. Above this value the enzymatic activity decreases rapidly. Other studies performed by Niu et al. [29] concluded that higher temperature, such as 37°C, could inhibit the expression of the uptake hydrogenase, as well as stimulate the expression of H_2 evolving hydrogenase.

The pH is often one of the most important factors influencing the performance of the fermentation process for the biohydrogen production. In this study regarding to the mathematical model, the linear effect and the interaction between the variables of temperature and initial concentration of glucose according to the ANOVA showed no significant effect since values of p are greater than 0.05. In terms of the quadratic model, this variable showed a significant effect according to the ANOVA (Table 3).

The response surface plots (figures 1a and 1e) show that the biohydrogen yield increases with the increment of initial pH from 4.8 to 6 in both variables. Reaching the highest increase in biohydrogen yield at a value of pH of 6.8, the decrease in biohydrogen yield is shown from higher values of pH. Changes in external pH

values also affect several physiological parameters in cells such as the proton motive force and membrane potential [30]. In this study at pH values below 4.8 the lack of hydrogen production may be due to the extremely acidic microenvironment pH < 4.5 was detrimental to the ability of the bacteria to produce biohydrogen as reported in other studies [31].

While at a value of pH 8.8 alkaline microenvironment is presented and fermentative pathways are prone to solventogenesis [32]. Other studies mention that hydrogenase enzyme activity gets inhibited by maintaining low or high pH beyond the optimum range [33]. The optimum pH value of 6.8 obtained in this study is in the optimum range for other biohydrogen producing bacteria that is between 6.0-6.8. In this pH range it has been reported that it might be beneficial due to the prevention of solventogenesis [34, 35].

The initial glucose concentration was evaluated by the ANOVA showing that linear and quadratic effects were significant, since values of p <0.05 were obtained (Table 3). In figures 1c and 1e the response surface plots show that at low glucose concentrations of 15 g/dm3, temperature of 15°C and initial pH of 4.8 the yield of biohydrogen had the lowest level. As the glucose concentration increased, the biohydrogen yield increased reaching its maximum value at an initial glucose concentration of 28.4 g dm^{-3}. The increase in biohydrogen yield with the increase in initial glucose concentration may be due to the fact that it has been reported by Wu and Lin [36], that in an appropriate range, increasing of substrate concentration could increase the ability of bacteria to produce biohydrogen. In our study, it is shown that from the optimum concentration of 28.4 g dm^{-3}, the increase in the glucose concentration caused a decrease in the yield of biohydrogen. Furthermore, studies show that high substrate concentrations become inhibitory to the microorganisms as a result of a pH drop and hydrogen pressure increase [37, 38]. Prakasham et al. [39], also reported that higher concentrations of glucose can also negatively impact on biohydrogen production.

3.2. Optimization of nutrient formulation for biohydrogen production by strain N92

The effect of the nutrient concentration levels added to the formulation was evaluated using a central composite design with two center points. From regression analysis of the experimental results, a second order polynomial model for biohydrogen yield Equation 3 was obtained.

$$Y = 1.51 + 0.092X_4 + 0.075X_5 + 0.13X_6 + 0.050X_4X_5 + 5.732e^{-3}X_4X_6 + 0.057X_5X_6 - 0.39X_4^2 - 0.47X_5^2 - 0.36X_6^2 \quad \text{Eq. 3}$$

Where *Y* is the biohydrogen yield, X_4 is the initial $FeSO_4$ concentration, X_5 is the initial $(NH_4)_2SO_4$ concentration and X_6 is the initial $NaHCO_3$ concentration.

In Table 4 the ANOVA demonstrates that the second order model for biohydrogen yield is highly significant as evident from the calculated F value of 7.05 and a very low probability value p model < *F* 0.05.

Table 4. ANOVA of the fitting model of the experimental response at various levels of $FeSO_4$, $(NH_4)_2SO_4$ and $NaHCO_3$ concentrations.

Source	Sum of Squares	df	Mean Square	*F* value	*p*-value
Model	3.12	9	0.35	7.05	0.0137
X_4-$FeSO_4$	0.11	1	0.11	2.33	0.1778
X_5-$(NH_4)_2SO_4$	0.077	1	0.077	1.57	0.2567
X_6-$NaHCO_3$	0.25	1	0.25	5.01	0.0664
X_4X_5	0.02	1	0.02	0.41	0.5436
X_4X_6	2.63E-04	1	2.63E-04	5.35E-03	0.9441
X_5X_6	0.026	1	0.026	0.53	0.4959
X_4^2	1.42	1	1.42	28.81	0.0017
X_5^2	2.09	1	2.09	42.48	0.0006
X_6^2	1.21	1	1.21	24.67	0.0025
Residual	0.3	6	0.049		
Lack of Fit	0.29	5	0.059	215.33	0.0517
Pure Error	2.74E-04	1	2.74E-04		
Total	3.42	15			

In Table 4 the *p* values for each factor $(NH_4)_2SO_4$ and $FeSO_4$ concentration and their corresponding interaction were greater than 0.05 indicating that these factors have no significant effect on biohydrogen yield. However, in the quadratic terms of the model, both factors showed that $p < 0.05$ have a significant effect on the biohydrogen yield.

In figures 2b, 2d and 2f the contour plots of both factors show elliptical shapes indicating the mutual interactions between $NaHCO_3$ and $FeSO_4$.

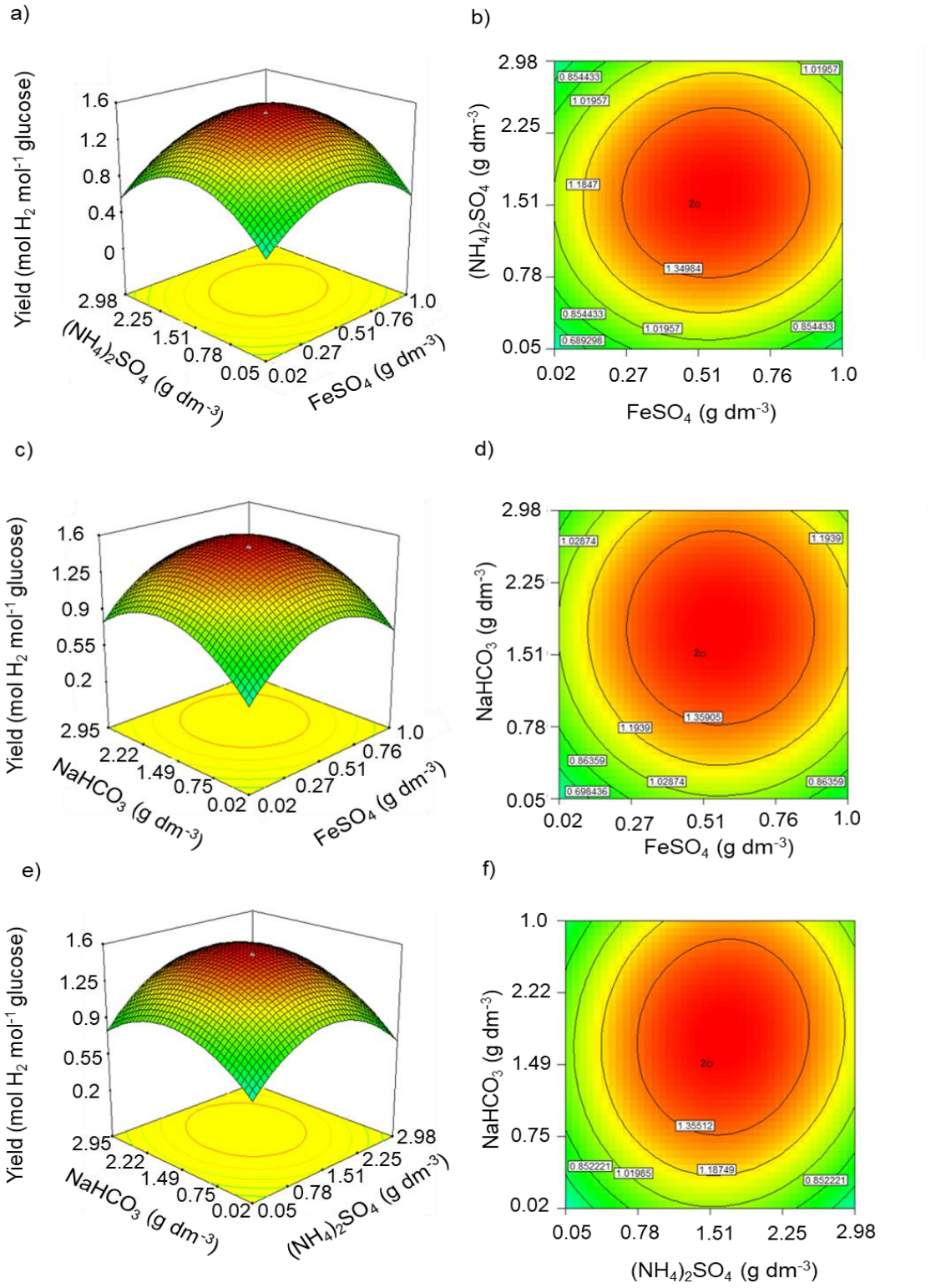

Figure 2. Response surface plots and contour plots showing the interactive effect of different concentrations of $(NH_4)_2SO_4$, $NaHCO_3$ and $FeSO_4$ on biohydrogen yield.

In figure 2a, response surface plot shows that the biohydrogen yield decreases when the $(NH_4)_2SO_4$ and $FeSO_4$ concentrations are presented in the lowest level being these 0.05 g dm^{-3} and 0.02 g dm^{-3} respectively.

The hydrogen yield increased as the $(NH_4)_2SO_4$ and $FeSO_4$ concentration increased, reaching their maximum yield at a concentration of 1.57 and 0.56 g dm^{-3} respectively. From this concentration, the increase in concentration caused a significant decrease in biohydrogen yield.

According to the results obtained at the concentration of $FeSO_4$ 0.02 g dm^{-3}, this condition did not favor the dark fermentation by strain N92 for biohydrogen production, since the yield showed the lowest value. However, the gradual augmentation of $FeSO_4$ favored the fermentation as the biohydrogen yield increased until reaching the maximum.

The increase in biohydrogen production may be attributed to the fact that Fe^{2+} increases the activity of hydrogenases, since Fe^{2+} is the metal in the catalytic center of hydrogenases which are responsible to catalyze the oxidation of hydrogen or the reduction of proton [40].

Others studies carried out by Wang et al. [41] showed that the cumulative hydrogen quantity in batch tests increased with increasing Fe^{2+} concentrations from 0 to 300 mg dm^{-3}, however, when the Fe2+ concentrations were higher than 300 mg dm^{-3}, the cumulative hydrogen quantity tended to decrease with increasing Fe^{2+} concentrations. Several studies have shown that suitable concentration of Fe^{2+} ranges were able to enhance the biohydrogen yield by the mixed cultures, while much lower or much higher Fe^{2+} concentrations than the suitable one are not favorable to raise the biohydrogen yield [41].

From the optimum Fe^{2+} concentration, the increase in concentration caused an inhibition during dark fermentation since the biohydrogen yield decreased significantly, it has been reported that in an excess concentration of ferrous iron exerts a slight inhibitive influence on hydrogen production.

Related reports carried out by Ding et al. [42] studied the effect of the Fe^{2+} concentrations ranging from 0 to 1473.7 mg dm^{-3} on the fermentative hydrogen

production from glucose by mixed cultures, obtaining the maximum hydrogen yield at the Fe^{2+} concentration of 200 mg dm^{-3}.

The results obtained in this study show that the addition of the lower concentration levels of $(NH_4)_2SO_4$ does not increase the biohydrogen yield. However, the increase in $(NH_4)_2SO_4$ concentration showed a positive effect on the fermentation by strain N92, as the biohydrogen yield increased to reach the maximum. But from this ammonium concentration, the increase caused a gradual decrease of the yield until reaching the lowest levels of biohydrogen production.

This behavior is similar to that described by several studies, demonstrating that in an appropriate concentration range, ammonia nitrogen is beneficial to fermentative biohydrogen production, while at a much higher concentration, ammonia nitrogen could inhibit fermentative hydrogen production, for it may change the intracellular pH of hydrogen producing bacteria, increase the maintenance energy requirement for hydrogen producing bacteria or inhibit specific enzymes related to fermentative biohydrogen production [43].

Table 4 shows p values for the carbonate and ferrous iron and their interaction, only the linear and quadratic terms of the model for the $NaHCO_3$ concentration had a significant effect since the values of $p > 0.05$ for the linear interaction between the two factors has no significant effect ($p > 0.05$) on the biohydrogen yield. The response surface plot in figure 2c shows the interactive effect of these two factors on biohydrogen yield.

With the $FeSO_4$ and $NaHCO_3$ concentration at levels -1 (0.02 g dm^{-3} and 0.02 g dm^{-3}, respectively), the biohydrogen yield decreased below 0.52 mol mol^{-1} glucose .The maximum biohydrogen yield obtained in the optimum condition was 1.52 mol mol^{-1} glucose in $NaHCO_3$ and $FeSO_4$ concentrations of 1.65 g dm^{-3} and 0.5 g dm^{-3} respectively, from this concentration the increase in ferrous iron and carbonate concentration did not favor the fermentation by N92 to increase the biohydrogen yield, conversely caused the biohydrogen yield gradually decreased reaching the minimum at concentrations obtained in the level -1.

Regarding the results obtained, the carbonate in suitable concentrations has a significant effect on biohydrogen production since it has been shown in several

studies that the addition of carbonate is used to maintain the pH of 6.8, by neutralizing organic acids formed during fermentation and maintaining the necessary pH conditions in microorganisms environment, and increasing the biohydrogen production [44]. Other studies mention that the addition of carbonates restored the growth of the bacteria [45].

The increase in carbonate concentration, followed by the optimum concentration showed a decrease of biohydrogen since it has been mentioned that an increase in carbonate concentration in the feed increases the carbon dioxide concentration because of carbonate dissolution and therefore decreased the hydrogen content in the gas phase [23].

The interaction between carbonate and ammonium on biohydrogen production is shown in the table 4. The *p* value on interaction of both factors was greater than 0.05 indicating that both factors had no significant effect on biohydrogen yield. The effect of both factors is shown in figure 2e, showing that at the extreme levels -1 and +1 (Table 2) the biohydrogen yield decreased below 0.62, while at level 0 this increased to reach the maximum biohydrogen yield using $NaHCO_3$ and $FeSO_4$ 1.73 g dm^{-3} and 1.43 g dm^{-3} respectively.

3.3. Metabolites produced during dark fermentation by strain N92

Biohydrogen production is accompanied by the production of metabolites such as volatile fatty acids (VFAs) and solvents during anaerobic digestion. The analysis of the metabolic products of the second experimental design of optimization is shown in figures 3 and 4. The values average concentration in (g dm^{-3}) of VFAs and solvents of different experimental treatment were: 1.19 acetic acid, 1.06 butyric acid, 0.27 succinic acid, 0.27 propionic acid, 1.57 ethanol and 0.43 acetoin (see Fig. 5 and 6).

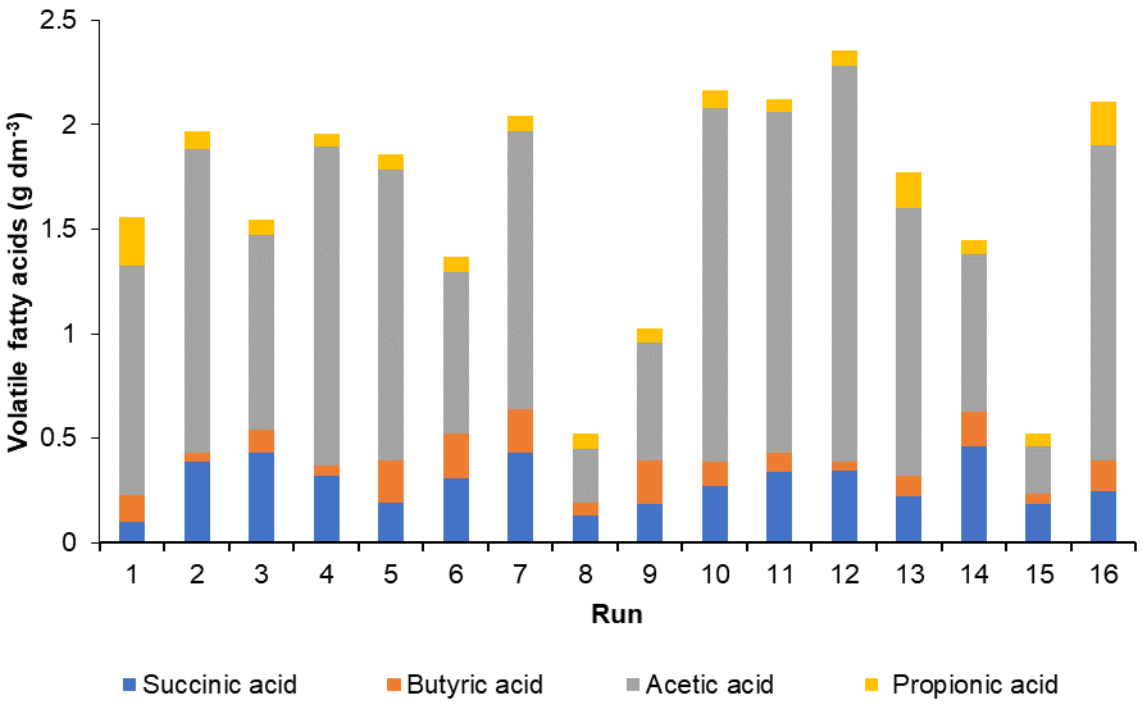

Figure 3. Distribution of final VFAs produced in different treatments.

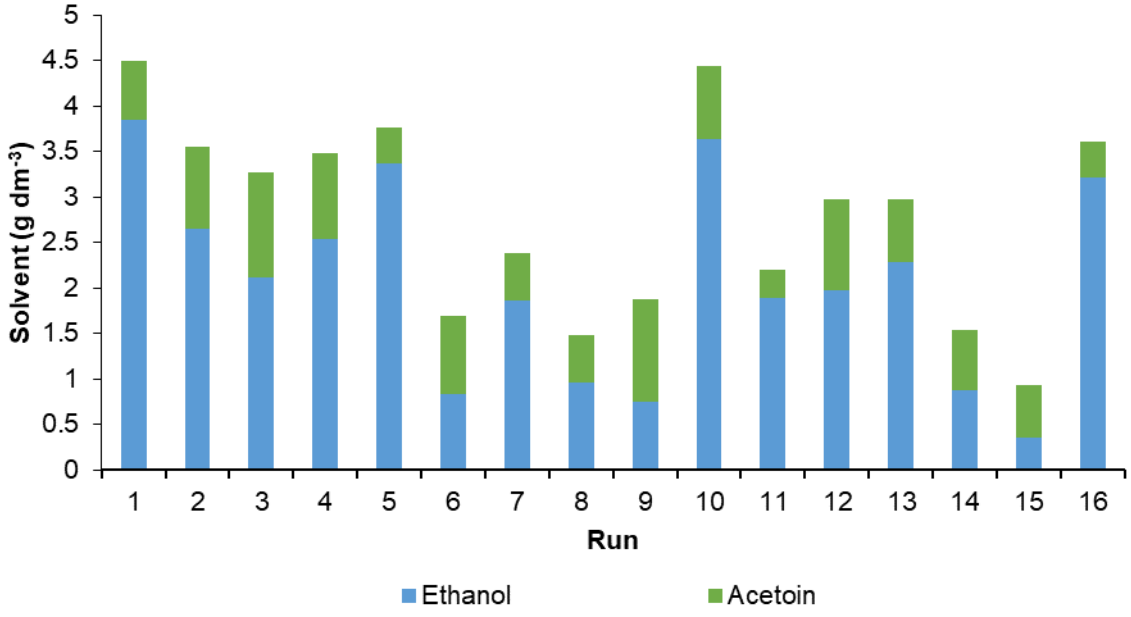

Figure 4. Solvents released from anaerobic fermentation by N92 strain at different treatments.

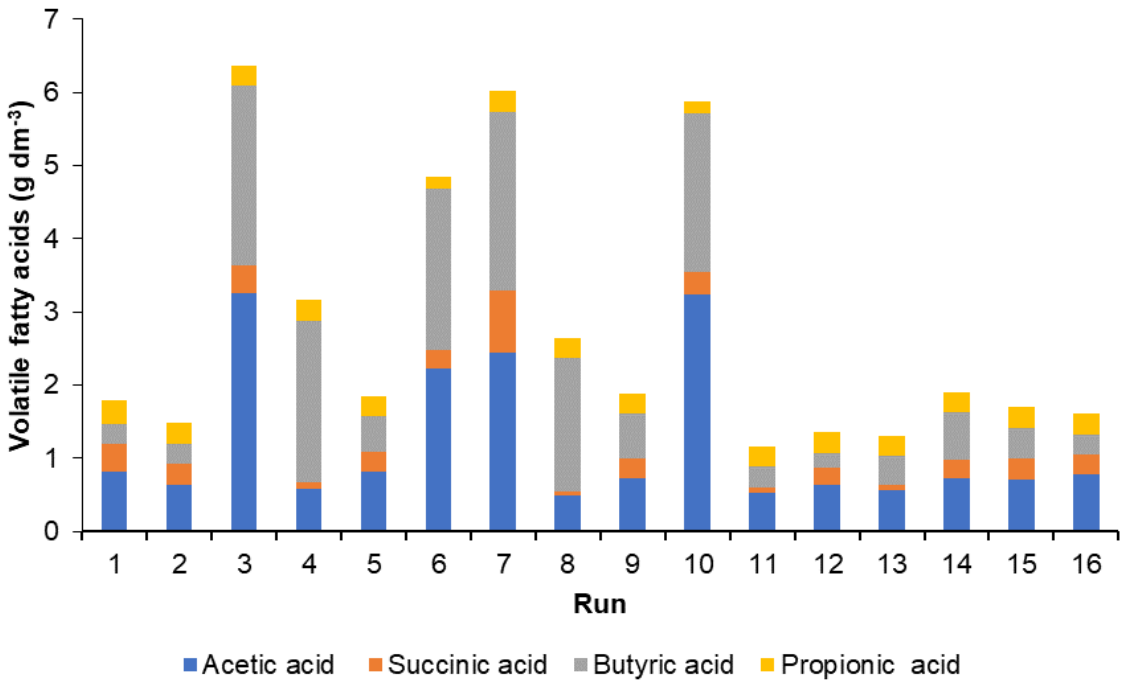

Figure 5. Organic acid produced in the dark fermentation by N92 strain by effect of the different concentrations of $(NH_4)_2SO_4$, $NaHCO_3$ and $FeSO_4$.

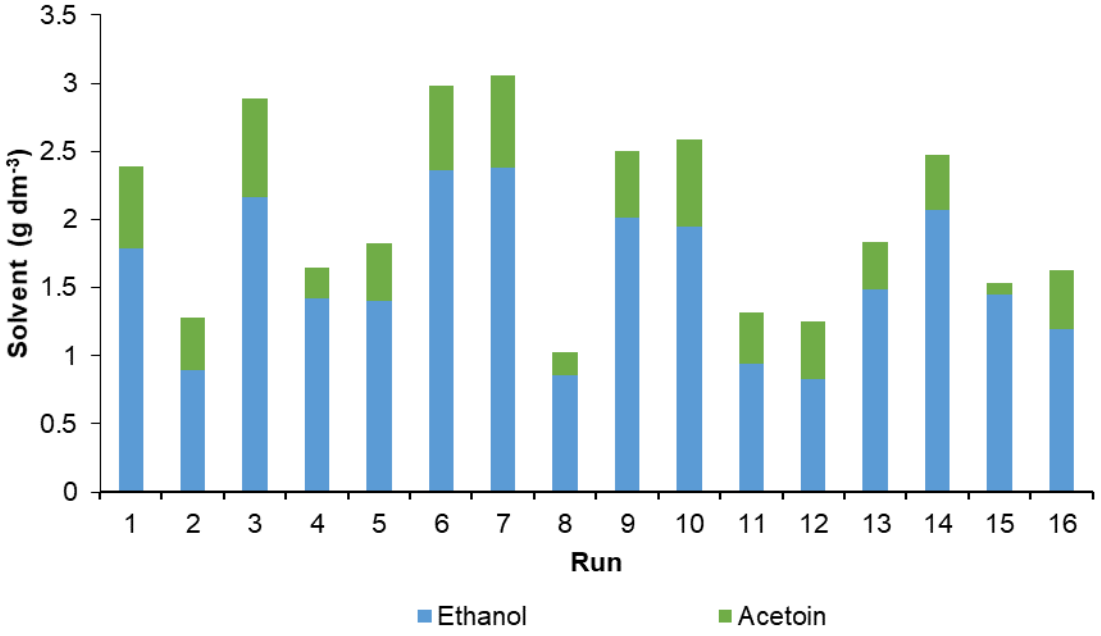

Figure 6. Ethanol and acetoin produced in the dark fermentation by N92 strain by effect of the different concentrations of $(NH_4)_2SO_4$, $NaHCO_3$ and $FeSO_4$.

The formation of VFAs obtained from the acidogenic pathway of pyruvate showed that the metabolic activity presented by the N92 bacterium is oriented to two metabolic reactions for biohydrogen production, which are that of acetic acid and butyric acid.

$C_6H_{12}O_6 + 2H_2O \rightarrow 2CH_3COOH + 2CO_2 + 4H_2$ Acetic acid pathway

$C_6H_{12}O_6 \rightarrow CH_3CH_2CH_2COOH + 2CO_2 + 2H_2$ Butyric acid pathway

Studies report that the accumulation of both acetic and butyric acid caused the greatest decrease in biohydrogen yield [46]. Hüsemann et al. [47] found that the undissociated acetic acid concentration did not correlate with the initiation of solventogenesis but undissociated butyric acid did. However, there is no general agreement on why butyric acid is more toxic than acetic acid, but likely it is a consequence of NAD^+ regeneration [46].

Studies show that accumulation of VFAs such as succinic acid and propionic acid beyond a certain level inhibits cell growth, since it has been shown that the presence of these acids are able to cross the cell membrane at a low pH and then dissociate in the cell at the higher cytoplasm pH releasing a proton inside the cell [48, 49]. The uptake of protons in this way uncouples the proton motive force, which causes an increase in maintenance of energy requirements to maintain the intracellular pH near to neutrality. The uptake of acid also causes a decrease in the available coenzyme A and phosphate pools which decreases the flux of glucose through glycolysis [50].

The accumulation of ethanol and acetoin produced by N92 strain in our study can affect the production of biohydrogen since studies have reported that the appearance of these solvents produced during the dark fermentation can cause the inhibition of the enzyme hydrogenase by carbon monoxide diverting reducing equivalents from H_2 a major electron sink to solvent production [51, 52]. Other studies have reported that the presence of alcohols on bacteria causes chaotropic effects on the membrane structure due to perturbation of the orderly array of the

fatty acid side chains of the phospholipids, that affect the ability of the cells to retain and exclude electrolytes and nonelectrolytes [53].

3.4. Experimental validation

An experimental validation was conducted to check the effectiveness of optimum conditions of pH, temperature, concentration of glucose and compound formulation obtained. The experiments were performed in duplicate (CE-1 and CE-2) showing the results in Table 5. The results showed that the maximum biohydrogen yield of 1.7 mol mol^{-1} glucose was obtained under optimization conditions.

Table 5. Estimated hydrogen yield coefficients and metabolic products of the fermentation at the optimum conditions.

				Volatile fatty acids (g dm^{-3})				Solvent (g dm^{-3})	
Run	**H_2 yield (mol mol^{-1} glucose)**	**H_2 production rate ($cm^3/dm^3/h$)**	**Energy efficiency %**	**Acetic acid**	**Propionic acid**	**Butyric acid**	**Succinic acid**	**Ethanol**	**Acetoin**
CE-1	1.66	12.28	0.76	0.856	0.31	0.715	0.297	2.121	0.497
CE-2	1.67	12.44	0.78	0.832	0.302	0.691	0.289	2.252	0.51

To ensure the reproducibility of the data from the optimization models, the chow test was carried out covering the different periods of biohydrogen production, resulting that the F-value in both models turned out to be less than 4.0 indicating the stability of the parameters.

Table 5 also shows the energy conversion efficiencies of these confirmation experiments showing that the efficiency obtained by the psychrophilic N92 strain in the optimum conditions is 0.77% which is a low value considering that the theoretical conversion efficiency into hydrogen production by dark fermentation is 33.5%. This is the heat value ratio of 4 mol H_2 product to 1 mol glucose feedstock [54]. On the other hand, this low efficiency could be greatly improved by a sequential process of photo-fermentation, in which photosynthetic bacteria reutilize the volatile fatty acids produced during dark fermentation to produce more hydrogen in the presence of light, as reported by several authors [54-56].

Nonetheless, comparing the hydrogen production yields obtained in this study with respect to those reported, the yield obtained from our study is in a mean value of the reported range. The Table 6 shows hydrogen yields from others fermentation processes using cultures of mesophilic and thermophilic microorganisms in a range between 0.85 and 4.0 mol mol^{-1} hexose [57-63].

Table 6. Comparison of biohydrogen production in batch mode with respect to other mesophilic and thermophilic fermentative anaerobic processes using glucose as substrate.

Microorganism	T (°C)	Maximum Biohydrogen yield (mol mol^{-1} glucose)	Reference
Thermotoga maritima	80	4	(Schröder et al., 1994)
Thermotoga elfii	65	3.3	(Van Niel et al., 2002)
Escherichia coli MC13-14	37	1.2	(Ishikawa et al., 2006)
Sewage sludge	40	1.75	(Wu et al., 2005)
Soybean meal	35	0.85	(Mizuno et al., 2000)
Clostridium tyrobutyricum	35	1.47	(Lin et al., 2007)
Klelsiella oxytocin	35	1	(Minnan et al., 2005)
N92	29	1.7	This study

However, these studies were performed at temperatures above the optimum of our fermentation process constituting for our process an energetic advantage since the reactor can be operable at room temperature reducing the operational costs of biohydrogen production process, and making up an alternative process for those cold countries. To date, most of the hydrogen production methods are energy-intensive and expensive. Nevertheless, the hydrogen generation via hydrolysis of metal hydrides such as $NaBH_4$, H-$CaMg_2$, Mg-oxide composites, Mg-La, Mg_3-RE,

MgH_2-NH_4Cl, H-Mg_3La have been recognized as potential chemical methods for generation of hydrogen due to their high hydrolysis yields [3-9]. Chemical hydrides can react with water and release high purity hydrogen at room temperature and atmospheric pressure, conversely to other chemical methods. For example, Ma et al. [5] reported that the hydrolysis of H-$CaMg_{1.9}Ni_{0.1}$ presented a hydrogen conversion and hydrolysis rate of 94.6% and 356 cm^3 g^{-1} min^{-1}, respectively. Huang et al. [3] reported a similar value of hydrogen conversion of 95.2% during the hydrolysis of Mg-MoO_3, with a higher hydrolysis rate of 857 cm^3 g^{-1} min^{-1}, while Zhong et al. [8] reported a single step process of hydrogen production and storage with an 89% hydrogen conversion in 10 min. There are other studies with exceptional hydrolysis rates. Such as Ouyang et al. [2] reported that the hydrolysis of Mg_3Mm (where Mm refers to a La and Ce-rich misch metal) produced 828 cm^3 g^{-1} in 15 min, while Huang et al. [4] achieved 1660 cm^3 g^{-1} in 30 min using a MgH_2-4.5 wt% NH_4Cl system. The hydrogen production rates achieved by these methods are higher than those attained by dark fermentative processes and particularly to the hydrogen production rate of 12.36 cm^3 dm^{-3} h^{-1} by N92 strain under the optimum conditions (Table 5). These are efficient and low-cost hydrogen production processes, but, hydrogen production by dark fermentation has several other advantages such as the ability to produce hydrogen from organic waste and therefore control and stabilize biological waste, which has a potential of contamination [64]. Besides hydrogen production by dark fermentation allows to obtain high-value chemicals such as alcohols. Current studies addressing the use of organic waste in dark fermentation are performed above 37°C [13]. Meanwhile, psychrophilic bacteria can metabolize the agroindustrial waste as substrate at low temperatures. Alvarez-Guzmán et al. [15] reported that the psychrophilic G088 strain isolated from Antarctica has the ability to ferment several monosaccharides and disaccharides which are abundant in agroindustrial waste and to produce simultaneously hydrogen, ethanol and 2,3-butanediol from glucose [65]. Other studies by Debowsky et al. [16] and Zielinski et al. [66] have shown the ability of psychrophilic bacteria to produce hydrogen from cheese whey as substrate. In this study, it has been demonstrated that the psychrophilic N92 strain is a natural

hydrogen-producing bacterium and additional investigations are necessary to the application of this psychrophilic strain in processes involving the use of organic wastes.

4. Conclusions

In this study, operational conditions initial pH, glucose concentration levels, temperature and initial nutrients in growth medium for enriching biohydrogen produced by N92 strain were optimized using a central composite design with two center points. Optimum conditions for biohydrogen production were estimated to be a temperature of 29.0°C, initial pH of 6.86 and glucose concentration of 28.4 g dm^{-3}. The optimum fermentation medium of nutrients was 1.64 4 g dm^{-3} $(NH_4)_2SO_4$, 0.53 g dm^{-3} $FeSO_4$ and 1.55 g dm^{-3} of $NaHCO_3$. The maximum biohydrogen yield obtained under these optimum conditions was 1.7 mol mol^{-1} glucose comparable to those reported for mesophilic and thermophilic microorganisms. Therefore, the results of our research indicate that this dark fermentation process with N92 strain has the potential to be used with agroindustrial residues as carbon source for biohydrogen production, with the advantage that it can be carried out at room temperature constituting a greater energy efficiency of the process.

5. Acknowledgments

Partial financial support from CONACyT Básicas Grant 281700. Postdoctoral fellowship by the CONACyT No. 229147. We also thank Lucia Aldana Navarro for the revision of the English manuscript.

6. References

[1] Ferchichi M, Crabbe E, Gil G-H, Hintz W, Almadidy A. Influence of initial pH on hydrogen production from cheese whey. Journal of biotechnology. 2005;120:402-9.

[2] Huang J, Ouyang L, Wen Y, Wang H, Liu J, Chen Z, et al. Improved hydrolysis properties of Mg 3 RE hydrides alloyed with Ni. international journal of hydrogen energy. 2014;39:6813-8.

[3] Huang M, Ouyang L, Chen Z, Peng C, Zhu X, Zhu M. Hydrogen production via hydrolysis of Mg-oxide composites. International Journal of Hydrogen Energy. 2017.
[4] Huang M, Ouyang L, Wang H, Liu J, Zhu M. Hydrogen generation by hydrolysis of MgH 2 and enhanced kinetics performance of ammonium chloride introducing. international journal of hydrogen energy. 2015;40:6145-50.
[5] Ma M, Duan R, Ouyang L, Zhu X, Peng C, Zhu M. Hydrogen generation via hydrolysis of H-CaMg 2 and H-CaMg 1.9 Ni 0.1. International Journal of Hydrogen Energy. 2017.
[6] Ouyang L, Huang J, Wang H, Wen Y, Zhang Q, Sun D, et al. Excellent hydrolysis performances of Mg 3 RE hydrides. international journal of hydrogen energy. 2013;38:2973-8.
[7] Ouyang L, Xu Y, Dong H, Sun L, Zhu M. Production of hydrogen via hydrolysis of hydrides in Mg–La system. international journal of hydrogen energy. 2009;34:9671-6.
[8] Zhong H, Ouyang LZ, Ye JS, Liu JW, Wang H, Yao XD, et al. An one-step approach towards hydrogen production and storage through regeneration of NaBH 4. Energy Storage Materials. 2017;7:222-8.
[9] Zhong H, Wang H, Liu J, Sun D, Fang F, Zhang Q, et al. Enhanced hydrolysis properties and energy efficiency of MgH 2-base hydrides. Journal of Alloys and Compounds. 2016;680:419-26.
[10] Manish S, Banerjee R. Comparison of biohydrogen production processes. International Journal of Hydrogen Energy. 2008;33:279-86.
[11] Cuetos M, Gomez X, Escapa A, Moran A. Evaluation and simultaneous optimization of biohydrogen production using 32 factorial design and the desirability function. Journal of power sources. 2007;169:131-9.
[12] Ghimire A, Frunzo L, Pirozzi F, Trably E, Escudie R, Lens PN, et al. A review on dark fermentative biohydrogen production from organic biomass: process parameters and use of by-products. Applied Energy. 2015;144:73-95.
[13] Wang J, Wan W. Factors influencing fermentative hydrogen production: a review. International journal of hydrogen energy. 2009;34:799-811.

[14] Alvarado-Cuevas ZD, López-Hidalgo AM, Ordoñez LG, Oceguera-Contreras E, Ornelas-Salas JT, De León-Rodríguez A. Biohydrogen production using psychrophilic bacteria isolated from Antarctica. International Journal of Hydrogen Energy. 2015;40:7586-92.

[15] Alvarez-Guzmán CL, Oceguera-Contreras E, Ornelas-Salas JT, Balderas-Hernández VE, De León-Rodríguez A. Biohydrogen production by the psychrophilic G088 strain using single carbohydrates as substrate. International Journal of Hydrogen Energy. 2016;41:8092-100.

[16] Dębowski M, Korzeniewska E, Filipkowska Z, Zieliński M, Kwiatkowski R. Possibility of hydrogen production during cheese whey fermentation process by different strains of psychrophilic bacteria. International journal of hydrogen energy. 2014;39:1972-8.

[17] Margesin R, Schinner F. Properties of cold-adapted microorganisms and their potential role in biotechnology. Journal of Biotechnology. 1994;33:1-14.

[18] García-Echauri S, Gidekel M, Gutiérrez-Moraga A, Santos L, De León-Rodríguez A. Isolation and phylogenetic classification of culturable psychrophilic prokaryotes from the Collins glacier in the Antarctica. Folia microbiologica. 2011;56:209-14.

[19] Kumari S, Das D. Improvement of biohydrogen production using acidogenic culture. International Journal of Hydrogen Energy. 2016;42:4083-94.

[20] Wang B, Wan W, Wang J. Effect of ammonia concentration on fermentative hydrogen production by mixed cultures. Bioresource technology. 2009;100:1211-3.

[21] Hay JXW, Wu TY, Teh CY, Jahim JM. Optimized growth of Rhodobacter sphaeroides OU 001 using response surface methodology (RSM). Journal of scientific & industrial research. 2012;71:149-54.

[22] Assawamongkholsiri T, Reungsang A. Photo-fermentational hydrogen production of Rhodobacter sp. KKU-PS1 isolated from an UASB reactor. Electronic Journal of Biotechnology. 2015;18:221-30.

[23] Lin C-Y, Lay C. Effects of carbonate and phosphate concentrations on hydrogen production using anaerobic sewage sludge microflora. International Journal of Hydrogen Energy. 2004;29:275-81.

[24] Oztekin R, Kapdan IK, Kargi F, Argun H. Optimization of media composition for hydrogen gas production from hydrolyzed wheat starch by dark fermentation. International Journal of Hydrogen Energy. 2008;33:4083-90.
[25] Romão B, Batista F, Ferreira J, Costa H, Resende M, Cardoso V. Biohydrogen production through dark fermentation by a microbial consortium using whey permeate as substrate. Applied biochemistry and biotechnology. 2014;172:3670-85.
[26] Chong M-L, Yee PL, Aziz SA, Rahim RA, Shirai Y, Hassan MA. Effects of pH, glucose and iron sulfate concentration on the yield of biohydrogen by Clostridium butyricum EB6. International journal of hydrogen energy. 2009;34:8859-65.
[27] Rosales-Colunga LM, Razo-Flores E, Ordoñez LG, Alatriste-Mondragón F, De León-Rodríguez A. Hydrogen production by Escherichia coli ΔhycA ΔlacI using cheese whey as substrate. International Journal of Hydrogen Energy. 2010;35:491-9.
[28] Das D, Khanna N, Dasgupta CN. Biohydrogen production: fundamentals and technology advances. London: CRC Press; 2014.
[29] Niu K, Zhang X, Tan W-S, Zhu M-L. Effect of culture conditions on producing and uptake hydrogen flux of biohydrogen fermentation by metabolic flux analysis method. Bioresource technology. 2011;102:7294-300.
[30] Fan Y, Li C, Lay J-J, Hou H, Zhang G. Optimization of initial substrate and pH levels for germination of sporing hydrogen-producing anaerobes in cow dung compost. Bioresource Technology. 2004;91:189-93.
[31] Chandrasekhar K, Lee Y-J, Lee D-W. Biohydrogen production: strategies to improve process efficiency through microbial routes. International Journal of Molecular Sciences. 2015;16:8266-93.
[32] Mohan SV, Chandrasekhar K, Chiranjeevi P, Babu PS. Biohydrogen. In: Pandey A, editor. Biohydrogen. First ed. San Diego, CA, USA: Elsevier Inc.; 2013. p. 223-46.
[33] Fan Y-T, Zhang Y-H, Zhang S-F, Hou H-W, Ren B-Z. Efficient conversion of wheat straw wastes into biohydrogen gas by cow dung compost. Bioresource Technology. 2006;97:500-5.

[34] Mohan SV, Bhaskar YV, Krishna PM, Rao NC, Babu VL, Sarma P. Biohydrogen production from chemical wastewater as substrate by selectively enriched anaerobic mixed consortia: influence of fermentation pH and substrate composition. International Journal of Hydrogen Energy. 2007;32:2286-95.
[35] Mohan SV, Srikanth S, Babu ML, Sarma P. Insight into the dehydrogenase catalyzed redox reactions and electron discharge pattern during fermentative hydrogen production. Bioresource technology. 2010;101:1826-33.
[36] Wu J-H, Lin C-Y. Biohydrogen production by mesophilic fermentation of food wastewater. Water Science and Technology. 2004;49:223-8.
[37] Ginkel SV, Sung S, Lay J-J. Biohydrogen production as a function of pH and substrate concentration. Environmental science & technology. 2001;35:4726-30.
[38] Lo Y-C, Chen W-M, Hung C-H, Chen S-D, Chang J-S. Dark H2 fermentation from sucrose and xylose using H2 producing indigenous bacteria: feasibility and kinetic studies. Water research. 2008;42:827-42.
[39] Prakasham R, Brahmaiah P, Sathish T, Rao KS. Fermentative biohydrogen production by mixed anaerobic consortia: impact of glucose to xylose ratio. International Journal of Hydrogen Energy. 2009;34:9354-61.
[40] Frey M. Hydrogenases: hydrogen-activating enzymes. ChemBioChem. 2002;3:153-60.
[41] Wang J, Wan W. Effect of Fe2+ concentration on fermentative hydrogen production by mixed cultures. International Journal of Hydrogen Energy. 2008;33:1215-20.
[42] Ding J, Ren N, Liu M, Ding L. Effect of Fe and Fe2+ on hydrogen production capacity with mixed culture. Environmental Science. 2004;25:48-53.
[43] Wang J, Wan W. Experimental design methods for fermentative hydrogen production: a review. International Journal of Hydrogen Energy. 2009;34:235-44.
[44] Richmond C, Han B, Ezeji T. Stimulatory effects of calcium carbonate on butanol production by solventogenic Clostridium species. Continental Journal of Microbiology. 2011;5:18-28.

[45] Maruyama K, Kitamura H. Mechanisms of growth inhibition by propionate and restoration of the growth by sodium bicarbonate or acetate in Rhodopseudomonas sphaeroides S. The Journal of Biochemistry. 1985;98:819-24.
[46] Van Ginkel S, Logan BE. Inhibition of biohydrogen production by undissociated acetic and butyric acids. Environmental science & technology. 2005;39:9351-6.
[47] Hüsemann MH, Papoutsakis ET. Solventogenesis in Clostridium acetobutylicum fermentations related to carboxylic acid and proton concentrations. Biotechnology and Bioengineering. 1988;32:843-52.
[48] Jones DT, Woods DR. Acetone-butanol fermentation revisited. Microbial and Molecular Biology Reviews. 1986;50:484-524.
[49] Oh Y-K, Raj SM, Jung GY, Park S. Metabolic Engineering of Microorganisms for Biohydrogen Production. In: Pandey A, editor. Biohydrogen. First ed. San Diego,CA,USA: Elsevier 2013. p. 45-60.
[50] Gottwald M, Gottschalk G. The internal pH of Clostridium acetobutylicum and its effect on the shift from acid to solvent formation. Archives of microbiology. 1985;143:42-6.
[51] Datta R, Zeikus J. Modulation of acetone-butanol-ethanol fermentation by carbon monoxide and organic acids. Applied and Environmental Microbiology. 1985;49:522-9.
[52] Meyer C, McLaughlin J, Papoutsakis E. The effect of CO on growth and product formation in batch cultures of Clostridium acetobutylicum. Biotechnology letters. 1985;7:37-42.
[53] Terracciano JS, Kashket ER. Intracellular conditions required for initiation of solvent production by Clostridium acetobutylicum. Applied and Environmental Microbiology. 1986;52:86-91.
[54] Su H, Cheng J, Zhou J, Song W, Cen K. Combination of dark-and photo-fermentation to enhance hydrogen production and energy conversion efficiency. International Journal of Hydrogen Energy. 2009;34:8846-53.

[55] Zong W, Yu R, Zhang P, Fan M, Zhou Z. Efficient hydrogen gas production from cassava and food waste by a two-step process of dark fermentation and photo-fermentation. Biomass and bioenergy. 2009;33:1458-63.
[56] Tao Y, Chen Y, Wu Y, He Y, Zhou Z. High hydrogen yield from a two-step process of dark-and photo-fermentation of sucrose. International Journal of Hydrogen Energy. 2007;32:200-6.
[57] Ishikawa M, Yamamura S, Takamura Y, Sode K, Tamiya E, Tomiyama M. Development of a compact high-density microbial hydrogen reactor for portable bio-fuel cell system. International Journal of Hydrogen Energy. 2006;31:1484-9.
[58] Lin P-Y, Whang L-M, Wu Y-R, Ren W-J, Hsiao C-J, Li S-L, et al. Biological hydrogen production of the genus Clostridium: metabolic study and mathematical model simulation. International Journal of Hydrogen Energy. 2007;32:1728-35.
[59] Minnan L, Jinli H, Xiaobin W, Huijuan X, Jinzao C, Chuannan L, et al. Isolation and characterization of a high H2-producing strain Klebsiella oxytoca HP1 from a hot spring. Research in microbiology. 2005;156:76-81.
[60] Mizuno O, Dinsdale R, Hawkes FR, Hawkes DL, Noike T. Enhancement of hydrogen production from glucose by nitrogen gas sparging. Bioresource Technology. 2000;73:59-65.
[61] Schröder C, Selig M, Schönheit P. Glucose fermentation to acetate, CO2 and H2 in the anaerobic hyperthermophilic eubacterium Thermotoga maritima: involvement of the Embden-Meyerhof pathway. Archives of Microbiology. 1994;161:460-70.
[62] Van Niel E, Budde M, De Haas G, Van der Wal F, Claassen P, Stams A. Distinctive properties of high hydrogen producing extreme thermophiles, Caldicellulosiruptor saccharolyticus and Thermotoga elfii. International Journal of Hydrogen Energy. 2002;27:1391-8.
[63] Wu SY, Hung CH, Lin CN, Chen HW, Lee AS, Chang JS. Fermentative hydrogen production and bacterial community structure in high-rate anaerobic bioreactors containing silicone-immobilized and self-flocculated sludge. Biotechnology and bioengineering. 2006;93:934-46.

[64] Dincer I, Acar C. Review and evaluation of hydrogen production methods for better sustainability. International journal of hydrogen energy. 2015;40:11094-111.
[65] Alvarez-Guzmán CL, Balderas-Hernández VE, González-García R, Ornelas-Salas JT, Vidal-Limón AM, Cisneros-de la Cueva S, et al. Optimization of hydrogen production by the psychrophilic strain G088. International Journal of Hydrogen Energy. 2017;42:3630-40.
[66] Marcin Z, Ewa K, Zofia F, Marcin D, Monika H, Rafał K. Biohydrogen production at low load of organic matterby psychrophilic bacteria. Energy. 2017.

Chapter 2

Coproduction of hydrogen, ethanol and 2,3-butanediol from agroindustrial residues by the Antarctic psychrophilic GA0F bacterium

Abstract

In this study, the simultaneous production of hydrogen, ethanol, and 2,3-butanediol was assessed using three agro-industrial residues: cheese whey powder (CWP), wheat straw hydrolysate (WSH) and sugarcane molasses (SCM), by the Antarctic psychrophilic GA0F bacterium [EU636050], which is closely related to *Pseudomonas antarctica* [KX186936.1]. The main soluble metabolites produced in all the fermentations were ethanol and 2,3-butanediol. CWP demonstrated to be the most effective carbon source, since fermentation of this substrate resulted in the highest yields of H_2 (73.5 ± 10 cm^3 g^{-1}), ethanol (0.24 ± 0.03 g g^{-1}) and 2,3-butanediol (0.42 ± 0.04 g g^{-1}), followed by the use of SCM, whereas WSH showed to have an inhibitory effect during the fermentation process, showing the lowest production values. Our results demonstrated the ability of the Antarctic psychrophilic GA0F bacterium to produce valuable products using low-cost substrates at room temperature conditions.

Keywords: Biofuels; Dark fermentation; Hydrogen; Ethanol; 2,3-butanediol.

Alvarez-Guzmán CL, Balderas-Hernández VE, De Leon-Rodriguez A. Coproduction of hydrogen, ethanol and 2,3-butanediol from agro-industrial residues by the Antarctic psychrophilic GA0F bacterium. Int J Hydrogen Energy 2020. https://doi.org/10.1016/j.ijhydene.2020.02.105.

1. Introduction

Biofuels have been considered as an option to replace fossil fuels. However, they must be derived from feed-stocks produced with much lower life-cycle and green-house emissions than traditional fossil fuels and with little or no competition with food production [1]. In this regard, renewable biomass is the most versatile non-petroleum-based resource that is generated from various industries as waste materials [2]. Lignocellulosic materials such as cereal straw, maize cob residues, food and starch-based materials, as well as organic industry wastewater, represent a vast source of raw materials that can be easily converted into sustainable energy carriers [3]. Among many alternatives, hydrogen and ethanol could emerge as important sustainable fuel sources in the foreseeable future. Biohydrogen can be used directly in combustion engines for transportation or in fuel cells for electricity generation, its high energy density (122 kJ g^{-1}), and the fact that water is the only by-product generated, makes hydrogen an ideal alternative to fossil fuels [4]. Furthermore, ethanol is the most employed liquid biofuel either as a fuel or as a gasoline enhancer; it has a high oxygen content that allows better oxidation of the gasoline hydrocarbons with the consequent reduction in the emission of CO2 to the atmosphere [5]. 2,3-Butanediol is a high-value chemical with high heating value (27.20 kJ g^{-1}) which compares favorably with other liquid fuels (methanol 22.08 kJ/g, ethanol 29.06 kJ g^{-1}) [6]. Likewise, 2,3-butanediol is used as a precursor in the manufacture of a range of chemical products (i.e., perfumes, fumigants, moistening foods, antifreeze, and pharmaceuticals) [7, 8]. The production of hydrogen, ethanol, and 2,3-butanediol can be carried out throughout fermentative processes such as dark fermentation. This method is environmentally friendly and more cost-effective compared to its chemical and thermochemical counterparts [9]. Different substrates such as corncob molasses, cheese whey and pre-treated lignocellulosic biomass have been used to produce H_2, ethanol and 2,3-butanediol [10-12]. Although the development of fermentation processes using economical carbon sources is an important issue for the production of these bio-commodities on a commercial scale, it is also desirable to find microorganisms with the ability to improve the production of these value-added compounds with the concomitant

reduction in energy consumption. From this perspective, the study of Antarctic ecosystems and their microorganisms have received greater attention to produce hydrogen at temperatures close to room temperature [13, 14]. These microorganisms, which have the ability to grow at low temperatures (0-25°C) [15], are characterized by their high catalytic efficiencies, that make them attractive for different biotechnological areas [16]. These studies were carried out using pure simple carbon sources, while to our knowledge, there are no reports regarding biofuel production by Antarctic psychrophilic bacteria using complex substrates such as agro-industrial residues. Therefore, the aim of this study was to evaluate the dark fermentation of different complex substrates such as cheese whey powder (CWP), wheat straw hydrolysate (WSH) and sugarcane molasses (SCM) by the Antarctic psychrophilic GA0F bacterium.

2. Materials and methods

2.1. Bacterium and substrates

Psychrophilic GA0F bacterium [EU636050] was used as fermentative organism. GA0F bacterium was previously isolated from glacier sediments from Antarctica [17] and it is closely related to *Pseudomonas antarctica* [KX186936.1] (according to NCBI). GA0F bacterium was routinely grown in solid YPG medium [13]. The agro-industrial residues CWP, SCM, and WSH were evaluated as potential carbon sources for GA0F bacterium for dark fermentation cultivations. CWP was purchased from Land O'Lakes Inc. (Arden Hills, Minnesota), and SCM was obtained from a local industry in San Luis Potosí, Mex, while WSH was obtained from CUCBA (University of Guadalajara, Jalisco, Mex). Fermentations using CWP 20 g dm^{-3} contained 13.5 g dm^{-3} of total sugars. SCM were diluted from a stock solution (380 g dm-3 total sugars) to a final total sugar concentration of 21 g dm^{-3}. For fermentations using WSH, the concentrated liquid fraction obtained from evaporation (at 70°C) of the slurred wheat straw that was pre-treated at 121°C for 1 h in a steam sterilizer in dilute H_2SO_4 (0.75% v v^{-1}) at 4% (w v^{-1}) was used. The WSH concentrated liquid fraction contained 20.4 g dm^{-3} of total sugars (composed

of glucose 3.2 g dm^{-3}, xylose 14.2 g dm^{-3}, and arabinose 3.0 g dm^{-3}), organic acids such as formic acid 1.0 g dm^{-3}, and acetic acid 2.2 g dm^{-3}, and furfural 0.6 g dm^{-3}.

2.2. Batch dark fermentation experiments

For dark fermentation experiments, preinocula of GA0F bacterium were grown in liquid YPG medium and incubated at 25°C and 120 rpm. After overnight growth cells were harvested by centrifugation, washed and then inoculated into 120 cm^3 anaerobic serological bottles (Prisma, DF, Mex) containing 110 cm3 of production medium containing 0.25 g dm^{-3} yeast extract and 2.75 g dm^{-3} Bacto-tryptone supplemented with each of the agro-industrial substrates (CWP, WSH or SCM). Serological bottles were rubber stopper capped with an aluminum crimp cap to avoid gas leakage. The production medium was supplemented with 1 cm^3 dm^{-3} trace elements solution [13]. The cultures were started at an optical density at 600 nm wavelength (OD_{600nm}) of 0.1. Initial pH was adjusted at 7, and incubated at 25°C and 180 rpm as suggested by Wu et al. [18]. All the experiments were carried out in triplicate.

2.3. Analytical methods

The volume of produced biogas was measured by the water displacement method using an inverted burette with acidic water (pH < 2). The percentage of hydrogen in the biogas was determined by gas chromatography using a thermal conductivity detector (Agilent Technologies Wilmington, DE, USA) as previously described [13]. 1 cm^3 samples were taken at different times during fermentation, then were diluted and filtered using a 0.22 µm syringe filter (Millipore, Bedford, Massachusetts, USA). End-fermentation metabolites such as succinic acid, lactic acid, formic acid, acetic acid, ethanol, and 2,3-butanediol were quantified by High-Performance Liquid Chromatography (HPLC, Infinity LC 1220, Agilent Technologies, Santa Clara CA, USA) using a Refractive Index Detector, with a column Phenomenex Rezex ROA (Phenomenex Torrance, CA, USA) at 60°C, and 0.0025 M H_2SO_4 as mobile phase at 0.5 cm^3 min^{-1}. The carbohydrates content in each agro-industrial substrate (CWP, WSH, and SCM) was analyzed by the colorimetric method for

determination of sugars and related substances [19, 20]. Furfural present in WSH was spectrophotometrically determined by the method established by Mexican standard regulation NMX-V-004-1972 [21].

2.4. Statistical analysis

The statistical analysis of the different experiments was determined by analysis of variance (ANOVA) and unpaired Student's t-test. Treatments with $p < 0.05$ were considered as statistically significant. The statistical analysis was performed using Excel v16 and GraphPad Prism v5.

3. Results

3.1. Cheese whey fermentation

Cheese whey is a cheap substrate and raw material nutritionally rich used for biofuel production [22]. This by-product is the liquid remaining from cheese production and represents about 85-95% of the milk volume. Typically, this residue contains lactose (4.5-5% w v^{-1}), soluble proteins (0.6-0.8% w v^{-1}) and lipids (0.4-0.5% w v^{-1}) [23]. Cheese whey powder (CWP) is a dried and concentrated form of cheese whey, it has some obvious advantages, such as reduced volume, concentrated source of lactose (75-80%), long term stability and ease of storage and transportation [24, 25]. In this work, 20 g dm^{-3} of CWP, which contained 13.5 g dm^{-3} of total sugars, were used as the substrate for batch fermentations. Fig. 7 shows the hydrogen production kinetics using CWP as substrate. As it is noted, most of the lactose present in CWP was rapidly consumed within the first 48 h of fermentation. After lactose was depleted from the medium, approximately at 150 h, the maximum hydrogen production attained by GA0F bacterium was 923.2 ± 130 cm^3 dm^{-3}.

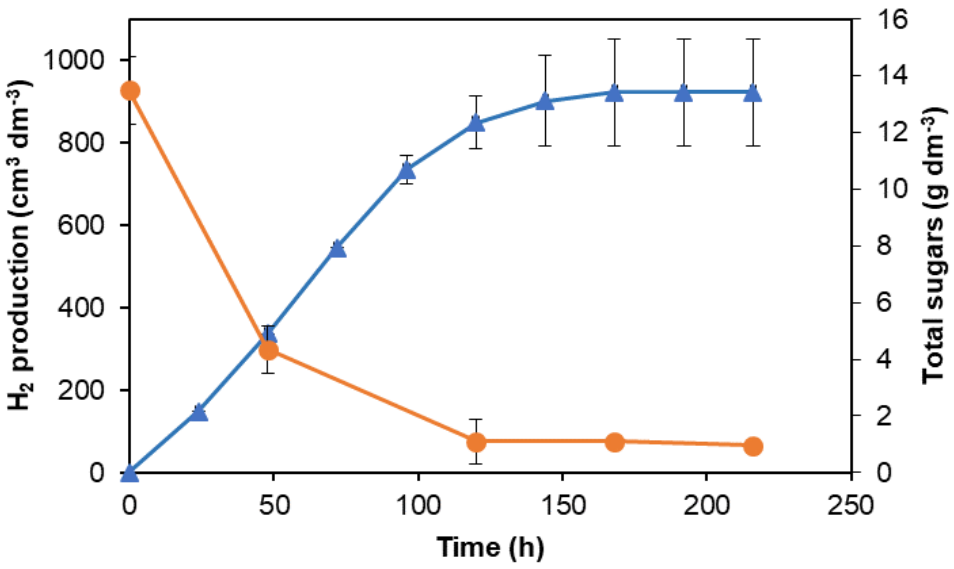

Figure 7. Hydrogen production profile of batch fermentation by the GA0F bacterium using CWP as substrate.

The use of CWP as substrate turned out to be beneficial for the psychrophilic bacterium, which was probably due to the nutrients present in the solution, including nitrogen and minerals. The hydrogen production observed can be compared to those attained by mesophilic and thermophilic bacteria. For example, Kargi et al. [26] reported the hydrogen production by anaerobic sludge using CWP under mesophilic (35°C) and thermophilic (55°C) conditions showing that the highest hydrogen production of 1,144 cm^3 H_2 dm^{-3} was reached under thermophilic conditions with a maximum production rate of 3.46 cm^3 H_2 dm^{-3} h^{-1}. Instead, in this study psychrophilic GA0F bacterium reached 923.20 ± 130 cm^3 H_2 dm^{-3}, with a maximum production rate of 7.60 ± 0.4 cm^3 H_2 dm^{-3} h^{-1}, which represents two-fold the production rate reported for the thermophilic sludge. Furthermore, the process required 30°C less than the thermophilic fermentation, which denotes an economic advantage, since it is possible to carry out the process at room temperature. In several studies [10, 26] cheese whey has proved to be a suitable substrate for hydrogen production using mesophilic and thermophilic bacteria. Nevertheless, there are few reports regarding the use of cheese whey for hydrogen production by

psychrophilic bacteria. Recently, Debowski et al. [27] reported the evaluation of hydrogen production by psychrophilic bacteria isolated from underground water and from demersal lake water using cheese whey as substrate. From 12 strains evaluated, Rhanella aquatilis (RA7) reached the highest hydrogen production of 134 cm^3 dm^{-3}, while the hydrogen production achieved by GA0F bacterium was almost 7 times higher than the production attained by RA7. These data prove the feasibility of Antarctic psychrophilic microorganisms to convert complex substrates such as CWP into hydrogen. Besides hydrogen, fermentation of CWP resulted in the production of several soluble metabolites. As shown in Fig. 8, the main metabolite produced was 2,3-butanediol (5.3 ± 0.5 g dm^{-3}) followed by ethanol (3.0 ± 0.04 g dm^{-3}), succinic acid (0.5 ± 0.08 g dm^{-3}), and acetic acid (0.3 ± 0.06 g dm^{-3}), which decreased the initial pH of 7.0 to 5.7.

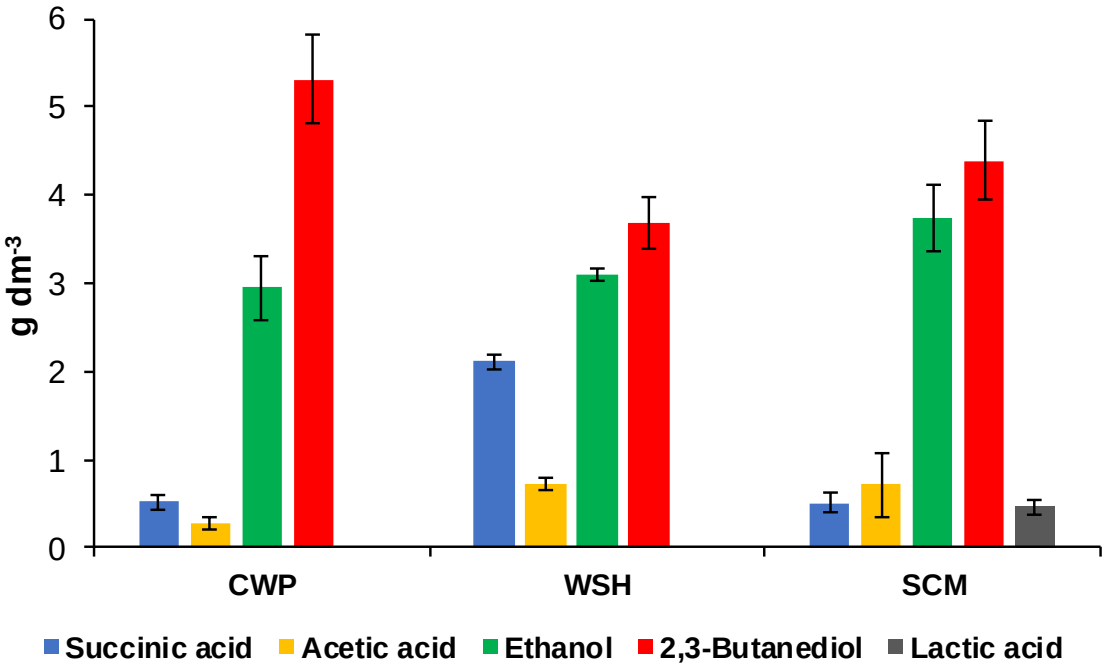

Figure 8. Production of soluble metabolites at the end of the fermentation of CWP, WSH and SCM by the psychrophilic GA0F bacterium.

This metabolite profile is typical of the mixed acid fermentation by sugar fermenting bacteria belonging to genus Enterobacter, Klebsiella, Bacillus, Serratia, and others. [28]. Guo et al. [24] reported the 2,3-butanediol production from CWP by Klebsiella

pneumoniae CICC 10781 reaching a yield of 0.42 g g^{-1}, likewise, another study by Lee and Maddox [29] showed a high 2,3-butanediol yield of 0.46 g g^{-1} using rennet whey permeate as substrate. Meanwhile, in this study, the 2,3-butanediol yield of 0.42 g g^{-1} lactose, which represents 78% of the maximum theoretical 2,3-butanediol yield of 0.538 g g^{-1} carbohydrate.

3.2. Wheat straw hydrolysate fermentation

Wheat straw is an abundant agro-industrial residue with low commercial value. Like any other biomass of lignocellulosic composition, it is composed by a complex mixture of cellulose (40-50%), hemicellulose (25-35%) and lignin (15-20%), therefore, this biomass requires to be hydrolyzed to expose the carbohydrates and make them accessible for the microorganisms [30]. After pretreatment, a broth rich in glucose, xylose, and arabinose is produced; in addition, other compounds such as furfural, phenolic compounds, and weak acids are formed [31]. In this work, the composition of WSH was 20.4 g dm^{-3} total sugars (which included 3.2 g dm^{-3} glucose, 14.2 g dm^{-3} xylose, 3.0 g dm^{-3} arabinose), 1.0 g dm^{-3} formic acid, 2.2 g dm^{-3} acetic acid and 0.6 g dm^{-3} furfural. Fig. 9 depicts the hydrogen production kinetics by the GA0F bacterium using WSH as substrate.

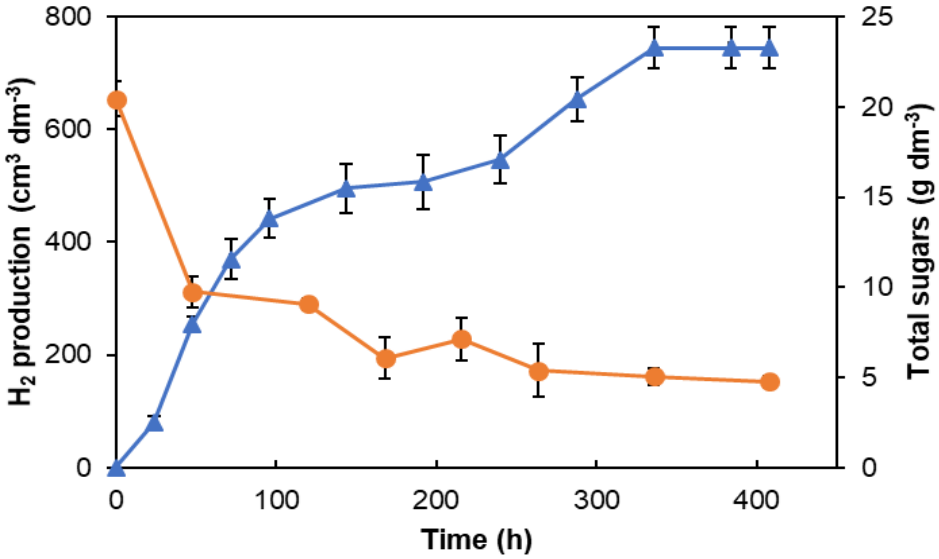

Figure 9. Hydrogen production profile of batch fermentation by the GA0F bacterium using WSH as substrate.

As it can be seen, hydrogen production started at 24 h, followed by a lag phase from 100 to 192 h. After that, hydrogen production restarted and continued until 336 h. When bacterial cells are exposed to multiple sugars, they do not metabolize all sugars simultaneously, but rather a sequential utilization of carbon sources is carried out. This phenomenon is characterized by two growth phases often separated with lag periods. Fig. 9 shows that total sugar concentration decreased by almost half of the initial concentration at the first 48 h of fermentation. Afterward, the total sugar concentration was maintained at the same concentration in agreement with the diauxic shift in hydrogen production, subsequently, another portion of the carbon source was consumed. The maximum hydrogen production and hydrogen production rate reached were 744.8 ± 36 cm^3 H_2 dm^{-3} and 5.4 ± 0.5 cm^3 H_2 dm^{-3} h^{-1}, respectively (Table 7).

Table 7. Hydrogen, ethanol and 2,3-butanediol production parameters obtained by the psychrophilic GA0F bacterium using CWP, WSH and SCM.

Substrate	**H_2 (cm^3 dm^{-3})**	**Y_{H2} (cm^3 g^{-1})**	**EtOH (g dm^{-3})**	**Y_{EtOH} (g g^{-1})**	**BDO (g dm^{-3})**	**Y_{BDO} (g g^{-1})**
CWP	923.2 ± 130	73.5 ±10	3.0 ± 0.04	0.24 ± 0.03	5.3 ± 0.5	0.42 ± 0.04
WSH	744.8 ± 36	43.6 ± 2	3.1 ± 0.1	0.19 ± 0.01	3.7 ± 0.3	0.23 ± 0.05
SCM	979.3 ± 74	52.4 ± 4	3.7 ± 0.4	0.20 ± 0.02	4.4 ± 0.4	0.24 ± 0.02

CWP: Cheese whey powder, WSH: Wheat straw hydrolysate, SCM: Sugarcane molasses, Y_{H2}: Hydrogen yield, EtOH: Ethanol, Y_{EtOH}: Ethanol yield, BDO: 2,3-butanediol, Y_{BDO}: 2,3-butanediol yield.

This hydrogen production was low compared to other studies reported in the literature (Table 7). For instance, Sagnak et al. [32] reported the production of 2,785 cm^{-3} H_2 dm^{-3} by mesophilic anaerobic sludge (37°C) using hydrolyzed waste ground wheat containing 27.5 g dm^{-3} total sugar. In the same way, Khamtib et al. [33] reported the production of 1,947 cm^{-3} H_2 dm^{-3} by hot spring enriched culture from oil palm trunk hydrolysate at 55°C using an initial substrate concentration of 22.07 g dm^{-3}, while Cakir et al. [34] at the same temperature using heat-treated

anaerobic sludge produced 3,008 cm^{-3} H_2 dm^{-3} from acid-hydrolyzed ground wheat starch with an initial total sugar concentration of 18.5 g dm^{-3}.

Table 8. Comparison of production and yield of hydrogen, ethanol, and 2,3-butanediol reported by different microorganisms using different substrates.

Substrate	Microorganism	T (°C)	H_2 (cm^3 dm^{-3})	Y_{H2} (cm^3 g^{-1})	EtOH (g dm^{-3})	Y_{EtOH} (g g^{-1})	BDO (g dm^{-3})	Y_{BDO} (g g^{-1})	Reference
CWP	GA0F	25	923.2	73.5	3.0	0.24	5.3	0.42	This study
	Rhanella aquatilis (RA7)	20	134*	NR	NR	NR	NR	NR	[27]
	Anaerobic sludge	55	1144	1.03[a]	NR	NR	NR	NR	[26]
	Klebsiella pneumoniae NCIB 8017	30	NR	NR	NR	NR	7.5	0.46	[29]
WSH	GA0F	25	744.8	43.6	3.1	0.19	3.7	0.23	This study
	Hot spring enriched cultured	55	1947	0.71	0.24	0.01	NR	NR	[33]
	Klebsiella pneumoniae	30	NR	NR	1.12	0.09	3.37	0.4	[43]
	Enterobacter aerogenes	39	NR	NR	NR	NR	8.8	0.88[a]	[47]
SCM	GA0F	25	979.3	52.4	3.7	0.20	4.4	0.24	This study
	Anaerobic sludge	35	1770	1.32[b]	NR	NR	NR	NR	[53]
	Enterobacter aerogenes	39	NR	NR	NR	NR	5.3	0.86[a]	[47]
	Klebsiella sp.	37	NR	0.67[a]	NR	0.59[a]	NR	0.59[a]	[12]

CWP: Cheese whey powder, WSH: Wheat straw hydrolysate, SCM: Sugarcane molasses, NR: Not reported, Y_{H2}: Hydrogen yield, EtOH: Ethanol, Y_{EtOH}: Ethanol yield, BDO: 2,3-butanediol, Y_{BDO}: 2,3-butanediol yield, [a]mol mol substrate^{-1}, [b]H_2_glu eq^{-1} (Glucose_equivalent: mmol of sugar as glucose), *Converted from original data.

One of the factors that could have affected hydrogen production is the adverse effect of inhibitory compounds present in WSH. Van Ginkel and Logan [35] reported the addition of 25 mM of acetic acid to the fermentation resulted in a decrease in hydrogen yield by 13%. During acid hydrolysis, acetic acid is released from acetylxylan from hemicellulose [36]. The unfavorable effect of acetic acid is attributed to its diffusion into the cytosol where the dissociation of the acid occurs, decreasing the cytosolic pH [37]. Likewise, furfural produced from pentoses inhibits dark fermentation by decreasing the enzyme activities, inhibiting protein and RNA synthesis and also breaking down DNA [38]. An initial concentration of 2.2 g dm^{-3}

(36.6 mM) acetic acid and 0.6 g dm^{-3} furfural could have had a negative effect on dark fermentation by psychrophilic GA0F bacterium. Cao et al. [39], demonstrated that a concentration of 1 g dm^{-3} furfural and hydroxymethylfurfural (HMF) exerted a large negative influence on growth and hydrogen production. While Panagiotopoulos et al. [40] observed inhibition of the fermentation of mild-acid pretreated corn stalks by furfural concentrations in a range of 0.08-0.17 g dm^{-3}. Likewise, Bellido et al. [41] described a complete inhibition of ethanol fermentation by using WSH due to the presence of 1.5 g dm^{-3} acetic acid, 0.15 g dm^{-3} furfural and 0.05 g dm^{-3} HMF. As stated by Sivagurunathan et al. [42] the threshold inhibition concentration of the by-products released during the pretreatment of lignocellulosic biomass is specific to the type of microorganism applied as inoculum. To our knowledge, there are no previous reports regarding the use of psychrophilic bacteria using lignocellulosic hydrolysates for biofuel production, therefore more research is needed to characterize the psychrophilic bacteria tolerance to this kind of fermentation inhibitors. The application of several mesophilic and thermophilic microorganisms using different hydrolysates of lignocellulosic materials such as wood [43], oil palm frond [44], wheat straw [11], corn stover [45], sugarcane bagasse [46], has been widely studied for 2,3-butanediol or ethanol production. Perego et al. [47] reported a 2,3-butanediol production of 8.8 g dm^{-3} using starch hydrolysate, likewise, Hazeena et al. [48] reached 7.2 g dm^{-3} using oil palm frond hydrolysate. Another study by Yu et al. [43] shows the production of 1.12 g dm^{-3} ethanol and 3.37 g dm^{-3} 2,3-butanediol at 30°C by Klebsiella pneumoniae from steam-exploded aspen presoaked in acid. While in this study, GA0F bacterium attained a 2,3-butanediol and ethanol production of 3.7 ± 0.3 g dm^{-3} and 3.1 ± 0.07 g dm^{-3}, respectively (Fig. 9). The yields of 2,3-butanediol and ethanol reported in the literature are in a range of 0.2 to 0.5 g g^{-1} carbohydrate consumed. In this study, ethanol (0.19 ± 0.01 g g^{-1}) and 2,3-butanediol (0.23 ± 0.05 g g^{-1}) yields using WSH were within the range mentioned above, although low with respect to the theoretical yield of 0.5 g g^{-1}. Beside alcohols, several organic acids such as succinic acid (2.1 ± 0.08 g dm^{-3}) and acetic acid (0.7 ± 0.2 g dm^{-3}) were produced (Fig. 9). This led to a drop in the

initial pH from 7 to 4.4, which also might have affected the synthesis of hydrogen, ethanol and 2,3-butanediol. The toxic effect of some compounds from the WSH on GA0F bacterium could be further improved as suggested by Palmqvist and Hahn-Hagerdal [37] through an optimization of the pretreatment and hydrolysis conditions of wheat straw and by detoxification methods for the removal of inhibitors prior to fermentation, as well as by acclimatization of the strains to hydrolysates through serial sub-culturing [43].

3.3. Sugarcane molasses

Sugarcane molasses are an agro-industrial by-product of the sugar manufacturing process, which contain sucrose as the most abundant sugar and small quantities of glucose, fructose and raffinose [49]. SCM are also rich in nutrients required by most microorganisms (metals, vitamins and nitrogen compounds) [50]. This by-product represents a cheap raw material, readily available, and accessible for conversion with limited pretreatments as compared to starchy or lignocellulosic materials, since all sugars are present in an easily fermentable form [51]. In this work, the use of diluted SCM (21 g dm^{-3} total sugars) led to a hydrogen production of 979.3 ± 74 cm^3 dm^{-3} and a production rate of 8.5 ± 0.8 cm^3 dm^{-3} h^{-1} (Table 1). Similar hydrogen production parameters are found in the literature. For instance, Kumar et al. [52] reported 1,800 cm^3 H_2 dm^{-3} by *Enterobacter aerogenes* at 30°C using 40 g dm^{-3} cane molasses. da Silva et al. [53] evaluated the use SCM combined with leachate, which originates from the disposal of plastics, batteries and mercury lamps, for hydrogen production under mesophilic conditions (35°C). Their results showed that hydrogen production was improved from 663 cm^3 H_2 dm^{-3} using SCM plus a nutrient solution, to 1,770 cm^3 H_2 dm^{-3} upon addition of the leachate to SCM. In our study, psychrophilic GA0F bacterium reached 979.3 ± 74 cm^3 H_2 dm^{-3} using SCM only with the addition of a nutrient solution (see section 2.2), similar to the one used in the aforementioned study, this represents an advantage since GA0F bacterium required 10°C less to carry out the fermentation. Fig. 10 illustrates hydrogen production kinetics using SCM as substrate.

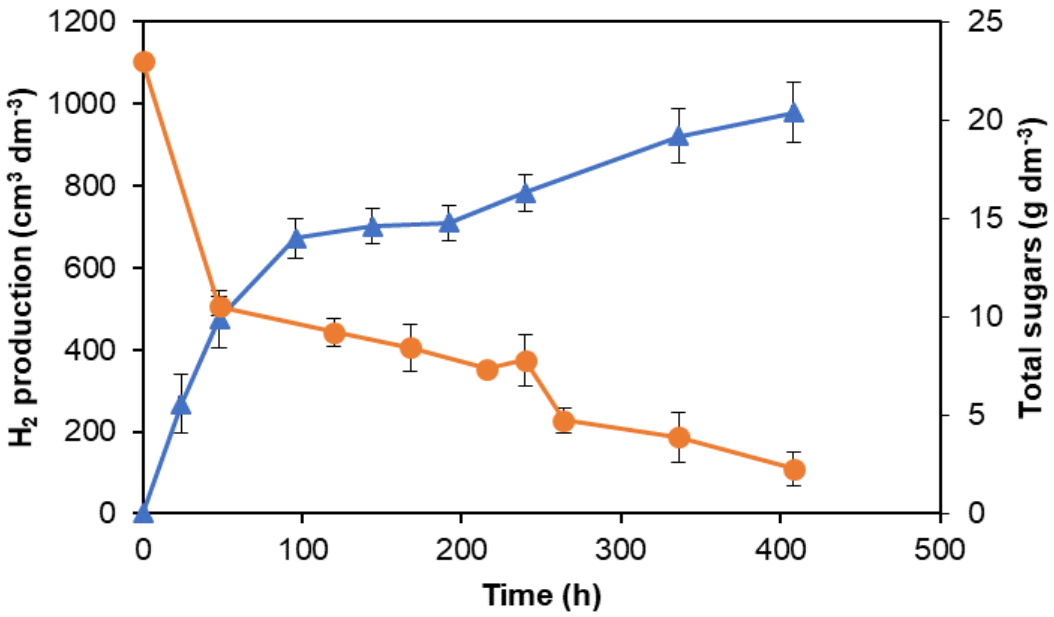

Figure 10. Hydrogen production profile of batch fermentation by the GA0F bacterium using SCM.

Similarly, as observed in fermentations using WSH, a biphasic behavior was present on hydrogen evolution from soluble sugars in SCM. Hydrogen production started at 24 h and continued until 96 h, after that a lag phase of 100 h was observed. Subsequently, the hydrogen production restarted until 408 h. The analysis of soluble metabolites showed that hydrogen production was accompanied principally by the production of solvents, and to a low extent by volatile fatty acids such as acetic acid (0.7 ± 0.2 g dm^{-3}), succinic acid (0.5 ± 0.1 g dm^{-3}) and lactic acid (0.5 ± 0.08 g dm^{-3}) (Fig. 8) which managed to lower the pH from 7 to 4.8. 2,3-butanediol production attained was 4.4 ± 0.4 g dm^{-3}, whereas the ethanol production was 3.7 ± 0.4 g dm^{-3}. Considering the substrate consumption, the yield achieved for both alcohols was 0.24 ± 0.02 g g^{-1} and 0.20 ± 0.02 g g^{-1}, respectively (Table 1). Perego et al. [47] reached a similar 2,3-butanediol yield from raw molasses (0.20 g g^{-1}) and decolored molasses (0.26 g g^{-1}) using Enterobacter aerogenes at 39°C. Dai et al. [54] reported 0.39 g g^{-1} by Enterobacter cloacae (GMCC 6053) at 37°C. Likewise, Afschar et al. [55], achieved 0.42 g g^{-1} using Klebsiella oxytoca. In addition, Cazetta et al. [56] reported an ethanol yield of

0.33 g g^{-1}, using Zymomonas mobilis, whereas Razmovski et al. [57] attained 0.49 g g^{-1} using Saccharomyces cerevisiae. These studies successfully achieved a high 2,3-butanediol or ethanol yield using SCM. In our study, the low ethanol and 2,3-butanediol production are compensated by the fact that hydrogen, ethanol, and 2,3-butanediol are produced simultaneously under room temperature conditions.

3.4. Comparison of hydrogen, ethanol and 2,3-butanediol production from CWP, HWS, and SCM by the GA0F bacterium

In this study, three different substrates CWP, WSH, and SCM were compared to determine the most suitable carbon source for the production of biofuels by GA0F bacterium. Hydrogen, ethanol, and 2,3-butanediol were produced in all cases; nevertheless, hydrogen yield (73.5 ± 10 cm^3 g^{-1}) from CWP was significantly higher ($p < 0.05$) compared to the yield achieved using the other two substrates (Table 7). This could be attributed to the fact that CWP is composed of a single carbon source plus nutrients like vitamins and proteins, which makes it easily and rapidly metabolized; also, CWP solution was probably nutritionally richer than the other substrates resulting in higher hydrogen yield. Moreover, this substrate is free from inhibitory compounds unlike WSH, which clearly affected the fermentation of hexoses and pentoses available in the medium. In the same way, a significantly ($p < 0.05$) higher 2,3-butanediol yield was obtained by the use of CWP, where GA0F bacterium reached 0.42 ± 0.04 g g^{-1}, which corresponds to 78% of the theoretical yield. 2,3-Butanediol is an important intermediate in diverse industrial areas such as printing, cosmetics, food processing, fumigants, antifreeze, etc. [58], also, 2,3-butanediol is a potentially valuable fuel additive with a heating value of 27.20 kJ g^{-1} which compares favorably with other liquid fuels (methanol 22.08 kJ g-1 and ethanol 29.06 kJ g^{-1}) [6]. Bacteria belonging to *Enterobacter*, *Klebsiella*, *Bacillus* and *Serratia* genus can produce this solvent through the mixed acid fermentation. Under anaerobic conditions 2,3-butanediol is formed from pyruvate, where three key enzymes are involved, i.e., α-acetolactate synthase (ALS, E.C. 4.1.3.18), α-acetolactate decarboxylase (ALDC, E.C.4.1.1.5), and 2,3-butanediol dehydrogenase (BDH, E.C. 1.1.1.76, also known as acetoin reductase). The first

step is the condensation of two molecules of pyruvate to yield α-acetolactate by ALS. Then, α-acetolactate is decarboxylated and converted into acetoin by ALDC. The final step is the reversible reduction of acetoin to 2,3-butanediol by BDH [28, 59]. Also, other enzymes such as lactate dehydrogenase (LDH, E.C. 1.1.1.27) and pyruvate formate lyase (PFL, E.C. 2.3.1.54) act upon pyruvate to generate lactic acid, formic acid and acetyl-CoA. Whereas, succinic acid originates from the phosphoenol pyruvate (PEP) branch point where is carboxylated to oxaloacetate and then to succinic acid [60]. 2,3-butanediol can also be produced under aerobic conditions where α-acetolactate can undergo to spontaneous decarboxylation producing diacetyl. Then diacetyl reductase (DAR, E.C. 1.1.1.303) converts diacetyl into acetoin. Finally, BDH reduces acetoin to 2,3-butanediol [58]. Several authors have reported the improvement of 2,3-butanediol production through micro-aeration conditions. For instance, Jung et al. [61], improved the 2,3-butanediol production by Enterobacter aerogenes from 69.5 g dm^{-3} to 118.05 g dm^{-3} with further optimization of the medium and aeration conditions. Similarly, Rebecchi et al. [62] reported that the oxygen transfer rate from 7 to 15 mmol dm^{-3} h^{-1} led to an optimal 2,3-butanediol yield of 0.43 ± 0.03 g g^{-1} in Bacillus licheniformis ATCC9789. However, micro-aeration causes the suppression of ethanol and hydrogen synthesis [58], which may not be convenient in the basis of a biorefinery concept. Through the synthesis of 2,3-butanediol, bacterial cells regulate intracellular $NADH/NAD^+$ and also prevent the medium acidification by changing the metabolism from acid production to the formation of neutral compounds [28]. The production of 2,3-butanediol by mesophilic and thermophilic bacteria is well documented; on the contrary, except by an earlier study of our group [13], no previous studies regarding to the production of 2,3-butanediol by cold-loving bacteria have been published so far, therefore, more studies are needed to understand the fermentative aspects of psychrophilic bacteria. As mentioned above, 2,3-butanediol is used as an anti-freeze in the industry due to its chemical properties; this fact may provide clues as to why psychrophilic bacteria synthesize 2,3-butanediol apart from the redox potential and pH regulation. As described by Hubálek [63], 2,3-butanediol can act as a cryoprotectant in harsh

environments, preventing the formation of large ice crystals within the cell and also reducing salt toxicity and excessive dehydration. On the other hand, ethanol yields achieved by GA0F bacterium ranged from 0.19-0.24 g g^{-1} where the highest value corresponds to CWP fermentation and the lowest to the WSH fermentation (Table 7). However, statistical analysis showed that there are not significant differences between the ethanol yields achieved. As shown in Fig. 2, the distribution of the organic acids produced was different for each substrate. When CWP was used as carbon source, only a small amount of succinic acid (0.5 ± 0.08 g dm^{-3}) and acetic acid (0.3 ± 0.06 g dm^{-3}) was produced. In contrast, when WSH was consumed, a significant ($p < 0.05$) concentration of succinic acid (2.1 ± 0.08 g dm^{-3}) was reached in comparison to the CWP and SCM metabolite profiles. The production of acetic acid was similar between the three substrates, being the CWP fermentation where the lowest concentration was observed. Ethanol production and yield were almost the same between the different substrates, however, as mentioned before, the highest 2,3-butanediol yield was attained using CWP (Table 7). This could be attributed to the effect of inhibitory compounds such as furan derivatives typically found in molasses and lignocellulosic hydrolysates. For instance, Horváth et al. [64] reported furan derivatives had a negative effect on 2,3-butanediol production, being furfural the one that showed stronger toxicity to cell growth and alcohol production.

On the other hand, the fermentation of SCM had lactic acid production, which was not observed on the other two fermentations; this reflects different carbon fluxes in the mixed acid pathway, which depend on the composition of each substrate (i.e., carbohydrates and inhibitory compounds). Therefore, in order to solve this differential carbon distribution among the different substrates, further analysis must be carried out, such as enzymatic activities and carbon flux balance analysis.

The fact that the psychrophilic GA0F bacterium used in this study preferentially produced solvents and hydrogen instead of acids represents a competitive advantage over other processes since it could be possible to establish an alcohol-

rich fermentation in which the end products are not toxic, as happens in ethanol or acetone-butanol fermentations.

4. Conclusions

In this work, the simultaneous production of hydrogen, ethanol, and 2,3-butanediol from different cheap substrates such as cheese whey powder, wheat straw hydrolysate and sugar cane molasses by the psychrophilic GA0F bacterium is demonstrated. The highest yields of hydrogen (73.5 ± 10 cm^3 H_2 g^{-1}), ethanol (0.24 ± 0.03 g g^{-1}) and 2,3-butanediol (0.42 ± 0.04 g g^{-1}) are obtained using cheese whey powder, which is an economical, concentrated source of lactose. This study also reveals the susceptibility of the GA0F bacterium to the inhibitory compounds present in wheat straw hydrolysate, which result in the lowest production of the three biofuels evaluated. Since fermentations carried out in this study resulted in a rich solvent production with concomitant hydrogen production, the use of the GA0F bacterium could be considered for a further application at industrial scale under conditions of room temperature.

5. Acknowledgments

We thank partial financial support from CONACyT-Basicas Grant 281700. Cecilia L. Alvarez-Guzmán thanks to CONACyT for her scholarship 330870. The authors wish to thank to Matthew Tippett for the English revision.

6. References

[1] Tilman D, Socolow R, Foley JA, Hill J, Larson E, Lynd L, et al. Beneficial biofuels—the food, energy, and environment trilemma. Science. 2009;325:270-1.

[2] Tabatabaei M, Rahim RA, Abdullah N, Wright A-DG, Shirai Y, Sakai K, et al. Importance of the methanogenic archaea populations in anaerobic wastewater treatments. Process Biochemistry. 2010;45:1214-25.

[3] Guo XM, Trably E, Latrille E, Carrere H, Steyer J-P. Hydrogen production from agricultural waste by dark fermentation: a review. International journal of hydrogen energy. 2010;35:10660-73.

[4] Ntaikou I, Antonopoulou G, Lyberatos G. Biohydrogen production from biomass and wastes via dark fermentation: a review. Waste and Biomass Valorization. 2010;1:21-39.

[5] Sanchez OJ, Cardona CA. Trends in biotechnological production of fuel ethanol from different feedstocks. Bioresource technology. 2008;99:5270-95.

[6] Garg S, Jain A. Fermentative production of 2, 3-butanediol: a review. Bioresource Technology. 1995;51:103-9.

[7] Köpke M, Mihalcea C, Liew F, Tizard JH, Ali MS, Conolly JJ, et al. 2, 3-Butanediol production by acetogenic bacteria, an alternative route to chemical synthesis, using industrial waste gas. Appl Environ Microbiol. 2011;77:5467-75.

[8] Magee RJ, Kosaric N. The microbial production of 2, 3-butanediol. Advances in Applied Microbiology: Elsevier; 1987. p. 89-161.

[9] Das D, Veziroğlu TN. Hydrogen production by biological processes: a survey of literature. International journal of hydrogen energy. 2001;26:13-28.

[10] Azbar N, Dokgöz FTÇ, Keskin T, Korkmaz KS, Syed HM. Continuous fermentative hydrogen production from cheese whey wastewater under thermophilic anaerobic conditions. International journal of Hydrogen energy. 2009;34:7441-7.

[11] Kaparaju P, Serrano M, Thomsen AB, Kongjan P, Angelidaki I. Bioethanol, biohydrogen and biogas production from wheat straw in a biorefinery concept. Bioresource technology. 2009;100:2562-8.

[12] Wang A, Wang Y, Jiang T, Li L, Ma C, Xu P. Production of 2, 3-butanediol from corncob molasses, a waste by-product in xylitol production. Applied microbiology and biotechnology. 2010;87:965-70.

[13] Alvarez-Guzmán CL, Balderas-Hernández VE, González-García R, Ornelas-Salas JT, Vidal-Limón AM, Cisneros-de la Cueva S, et al. Optimization of hydrogen production by the psychrophilic strain G088. International Journal of Hydrogen Energy. 2017;42:3630-40.

[14] Mohammed A, Abdul-Wahab MF, Hashim M, Omar AH, Md MR, Muhamad MS, et al. Biohydrogen Production by Antarctic Psychrotolerant *Klebsiella* sp. ABZ11. Polish journal of microbiology. 2018;67:283-90.

[15] Margesin R, Schinner F. Properties of cold-adapted microorganisms and their potential role in biotechnology. Journal of Biotechnology. 1994;33:1-14.

[16] Cavicchioli R, Charlton T, Ertan H, Omar SM, Siddiqui K, Williams T. Biotechnological uses of enzymes from psychrophiles. Microbial biotechnology. 2011;4:449-60.

[17] García-Echauri S, Gidekel M, Gutiérrez-Moraga A, Santos L, De León-Rodríguez A. Isolation and phylogenetic classification of culturable psychrophilic prokaryotes from the Collins glacier in the Antarctica. Folia microbiologica. 2011;56:209-14.

[18] Wu K-J, Saratale GD, Lo Y-C, Chen W-M, Tseng Z-J, Chang M-C, et al. Simultaneous production of 2, 3-butanediol, ethanol and hydrogen with a *Klebsiella* sp. strain isolated from sewage sludge. Bioresource technology. 2008;99:7966-70.

[19] Dubois M, Gilles KA, Hamilton JK, Rebers Pt, Smith F. Colorimetric method for determination of sugars and related substances. Analytical chemistry. 1956;28:350-6.

[20] Masuko T, Minami A, Iwasaki N, Majima T, Nishimura S-I, Lee YC. Carbohydrate analysis by a phenol–sulfuric acid method in microplate format. Analytical biochemistry. 2005;339:69-72.

[21] Mexicana NO, ALCOHOLICAS-CHARANDA-ESPECIFICACIONES B. NOM-144-SCFI-2000.

[22] Prazeres AR, Carvalho F, Rivas J. Cheese whey management: A review. Journal of Environmental Management. 2012;110:48-68.

[23] Göblös S, Portörő P, Bordás D, Kálmán M, Kiss I. Comparison of the effectivities of two-phase and single-phase anaerobic sequencing batch reactors during dairy wastewater treatment. Renewable Energy. 2008;33:960-5.

[24] Guo X, Wang Y, Guo J, Wang Q, Zhang Y, Chen Y, et al. Efficient production of 2, 3-butanediol from cheese whey powder (CWP) solution by *Klebsiella pneumoniae* through integrating pulsed fed-batch fermentation with a two-stage pH control strategy. Fuel. 2017;203:469-77.

[25] Kargi F, Ozmıhcı S. Utilization of cheese whey powder (CWP) for ethanol fermentations: Effects of operating parameters. Enzyme and Microbial Technology. 2006;38:711-8.

[26] Kargi F, Eren NS, Ozmihci S. Bio-hydrogen production from cheese whey powder (CWP) solution: comparison of thermophilic and mesophilic dark fermentations. international journal of hydrogen energy. 2012;37:8338-42.

[27] Dębowski M, Korzeniewska E, Filipkowska Z, Zieliński M, Kwiatkowski R. Possibility of hydrogen production during cheese whey fermentation process by different strains of psychrophilic bacteria. International journal of hydrogen energy. 2014;39:1972-8.

[28] Ji X-J, Huang H, Ouyang P-K. Microbial 2, 3-butanediol production: a state-of-the-art review. Biotechnology advances. 2011;29:351-64.

[29] Lee H, Maddox I. Microbial production of 2, 3-butanediol from whey permeate. Biotechnology letters. 1984;6:815-8.

[30] Domínguez-Bocanegra AR, Torres-Muñoz JA, López RA. Production of bioethanol from agro-industrial wastes. Fuel. 2015;149:85-9.

[31] Lin R, Cheng J, Ding L, Song W, Zhou J, Cen K. Inhibitory effects of furan derivatives and phenolic compounds on dark hydrogen fermentation. Bioresource technology. 2015;196:250-5.

[32] Sagnak R, Kargi F, Kapdan IK. Bio-hydrogen production from acid hydrolyzed waste ground wheat by dark fermentation. International Journal of Hydrogen Energy. 2011;36:12803-9.

[33] Khamtib S, Plangklang P, Reungsang A. Optimization of fermentative hydrogen production from hydrolysate of microwave assisted sulfuric acid pretreated oil palm trunk by hot spring enriched culture. International Journal of Hydrogen Energy. 2011;36:14204-16.

[34] Cakır A, Ozmihci S, Kargi F. Comparison of bio-hydrogen production from hydrolyzed wheat starch by mesophilic and thermophilic dark fermentation. International Journal of Hydrogen Energy. 2010;35:13214-8.

[35] Van Ginkel S, Logan BE. Inhibition of biohydrogen production by undissociated acetic and butyric acids. Environmental science & technology. 2005;39:9351-6.

[36] Lee SJ, Lee JH, Yang X, Kim SB, Lee JH, Yoo HY, et al. Phenolic compounds: Strong inhibitors derived from lignocellulosic hydrolysate for 2, 3-butanediol production by *Enterobacter aerogenes*. Biotechnology journal. 2015;10:1920-8.

[37] Palmqvist E, Hahn-Hägerdal B. Fermentation of lignocellulosic hydrolysates. II: inhibitors and mechanisms of inhibition. Bioresource technology. 2000;74:25-33.

[38] Nissilä ME, Lay C-H, Puhakka JA. Dark fermentative hydrogen production from lignocellulosic hydrolyzates–a review. biomass and bioenergy. 2014;67:145-59.

[39] Cao G-L, Ren N-Q, Wang A-J, Guo W-Q, Xu J-F, Liu B-F. Effect of lignocellulose-derived inhibitors on growth and hydrogen production by *Thermoanaerobacterium thermosaccharolyticum* W16. International Journal of Hydrogen Energy. 2010;35:13475-80.

[40] Panagiotopoulos I, Bakker R, Budde M, De Vrije T, Claassen P, Koukios E. Fermentative hydrogen production from pretreated biomass: a comparative study. Bioresource technology. 2009;100:6331-8.

[41] Bellido C, Bolado S, Coca M, Lucas S, González-Benito G, García-Cubero MT. Effect of inhibitors formed during wheat straw pretreatment on ethanol fermentation by *Pichia stipitis*. Bioresource technology. 2011;102:10868-74.

[42] Sivagurunathan P, Kumar G, Mudhoo A, Rene ER, Saratale GD, Kobayashi T, et al. Fermentative hydrogen production using lignocellulose biomass: an overview of pre-treatment methods, inhibitor effects and detoxification experiences. Renewable and Sustainable Energy Reviews. 2017;77:28-42.

[43] Yu E, Levitin N, Saddler J. Production of 2, 3-butanediol by *Klebsiella pneumoniae* grown on acid hydrolyzed wood hemicellulose. Biotechnology Letters. 1982;4:741-6.

[44] Sitthikitpanya S, Reungsang A, Prasertsan P, Khanal SK. Two-stage thermophilic bio-hydrogen and methane production from oil palm trunk hydrolysate using *Thermoanaerobacterium thermosaccharolyticum* KKU19. International Journal of Hydrogen Energy. 2017;42:28222-32.

[45] Li L, Li K, Wang K, Chen C, Gao C, Ma C, et al. Efficient production of 2, 3-butanediol from corn stover hydrolysate by using a thermophilic *Bacillus licheniformis* strain. Bioresource technology. 2014;170:256-61.

[46] Um J, Kim DG, Jung M-Y, Saratale GD, Oh M-K. Metabolic engineering of *Enterobacter aerogenes* for 2, 3-butanediol production from sugarcane bagasse hydrolysate. Bioresource technology. 2017;245:1567-74.

[47] Perego P, Converti A, Del Borghi A, Canepa P. 2, 3-Butanediol production by *Enterobacter aerogenes*: selection of the optimal conditions and application to food industry residues. Bioprocess Engineering. 2000;23:613-20.

[48] Hazeena SH, Pandey A, Binod P. Evaluation of oil palm front hydrolysate as a novel substrate for 2, 3-butanediol production using a novel isolate *Enterobacter cloacae* SG1. Renewable energy. 2016;98:216-20.

[49] Mladenović DD, Djukić-Vuković AP, Kocić-Tanackov SD, Pejin JD, Mojović LV. Lactic acid production on a combined distillery stillage and sugar beet molasses substrate. Journal of Chemical Technology & Biotechnology. 2016;91:2474-9.

[50] Liu Y-P, Zheng P, Sun Z-H, Ni Y, Dong J-J, Zhu L-L. Economical succinic acid production from cane molasses by *Actinobacillus succinogenes*. Bioresource technology. 2008;99:1736-42.

[51] El-Gendy NS, Madian HR, Amr SSA. Design and optimization of a process for sugarcane molasses fermentation by *Saccharomyces cerevisiae* using response surface methodology. International journal of microbiology. 2013;2013.

[52] Kumar V, Kothari R, Ahmad S, Tyagi S. Improvement of Biohydrogen Production with Optimized Initial pH using Industrial Organic Residue (Molasses) with *Enterobacter Aerogens*.

[53] da Silva IA, de Lima ST, Siqueira MR, da Veiga MAMS, Reginatto V. Landfill leachate enhances fermentative hydrogen production from glucose and sugarcane processing derivatives. Journal of Material Cycles and Waste Management. 2018;20:777-86.

[54] Dai J-Y, Zhao P, Cheng X-L, Xiu Z-L. Enhanced production of 2, 3-butanediol from sugarcane molasses. Applied biochemistry and biotechnology. 2015;175:3014-24.

[55] Afschar A, Bellgardt K, Rossell CV, Czok A, Schaller K. The production of 2, 3-butanediol by fermentation of high test molasses. Applied microbiology and biotechnology. 1991;34:582-5.

[56] Cazetta M, Celligoi M, Buzato J, Scarmino I. Fermentation of molasses by *Zymomonas mobilis*: Effects of temperature and sugar concentration on ethanol production. Bioresource technology. 2007;98:2824-8.

[57] Razmovski R, Vučurović V. Ethanol production from sugar beet molasses by S. cerevisiae entrapped in an alginate–maize stem ground tissue matrix. Enzyme and microbial technology. 2011;48:378-85.

[58] Celińska E, Grajek W. Biotechnological production of 2, 3-butanediol—current state and prospects. Biotechnology advances. 2009;27:715-25.

[59] Xiao Z, Lu JR. Strategies for enhancing fermentative production of acetoin: a review. Biotechnology advances. 2014;32:492-503.

[60] Syu M-J. Biological production of 2, 3-butanediol. Applied microbiology and biotechnology. 2001;55:10-8.

[61] Jung M-Y, Ng CY, Song H, Lee J, Oh M-K. Deletion of lactate dehydrogenase in *Enterobacter aerogenes* to enhance 2, 3-butanediol production. Applied Microbiology and Biotechnology. 2012;95:461-9.

[62] Rebecchi S, Pinelli D, Zanaroli G, Fava F, Frascari D. Effect of oxygen mass transfer rate on the production of 2, 3-butanediol from glucose and agro-industrial byproducts by *Bacillus licheniformis* ATCC9789. Biotechnology for biofuels. 2018;11:145.

[63] Hubalek Z. Protectants used in the cryopreservation of microorganisms. Cryobiology. 2003;46:205-29.

[64] Horváth IS, Franzén CJ, Taherzadeh MJ, Niklasson C, Lidén G. Effects of furfural on the respiratory metabolism of Saccharomyces cerevisiae in glucose-limited chemostats. Appl Environ Microbiol. 2003;69:4076-86.

Chapter 3

Autodisplay of alpha amylase from *Bacillus megaterium* in *E. coli* for the bioconversion of starch into hydrogen, ethanol and succinic acid

Abstract

In this work, the expression of an α-amylase from Bacillus megaterium on the cell surface of *Escherichia coli* strains WDHA (*Δ hycA* and *Δ ldhA*) and WDHFP (*Δ hycA*, *Δ frdD* and *Δ pta*) by the autodisplay AIDA system was carried out with the purpose to confer the ability to *E. coli* strains to degrade starch and thus produce hydrogen, ethanol and succinic acid. For the characterization of the biocatalyst, the effect of temperature (30-70°C), pH (3-6) and CaCl2 concentration (0-25 mM), as well as the thermostability of the biocatalyst (55-80°C) at several time intervals (15-60 min) were evaluated. The results show that the biocatalyst has a maximum activity at 55°C and pH 4.5. Calcium is required for the activity as well for the thermal stability of the biocatalyst. The calculated Vmax and Km values were 0.24 U cm^{-3} and 5.8 mg cm^{-3}, respectively. Furthermore, a set of anaerobic batch fermentations was carried out using 10 g dm^{-3} of starch and 1 g dm^{-3} of glucose as carbon sources in 120 cm^3 serological bottles, using WDHA and WDHFP strains harboring the pAIDA-amyA plasmid. The hydrogen production for WDHA was 1056.06 cm^3 dm^{-3} and the succinic acid yield was 0.68 g g^{-1} starch, whereas WDHFP strain produced 1689.68 cm^3 dm^{-3} of hydrogen and an ethanol yield of 0.28 g g^{-1} starch. This work represents a promising strategy to improve the exploitation of starchy biomass for the production of biofuels (hydrogen and ethanol) or succinate without the need of a pre-saccharification process.

Keywords: Whole-cell catalysis; α-amylase; starch hydrolysis; biofuels

Gutiérrez-García AK*, Alvarez-Guzmán CL*, De Leon-Rodriguez A. Autodisplay of alpha amylase from Bacillus megaterium in E. coli for the bioconversion of starch into hydrogen, ethanol and succinic acid. Enzyme Microb Technol 2020;134:109477. https://doi.org/10.1016/j.enzmictec.2019.109477. **Equal contribution.*

1. Introduction

The utilization of biomass as feedstock to produce biofuels and bio-based chemicals has recently become an attractive alternative option, due to the depletion of fossil fuels. One of the main feedstocks for biofuel and chemical production is starch-rich biomass, which is easily depolymerized by amylases to generate high yields of glucose [1]. Starch is contained in many staple foods (e.g. potatoes, wheat, corn, rice), therefore it is abundant and consists of a large number of glucose units conjugated with glycosidic bonds [2]. However, although starchy materials are available in abundance, a previous liquefaction and saccharification process of the biomass is required in order to hydrolyze polysaccharides into monosaccharides before its use as carbon source for biofuel or chemical production. Amylases are extracellular enzymes that hydrolyze starch molecules to give such diverse products as dextrins and progressively smaller polymers composed of glucose units. In this regard, α-amylases are endoamylases catalyzing the hydrolysis of internal α-1,4-glycosidic linkages in starch in a random manner, preferably in the immobilized form [3]. They are mainly produced by bacteria belonging to the genus *Bacillus* such as *B. subtilis*, *B. licheniformis*, *B. amyloliquefancies* and *B. stearothermophilus* [4]. Several strategies have been adopted for the construction of the starch-utilizing systems, such as the addition of large amounts of amylases. The use of pure enzymes in biocatalysis has several advantages such as the specificity for selected reactions, simple equipment and procedures [5]. Nevertheless, enzyme production, isolation and purification can be expensive and in addition, the enzymes are often used only once, which increases the cost of the process. On the contrary, the use of microorganisms as whole-cell biocatalysts avoids the purification steps and allows the recycling of the enzymes. The whole-cell biocatalysts have several advantages such as to provide a natural environment for the enzymes preventing conformational changes which could result in the loss of the activity, and microorganisms can efficiently regenerate the enzymes and restock their activity [6]. Among the different autodisplay for whole-cell catalysis, the AIDA (adhesin involved in diffuse adherence) system from *E. coli* has favorable features such as modularity and simplicity. This is an efficient

surface display system for Gram-negative bacteria and is based on the autotransporter secretion pathway. In general, it consists of a cassette that includes the β barrel of AIDA, the recombinant passenger protein to be transported that its coding sequence is simply introduced in frame between the signal peptide and the translocator domain [7]. This autodisplay offers the expression of more than 105 recombinant molecules per single cell, permits the multimerization of subunits expressed from monomeric genes at the cell surface and it results in a superior surface exposure of heterologous passenger [8]. Therefore, the aim of this study was to develop a whole cell biocatalyst for the fermentation of starch to produce hydrogen, ethanol and succinic acid using two *E. coli* strains metabolic engineered in the central carbon metabolism. For this, autodisplay AIDA system was used to express the α-amylase from *B. megaterium* in the cell surface of *E. coli*. The characterization of the enzyme activity and its effectiveness to hydrolyze starch in batch fermentations were assessed.

2. Material and methods

Strains of *E. coli* WDH were generated as previously described by Balderas et al [9]. Briefly, *E. coli* WDH strain (*ΔhycA*, negative regulator of the formate regulon) was used as parental strain [10]. Gene deletion was carried out by transduction with bacteriophage P1 [11]. Strains from a single-gene knockout mutant collection of the nonessential genes of the *E. coli* W3110 were used as donors. Deleted genes were *ldhA*: D-lactate dehydrogenase; *frdD*: fumarate reductase; and *pta*: phosphate acetyltransferase. Gene deletions and resistance loss were confirmed by PCR analysis using standard conditions and the primers described in Table 9.

Table 9. E. coli strains and primers used in this study

Strains Name	**Genotype description**	**Reference**
WDH	*E. coli* (lac^+, gal^+, F^-, λ^-, IN (rrnD-rrnE)1, rph-1) *ΔhycA*	[10]
WDHA	WDH *ΔldhA*	This work
WDHFP	WDH *ΔfrdD Δpta*	This work
Primers Name	**Sequence (5´to 3´)**	**Reference**

ldhA-FCK	TCGCCATCGGTCTACGGGC	[9]
ldhA-RCK	CATAACACCATTAGCGAAAT	
frdD-FCK	TCTGGTTTCCATACAA	
frdD-RCK	TTAGATTGTAACGACACCAATC	
pta-FCK	CTGCACGTTTCGGCAAATCT	This work
pta-RCK	ATTGCGGACATAGCGCAAAT	This work

2.1 Bacterial strain and growth conditions for molecular cloning

E. coli TOP 10 and pGEM-T easy vector were used for subcloning of PCR products and were obtained from Promega. Cells were routinely grown at 31°C in Luria-Bertani (LB) medium, containing 150 µg cm^{-3} of ampicillin. Solid media were prepared by the addition of agar (1.5% w v^{-1}).

2.2 Construction of artificial AIDA system

The design of the *amyA-AIDA* fusion gene was carried out to confer the ability to degrade starch to *E. coli*. For this, the DNA sequences were assembled with the Snapgene software (GSL Biotech LLC, Version 3.3) and MacVector (MacVector, Inc, Version 10.1). The design of the fusion genes for the autodisplay of proteins was based on the AIDA sequence reported by Maurer [7]. For the translocation to the internal membrane, the signal peptide of the toxin of the β-subunit of *Vibrio cholerae* (CtxB) was selected. The autotransporter gene for AIDA was used, which consists of a peptide and a β-barrel (amino acids from 839 to 1286, GenBank: X65022.1). The nucleotide sequences were optimized for their expression in *E. coli* (GenScript, New Jersey, USA). *Asc*I and *Xho*I restriction sites were added to be able to exchange the protein passenger when required. The gapAP1 promoter of the constitutive gapA gene of E. coli was selected as the transcriptional regulator of the amyA-AIDA gene since it works under aerobic and anaerobic conditions. Additionally, at the edges of the *amyA-AIDA* gene, homologous recombination arms were added with target to the *frdABCD* gene of *E. coli*. This construction was synthesized by Biomatik Corp (Delaware, USA) and cloned into pUC57 plasmid

(Thermo Fisher) using the *EcoR*V restriction sites. The resulting plasmid was called as pUC57-AIDA.

The *amyA* gene encoding for α-amylase was amplified by PCR of the *B. megaterium* genome (X07261.1). PCR product was inserted into pGEM-T easy vector from which it was cleaved using the restriction enzymes *Asc*I and *Xho*I before ligation into pUC57-AIDA plasmid, cleaved with the same enzymes to yield the pAIDA-amyA plasmid. The inserted gene was sequenced before its use in further experiments. This construction contained an in-frame fusion protein consisting of the CtxB signal peptide, α-amylase as the passenger, the linker region and the β-barrel autotransporter under the control of the gapAP1 promoter. The pAIDA-amyA plasmid was transformed into *E. coli* WDHA and WDHFP strains by electroporation.

2.3 α-Amylase activity visualization

The α-amylase activity was visually detected from the clearing zone around the colonies grown on starch plates containing 0.3% meat extract, 0.2% soluble starch, 0.5% peptone and 1.5% of agar. The starch agar plate was seeded with individual colonies of *E. coli* WDHA/pAIDA-amyA as well as a negative control *E. coli* WDHA and incubated for 48 h at 37°C. Subsequently, the plate was flooded with iodine reagent (0.01 M I_2-KI solution) and washed with 1 M NaCl.

2.4 Enzymatic reaction

100 cm^3 of LB medium with 200 µg cm^{-3} of ampicillin were inoculated with E. coli WDHA or WDHFP. The cells were cultured at 31°C and 180 rpm until an optical density at 600 nm ($O.D._{600nm}$) of 1 was reached. The cells were centrifuged and washed twice with reaction buffer. All the enzymatic reactions were carried out in triplicate, with a biomass $O.D._{600nm}$ of 10 and using 1% soluble starch as substrate. The reactions were stopped by centrifugation at 13,000 rpm for 5 min and the supernatant was used to measure the enzymatic activity.

2.5 Temperature and pH effect on the biocatalyst activity

The effect of temperature on the biocatalyst activity was determined by incubation in 0.1 M acetate buffer (0.2 M acetic acid and 0.2 M sodium acetate) pH 5.5 containing 1% starch and 5 mM $CaCl_2$ at temperatures ranging from 30 to 70°C at 1400 rpm for 30 min. The enzyme activity was then measured using the 3,5-dinitrosalicylic acid (DNS) method [12]. Meanwhile, the effect of pH on the biocatalyst was determined at different pH (3-6) using the universal Britton and Robinson´s buffer (50 mM phosphoric acid, 50 mM boric acid and 50 mM acetic acid), 1% starch and 5 mM $CaCl_2$ at 55°C and 1400 rpm for 30 min. A reaction, without cells, was used as a negative control.

2.6 Determination of biocatalyst thermostability

The thermal stability of the biocatalyst was determined by measuring the final activities of the biocatalyst after 15 to 60 min of incubation in acetate buffer pH 4.5 and temperature ranging from 55 to 80°C with and without 5 mM $CaCl_2$.

2.7 Effect of calcium on biocatalyst

The effect of different calcium concentrations on the biocatalyst was determined by incubation in Britton and Robinson´s buffer pH 4.5 at 55°C for 30 min with calcium concentration ranging from 0 to 25 mM at 1400 rpm. The negative controls were also evaluated. The activity assayed in the absence of calcium was recorded as 100%.

2.8 Determination of total reducing sugars

The biocatalyst activity was determined by measuring the reducing sugars released during starch hydrolysis by DNS method [12]. The reaction mixture contained 0.05 cm^3 of supernatant from centrifuged samples and 0.15 cm^3 of DNS reagent, the reaction mixture was boiled for 5 min at 100°C and stopped by cooling to room temperature. The absorbance was measured at 595 nm. Glucose served

as the calibration standard for total reducing sugar determination. 1 U was defined as the amount of enzyme that releases 1 µmol of reducing sugars per minute and for the biocatalyst specific activity as one unit of biocatalyst activity per mg of *E. coli* cells.

2.9 Kinetics parameters calculation

The maximum reaction rate (Vmax) and the Michaelis-Menten constant (Km) were calculated using the standard activity assay with different substrate concentrations (0-3% w v^{-1} soluble starch) in Britton and Robinson´s buffer (pH 4.5) at 55°C. Kinetic constants (Vmax and Km) were calculated by the method of Lineweaver-Burk using standard linear regression techniques.

2.10 Dark fermentation of starch by the biocatalyst

Dark fermentation by *E. coli* WDHA and WDHFP strains carrying the pAIDA-amyA plasmid were carried out as follow, pre-inocula were grown in LB medium (10 g dm^{-3} peptone, 5 g dm^{-3} yeast extract, 5 g dm^{-3} sodium chloride) supplemented with 200 µg cm^{-3} of ampicillin under aerobic conditions at 31°C for 16 h. Cells were harvested, centrifuged at 6000 rpm 10 min, washed and inoculated into 120 cm^3 anaerobic serological bottles containing 110 cm^3 of medium B (12.5 mg dm^{-3} $Na_2MoO_4 \cdot 2H_2O$, 15 mg dm^{-3} $MnSO_4 \cdot 7H_2O$, $CoCl_2 \cdot 8H_2O$ 3 mg dm^{-3}, 75 mg dm^{-3} $ZnCl_2$, 4500 mg dm^{-3} $NH_4H_2PO_4$, 11,867 mg dm^{-3} Na_2HPO_4, 125 mg dm^{-3} K_2HPO_4, 100 mg dm^{-3} $MgCl_2 \cdot 6H_2O$, 25 mg dm^{-3} $FeSO_4 \cdot 6H_2O$, 5 mg dm^{-3} $CuSO_4 \cdot 5H_2O$) [13], 0.5 g dm^{-3} $CaCl_2$, 1 cm^3 dm^{-3} trace elements solution [10], 1 g dm^{-3} yeast extract (Difco), 1 g dm^{-3} glucose and 10 g dm^{-3} soluble starch. Cultures were started at pH 7.5 and were incubated at 31°C and 180 rpm. Experiments were carried out in triplicate.

2.11 Analytical methods

The amount of hydrogen produced was measured by the acidic water (pH <2) displacement method in an inverted burette connected to serological bottles with rubber and a needle. The hydrogen percentage on the biogas was determined by gas chromatography using a thermal conductivity detector (Agilent Technologies Wilmington, DE, USA) as described elsewhere [14]. Samples of 1 cm^3 were taken at different times during fermentation; then cells were separated by 5 min centrifugation at 13000 rpm. The supernatants were filtered through a 0.22 µm membrane (Millipore, Bedford, Massachusetts, USA) [14]. Concentrations of soluble metabolites such as succinic acid, lactic acid, acetic acid, formic acid, and ethanol were analyzed by High-Performance Liquid Chromatography (HPLC, Infinity LC 1220, Agilent Technologies, Santa Clara CA, USA) using a Refraction Index Detector, a column Phenomenex Rezex ROA (Phenomenex Torrance, CA, USA) at 60°C, and 0.0025 M H_2SO_4 as mobile phase at 0.5 cm^3 min. An $O.D._{.600nm}$ of 1.0 was equivalent to 0.37 g (dry cell weight, DCW) cells dm^{-3}. Total sugar concentrations were measured using the phenol-sulfuric acid method [15].

2.12 Statistical analysis

All the experiments were carried out in triplicate and the statistical analysis of the treatments was determined by analysis of variance (ANOVA) and unpaired Student's *t*-test. Treatments with $p < 0.05$ were statistically significant. The statistical analysis was performed using Microsoft Excel v16.0 and GraphPad Prism v5.

3. Results and discussion

3.1 Design of AIDA-*amyA* expression system

The pAIDA-amyA plasmid (Fig. 11) contains the fusion gene which consists of 5' to 3' as follows: *Sma*I restriction site, 5' homologous recombination arm with target to

the *frdABCD* gene, *EcoR*I restriction site, promoter of the *gapA* gene of *E. coli*, *Nde*I restriction site, CtxB protein signal peptide, *Asc*I restriction site, passenger gene *amyA* that encodes the α-amylase from *B. megaterium*, *Xho*I restriction site, linker and β-barrel of the AIDA autotransporter of *E. coli*, *Bam*HI restriction site, Rho-independent terminator and homologous 3' recombination arm to the *frdABCD* gene and *Sma*I restriction site.

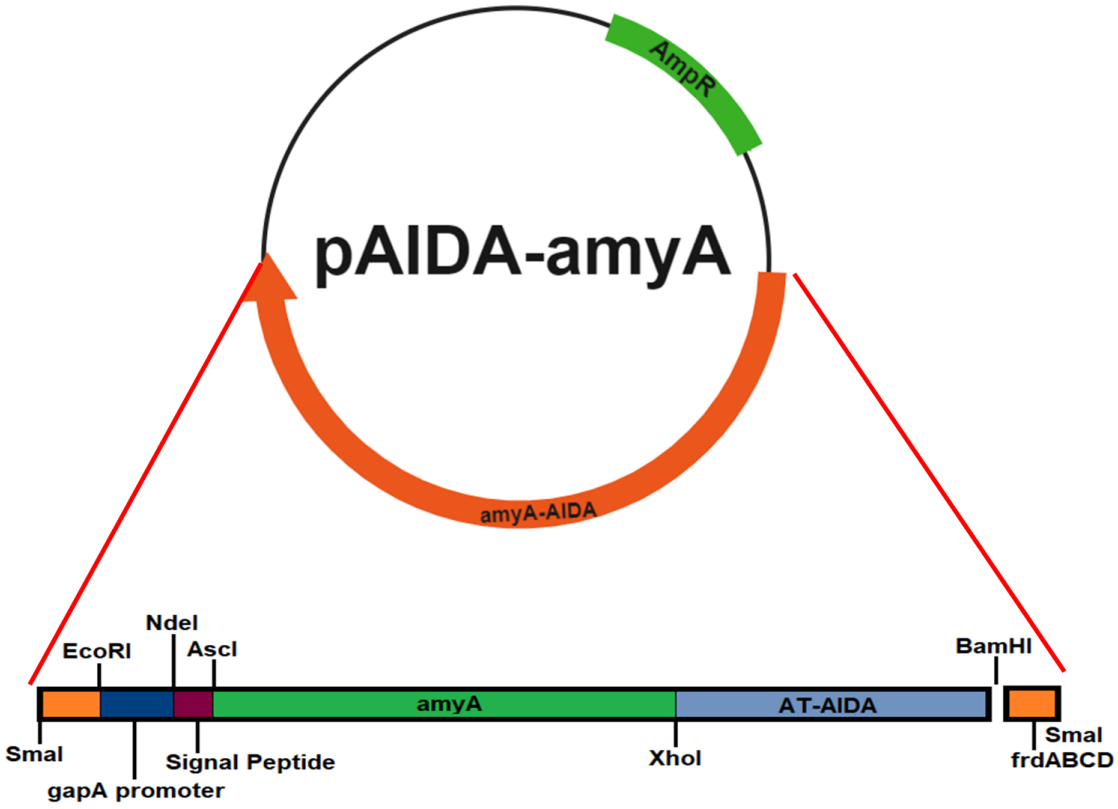

Figure 11. Structure of pAIDA-amyA plasmid used for the autodisplay of α-amylase using the AIDA system of *E. coli*. It consists of a signal peptide (CtxB) derived from *Vibrio cholerae*, followed by the gene encoding for α-amylase (*amyA*) from *B. megaterium*, and the β-barrel (AT-AIDA).

3.2 Detection of amylolytic activity on plate

It was performed a plate assay to determine if the pAIDA-amyA transformants gained amylolytic activity. The amylolytic activity was observed by a halo formation

on a starch-agar plate. Cells carrying the plasmid pAIDA-amyA or the strain without it as control were inoculated on a plate of solid medium containing soluble starch. After incubation for two days at 37°C, the plate was stained with an iodine solution and it is shown in Fig 12. Cells harboring the plasmid pAIDA-amyA hydrolyzed starch and produced a halo strictly around the colony, while no halo formation was observed around the control cells. This assay indicated that the former cells presented amylolytic activity due to the expression of the α-amylase AIDA system.

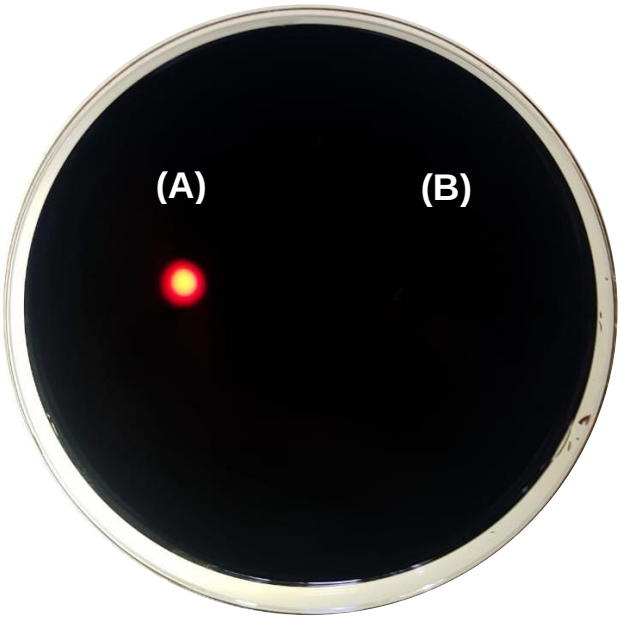

Figure 12. Agar plate test used for detection of the α-amylase activity by: (A) *E. coli* WDHA/pAIDA-amyA strain. (B) Negative control *E. coli* WDHA. The strains were cultured on a starch agar plate for 48 h at 37°C.

3.3 Effect of temperature and pH on biocatalyst activity

The effect of temperature on the biocatalyst activity was determined by assaying enzyme activity using starch (1%) at different temperatures in a range of 30 to 70°C (Fig. 13A). The gradual increase in temperature from 30 to 50°C enhanced the activity of the biocatalyst until 55°C, where the maximum activity was achieved.

The activity at 50 and 60°C showed to be over 70% of the maximum activity. A further increase in temperature caused a detrimental effect on the activity, and the biocatalyst remains active (51%) at 70°C. The optimum temperature (55°C) of the biocatalyst in this study was lower than that reported for the free α-amylase from *B. megaterium* (60°C) [16].

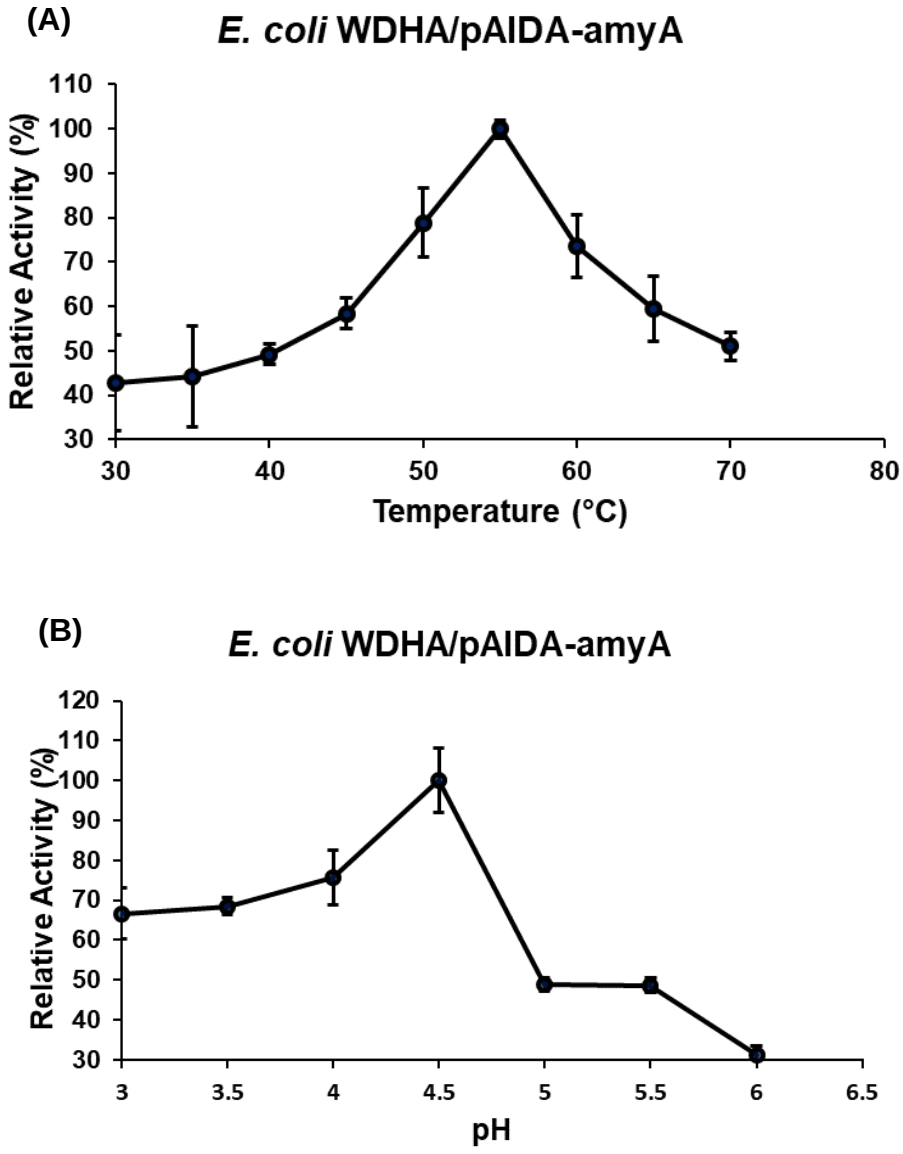

Figure 13. Determination of optimal conditions for the α-amylase biocatalyst. A) Temperature dependence (maximum at 55°C): B) pH dependence (optimal at 4.5). Values are expressed as the mean of the percentage of relative activity. Bars represent means ± standard deviations for three replicates.

The influence of pH on the activity of the biocatalyst was evaluated at various pH values in a range of 3 to 6. As showed in Fig. 13B, the biocatalyst had the maximum activity at pH 4.5, and rapidly declined at pH below 5.0 showing that only about 30% activity was retained at pH 6. The specific biocatalyst activity of 70 U g^{-1} was attained under the optimum conditions of 55°C and pH 4.5. The optimum pH value for the biocatalyst is similar to previous reports using free α-amylases from *Bacillus.* sp. Ferdowsicous (4.5)[19], and *Alicybacillus* sp. A4 (4.2) [21].

3.4 Thermostability of biocatalyst

To determine the thermostability of the biocatalyst used in this work, it was preincubated at different temperatures (55 to 80°C) with and without 5 mM $CaCl_2$ at different time intervals (15 to 60 min). As shown in Fig. 14, when the biocatalyst was incubated for 15 min in absence of calcium at every temperature evaluated, the relative activity was below to 80%.

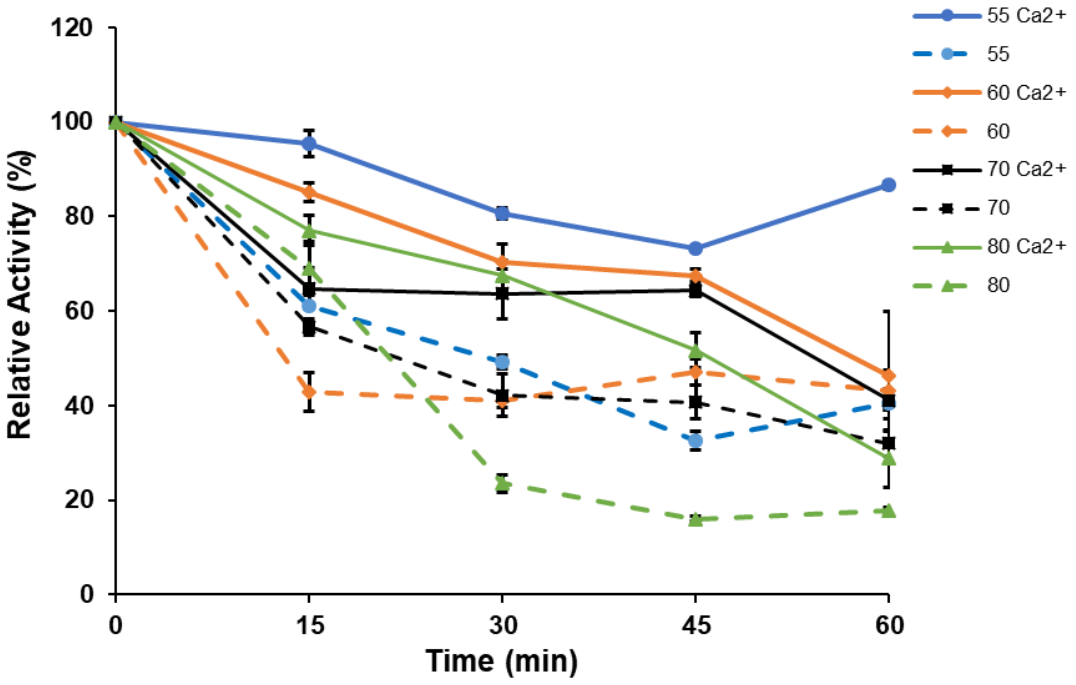

Figure 14. Thermal stability evaluation of the α-amylase biocatalyst. The enzyme was pre-incubated at different temperatures for 15 to 60 min in the presence or absence of 5 mM $CaCl_2$ and the remaining activity was determined incubating the

enzyme at the optimum temperature (55°C for 30 min). Continue line represents reaction mixture with 5 mM $CaCl_2$; the dotted line represents the reaction mixture without $CaCl_2$. Bars represent means ± standard deviations for three replicates.

In addition, a further increase in the incubation time to 60 min without calcium, showed a relative activity of less than 50% at all temperatures. Whereas, in all the conditions supplemented with 5 mM calcium, the biocatalyst retained more than 60% of its relative activity after 45 min of incubation. At 80°C the biocatalyst showed a remaining activity of 17% without calcium and 29% with 5 mM calcium. These results indicated that Ca^{2+} ions are required to maintain the folding and stability of the biocatalyst, which it has also been observed in α-amylases from *B. licheniformis* and *Pyrococcus furiosus* [23, 24].

3.5 Effect of calcium on the biocatalyst activity

The effect of the addition of different Ca^{2+} concentrations on the biocatalyst was also evaluated at 55°C and pH 4.5 (Fig. 15).

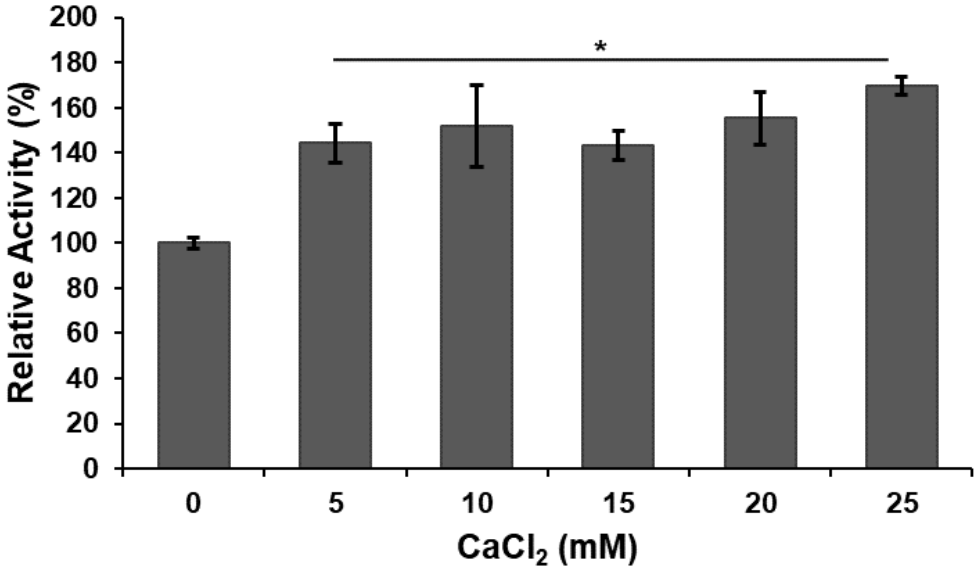

Figure 15. Effect of the addition of different $CaCl_2$ concentrations on the biocatalyst. Bars represent means ± standard deviations for three replicates ($p < 0.05$).

The presence of 5 mM of $CaCl_2$ and upper significatively increased the α-amylase activity almost 50% compared to the control without calcium ($p < 0.05$), and interestingly at 25 mM of $CaCl_2$ compared to 5 mM, the relative activity of the biocatalyst increased 20% ($p < 0.05$). As stated by Prakash and Jaiswal [25], the Ca^{2+} ion confers to the molecule of α-amylase structural rigidity by forming an intramolecular metal-chelate structure, and it is known that the presence of Ca^{2+} ions usually enhances the enzyme activity [22]. For instance, Burhan et al. [23] reported that the addition of 5 mM of $CaCl_2$ increased 110% of the activity of the α-amylase from *Bacillus* sp. ANT-6. While, Asgher et al. [26] observed that when 2 mM Ca^{2+} was added, the activity of the α-amylases from *B. subtilis* JS-2004 increased 117%.

3.6 Kinetic parameters of biocatalyst

Vmax and Km of the biocatalyst were determined according to the Lineweaver-Burk plot based on the hydrolysis reaction of starch using different concentrations between 0-3% w v^{-1} (Fig.16).

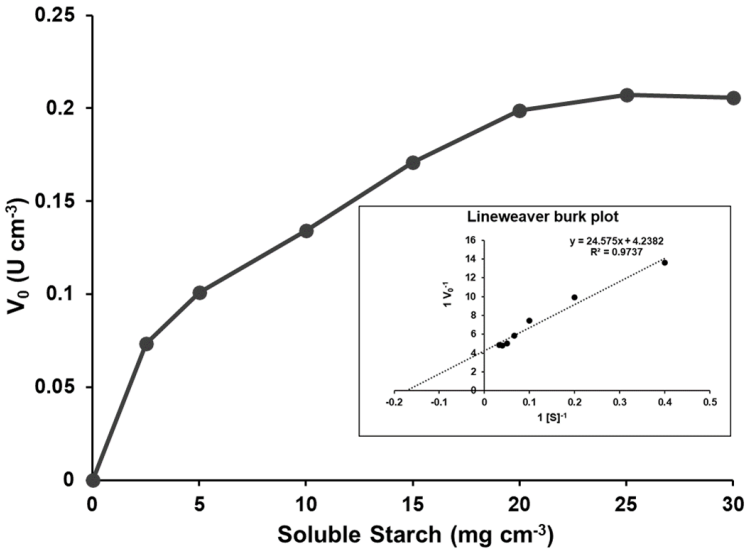

Figure 16. Michaelis-Menten type plot showing the biocatalyst hydrolysis rate using different starch concentrations**.** Bars represent means ± standard deviations for three replicates.

The resultant values were 0.24 U cm^{-3} and 5.8 mg cm^{-3}, respectively. Values for the free amylase were 1.62 U cm^{-3} and 2 mg cm^{-3} as reported by Ghollasi et al. [16]. The increment in the Km value indicates that the immobilized enzyme has a lower affinity for its substrate than the free enzyme. This behavior may be caused by structural changes in the enzyme by its immobilization [27]. This effect was observed by Dey et al. [30] for the biocatalyst of *B. circulans* GRS 313 when it was immobilized on coconut fiber (Table 10).

Table 10. Kinetic parameters of α-amylases by diverse types of immobilizations

Microorganism	Type of biocatalysis	Carrier	Specific activity	Km	Reference
B. amyloliquefaciens	Immobilization	Combi-MOF	-	0.58 µM	[37]
B. circulans GRS 313	Immobilization	Coconut fiber	38.7 U g^{-1}	14.11 mg cm^{-3}	[30]
B. circulans GRS 313	-	Free enzyme	197.8 U mg^{-1}	11.66 mg cm^{-3}	[39]
B. megaterium	-	Free enzyme	-	2 mg cm^{-3}	[16]
E. coli	Whole cell catalysis	Cell surface	70 U g^{-1}	5.8 mg cm^{-3}	This work

Combi-MOF: combi-metal organic frameworks

3.7 Production of valuable products from starch by the whole-cell biocatalyst

To evaluate the effectiveness of the biocatalyst on the bioconversion of starch into hydrogen, ethanol and succinic acid, a set of experiments with the *E. coli* strain WDHA/pAIDA-amyA and WDHFP/pAIDA-amyA were carried out (Fig. 17). Batch cultures with a biocatalyst concentration of 0.037 g dm^{-3} were anaerobically cultivated with 10 g dm^{-3} of soluble starch and 1 g dm^{-3} of glucose as carbon sources.

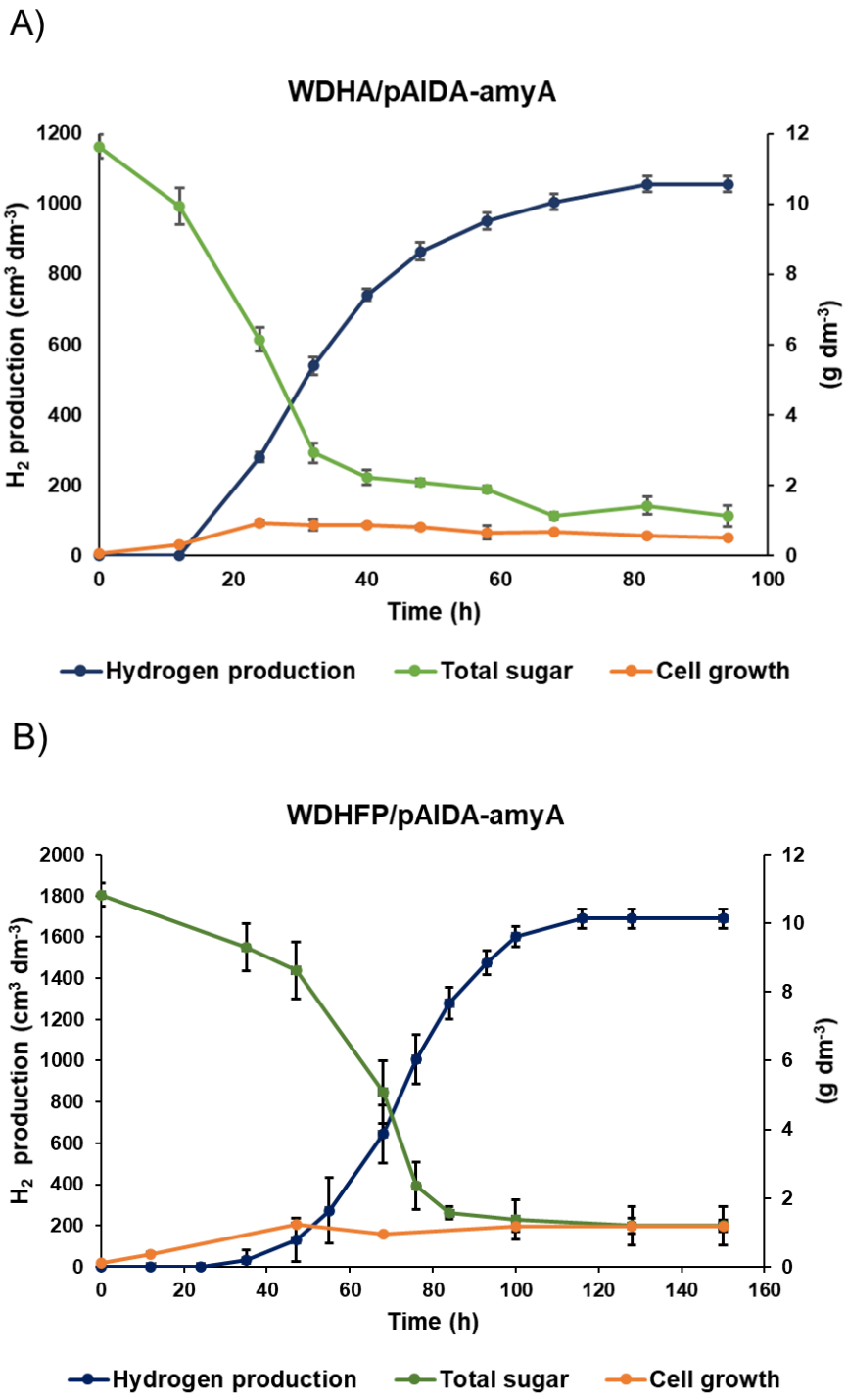

Figure 17. Kinetics of hydrogen production, cell growth and total sugar consumption by WDHA/pAIDA-amyA (A) and WDHFP/pAIDA-amyA (B) using 10 g dm^{-3} of starch and 1 g dm^{-3} of glucose, incubated at 31°C, initial pH 7.5 and 180 rpm. Bars represent means ± standard deviations for three replicates.

The results showed that cells carrying the pAIDA-amyA plasmid were able to utilize the starch in the medium as carbon source. As can be seen in Fig. 17A, strain WDHA/pAIDA-amyA proliferated to reach a maximum biomass of 0.92 g dm^{-3} at 24 h with an adaptation phase of 12 h. During this lag phase, it is assumed that WDHA/pAIDA-amyA strain used the small amount of glucose (1 g dm^{-3}) available in the medium to support the cellular growth and hence the α-amylase synthesis. After this phase, the biocatalyst started to hydrolyze the available starch releasing the reducing sugars needed for cellular growth. Also, with the concomitant cellular growth, hydrogen and several soluble metabolites were produced. Fig. 17A shows that hydrogen production began at 12 h and increased as the total sugar concentration decreased, to reach a maximum hydrogen production of 1056.06 cm^3 dm^{-3} after 82 h of fermentation and a hydrogen production rate of 26.8 cm^3 dm^{-3} h. Metabolic products formed during the fermentation are those typically reported by *E. coli* under anaerobic conditions (Fig. 18). The less abundant product was lactic acid (0.7 g dm^{-3}). Whereas succinic acid was the main metabolite (6.8 g dm^{-3}), followed by acetic acid (1.7 g dm^{-3}) and ethanol (1.3 g dm^{-3}).

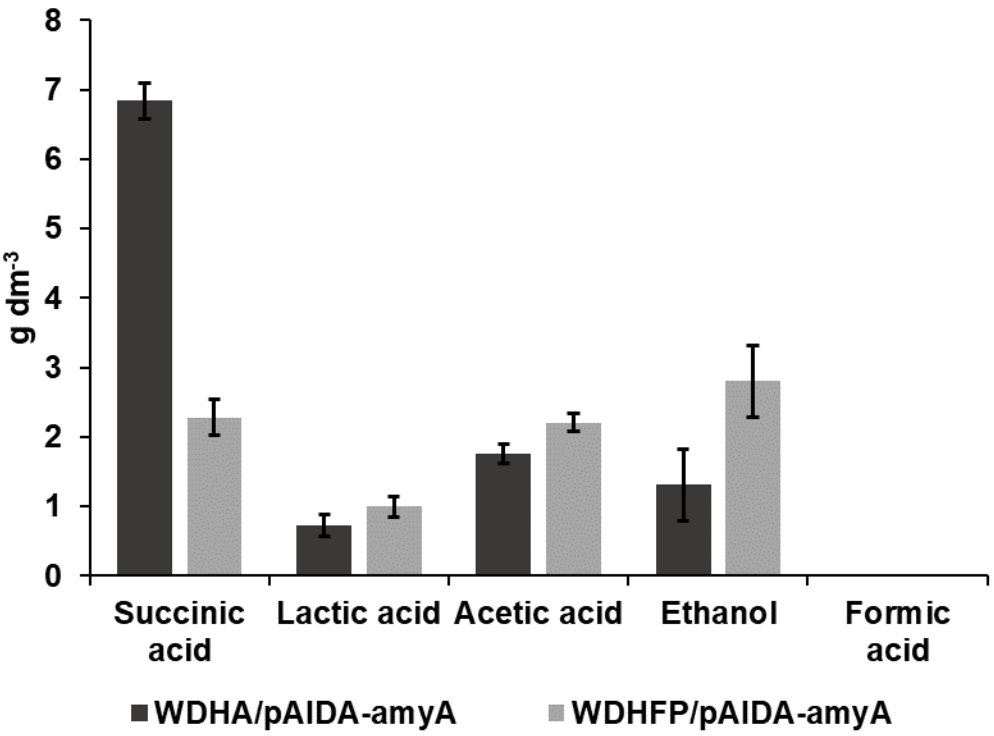

Figure 18. Comparison of fermentative metabolites produced by WDHA and WDHFP *E. coli* strains carrying the pAIDA-amyA plasmid. Bars represent means ± standard deviations for three replicates.

Since, succinic acid production competed with the hydrogen and ethanol production, a WDH *frdD*$^{-}$ *pta*$^{-}$ mutant strain designed as WDHFP was generated and it was transformed with the pAIDA-amyA plasmid to improve the flux of pyruvate to hydrogen and ethanol production. *frd*D gene encodes for the fumarate reductase [32], whereas the *pta* gene encodes for the phosphate acetyltransferase which is the first enzyme of the acetate pathway [33]. In Fig. 7B, it is noticeable that the hydrogen production and cellular growth by WDHFP/pAIDA-amyA strain presented a longer lag phase compared to the WDHA/pAIDA-amyA strain, this behavior can be attributed to the *pta* gene deletion. Chang et al. [33] reported the same effect in their study, where an *E. coli* JP231 strain which has deleted the *pta* gene showed a slower growth rate on various carbon sources compared to those of the wild type strain, the authors attributed this conduct to the perturbation of the pyruvate and acetyl CoA fluxes in the mutant. It has been previously described that

when *pta* gene is deleted in *E. coli*, pyruvate accumulates in the cell, therefore phosphoenol pyruvate (PEP)/pyruvate ratio is reduced, which results in a decrease on the consumption of the sugars transported by the phosphotransferase system (PTS) which requires PEP [33-35]. After 35 h, WDHFP/pAIDA-amyA started the hydrogen production and continued until 116 h of fermentation, where the maximum hydrogen production of 1689.68 cm^3 dm^{-3} was achieved with a production rate of 33.14 cm^3 dm^{-3} h^{-1}. This hydrogen production is significantly higher (60%) ($p < 0.05$) than the one attained by WDHA/pAIDA-amyA as well as the production rate ($p < 0.05$). In Fig. 17B it is observed that the total sugar concentration decreases with the simultaneous hydrogen production increment, hence this data confirms the effectiveness hydrolysis of starch in the medium and its utilization as carbon source. Regarding the metabolites produced in the fermentation, in Fig. 18 it can be observed that the metabolite distribution changed with respect to the profile shown by WDHA/pAIDA-amyA. In this case, the succinic acid reached a concentration of 2.3 g dm^{-3}, whereas acetic acid 2.2 g dm^{-3}, since *frd*D and *pta* genes were deleted from WDHFP/pAIDA-amyA, it was expected to observe no succinic and acetic acid production, however, there are alternative routes for the production of these acids in *E. coli*, which involve the glyoxylate shunt where succinic acid is formed from acetyl Co-A by the isocitrate lyase (aceA), and acetic acid can be produced directly from pyruvate by the pyruvate oxidase (poxB) [36]. Furthermore, ethanol production reached a concentration of 2.8 g dm^{-3}, which is significantly higher ($p < 0.05$) than the production achieved by WDHA/pAIDA-amyA. The results showed that the biocatalyst constructed by using the autodisplay AIDA system is an effective alternative for the use of a complex polysaccharide such as starch by *E. coli* without the requirement of a saccharification pre-treatment. Moreover, the ability of *E. coli* WDHA and WDHFP carrying the pAIDA-amyA plasmid for the production of biofuels like hydrogen and ethanol, as well as succinic acid which is an important building block in the chemical industry, shows the potential for these strains to be applied in industrial processes using starch-rich biomass.

4. Conclusions

The results show that the optimum activity of the biocatalyst by AIDA autodisplay is achieved at 55°C and pH 4.5. *E. coli* strains WDHA/pAIDA-amyA and WDHFP/pAIDA-amyA have the ability to convert starch into valuable products. *E. coli* WDHFP/pAIDA-amyA resulted in the highest hydrogen (1689.68 cm^3 dm^{-3}) and an ethanol yield of 0.28 g g^{-1} starch. While *E. coli* WDHA/pAIDA-amyA produces a succinic acid yield of 0.68 g g^{-1} starch. The expression of hydrolytic enzymes such as α-amylase on the cell surface of metabolic engineered *E. coli* strains promises to be an economic and efficient process for biofuels production.

5. Acknowledgments

Cecilia Alvarez and A. Gutiérrez, thanks to the National Council of Science and Technology (CONACyT) for their scholarships 330870, 297341, respectively. We thank Victor E. Balderas for his technical support.

Funding: This work was supported by CONACyT Ciencias básicas 281700.

6. References

[1] Tanaka, T. and A. Kondo, Cell surface engineering of industrial microorganisms for biorefining applications. Biotechnology advances, 2015. 33(7): p. 1403-1411.

[2] Yamamoto, K., T. Matsumoto, S. Shimada, T. Tanaka, and A. Kondo, Starchy biomass-powered enzymatic biofuel cell based on amylases and glucose oxidase multi-immobilized bioanode. New biotechnology, 2013. 30(5): p. 531-535.

[3] Gupta, R., P. Gigras, H. Mohapatra, V.K. Goswami, and B. Chauhan, Microbial α-amylases: a biotechnological perspective. Process biochemistry, 2003. 38(11): p. 1599-1616.

[4] Nigam, P. and D. Singh, Enzyme and microbial systems involved in starch processing. Enzyme and Microbial Technology, 1995. 17(9): p. 770-778.

[5] De Carvalho, C.C., Enzymatic and whole cell catalysis: finding new strategies for old processes. Biotechnology advances, 2011. 29(1): p. 75-83.

[6] Schüürmann, J., P. Quehl, G. Festel, and J. Jose, Bacterial whole-cell biocatalysts by surface display of enzymes: toward industrial application. Applied microbiology and biotechnology, 2014. 98(19): p. 8031-8046.

[7] Maurer, J., J. Jose, and T.F. Meyer, Characterization of the essential transport function of the AIDA-I autotransporter and evidence supporting structural predictions. Journal of bacteriology, 1999. 181(22): p. 7014-7020.

[8] Bielen, A., R. Teparić, D. Vujaklija, and V. Mrša, Microbial anchoring systems for cell-surface display of lipolytic enzymes. Food Technology and Biotechnology, 2014. 52(1): p. 16-34.

[9] Balderas-Hernandez, V.E., K.P.L. Maldonado, A. Sánchez, A. Smoliński, and A.D.L. Rodriguez, Improvement of hydrogen production by metabolic engineering of *Escherichia coli*: Modification on both the PTS system and central carbon metabolism. International Journal of Hydrogen Energy, 2019.

[10] Rosales-Colunga, L.M., E. Razo-Flores, L.G. Ordoñez, F. Alatriste-Mondragón, and A. De León-Rodríguez, Hydrogen production by *Escherichia coli* ΔhycA ΔlacI using cheese whey as substrate. international journal of hydrogen energy, 2010. 35(2): p. 491-499.

[11] Thomason, L.C., N. Costantino, and D.L. Court, *E. coli* genome manipulation by P1 transduction. Current protocols in molecular biology, 2007. 79(1): p. 1.17. 1-1.17. 8.

[12] Miller, G.L., Use of dinitrosalicylic acid reagent for determination of reducing sugar. Analytical chemistry, 1959. 31(3): p. 426-428.

[13] Davila-Vazquez, G., A. de León-Rodríguez, F. Alatriste-Mondragón, and E. Razo-Flores, The buffer composition impacts the hydrogen production and the

microbial community composition in non-axenic cultures. Biomass and bioenergy, 2011. 35(7): p. 3174-3181.

[14] Lopez-Hidalgo, A.M., A. Sánchez, and A. De León-Rodríguez, Simultaneous production of bioethanol and biohydrogen by *Escherichia coli* WDHL using wheat straw hydrolysate as substrate. Fuel, 2017. 188: p. 19-27.

[15] Masuko, T., A. Minami, N. Iwasaki, T. Majima, S.-I. Nishimura, and Y.C. Lee, Carbohydrate analysis by a phenol–sulfuric acid method in microplate format. Analytical biochemistry, 2005. 339(1): p. 69-72.

[16] Ghollasi, M., K. Khajeh, H. Naderi-Manesh, and A. Ghasemi, Engineering of a *Bacillus* α-amylase with improved thermostability and calcium independency. Applied biochemistry and biotechnology, 2010. 162(2): p. 444-459.

[17] Aguilar, G., J. Morlon-Guyot, B. Trejo-Aguilar, and J. Guyot, Purification and characterization of an extracellular α-amylase produced by *Lactobacillus manihotivorans* LMG 18010T, an amylolytic lactic acid bacterium. Enzyme and Microbial Technology, 2000. 27(6): p. 406-413.

[18] Manning, G.B. and L.L. Campbell, Thermostable α-amylase of *Bacillus stearothermophilus* I. Crystallization and some general properties. Journal of Biological Chemistry, 1961. 236(11): p. 2952-2957.

[19] Asoodeh, A., J. Chamani, and M. Lagzian, A novel thermostable, acidophilic α-amylase from a new thermophilic "*Bacillus* sp. Ferdowsicous" isolated from Ferdows hot mineral spring in Iran: Purification and biochemical characterization. International journal of biological macromolecules, 2010. 46(3): p. 289-297.

[20] Sajedi, R.H., H. Naderi-Manesh, K. Khajeh, R. Ahmadvand, B. Ranjbar, A. Asoodeh, and F. Moradian, A Ca-independent α-amylase that is active and stable at low pH from the *Bacillus* sp. KR-8104. Enzyme and Microbial Technology, 2005. 36(5-6): p. 666-671.

[21] Bai, Y., H. Huang, K. Meng, P. Shi, P. Yang, H. Luo, C. Luo, Y. Feng, W. Zhang, and B. Yao, Identification of an acidic α-amylase from *Alicyclobacillus* sp.

A4 and assessment of its application in the starch industry. Food Chemistry, 2012. 131(4): p. 1473-1478.

[22] Sharma, A. and T. Satyanarayana, Microbial acid-stable α-amylases: characteristics, genetic engineering and applications. Process Biochemistry, 2013. 48(2): p. 201-211.

[23] Burhan, A., U. Nisa, C. Gökhan, C. Ömer, A. Ashabil, and G. Osman, Enzymatic properties of a novel thermostable, thermophilic, alkaline and chelator resistant amylase from an alkaliphilic *Bacillus* sp. isolate ANT-6. Process Biochemistry, 2003. 38(10): p. 1397-1403.

[24] Brown, S.H. and R.M. Kelly, Characterization of amylolytic enzymes, having both α-1, 4 and α-1, 6 hydrolytic activity, from the thermophilic archaea *Pyrococcus furiosus* and *Thermococcus litoralis*. Appl. Environ. Microbiol., 1993. 59(8): p. 2614-2621.

[25] Prakash, O. and N. Jaiswal, α-Amylase: an ideal representative of thermostable enzymes. Applied biochemistry and biotechnology, 2010. 160(8): p. 2401-2414.

[26] Asgher, M., M.J. Asad, S. Rahman, and R. Legge, A thermostable α-amylase from a moderately thermophilic *Bacillus subtilis* strain for starch processing. Journal of food engineering, 2007. 79(3): p. 950-955.

[27] Chang, M.-Y. and R.-S. Juang, Activities, stabilities, and reaction kinetics of three free and chitosan–clay composite immobilized enzymes. Enzyme and Microbial Technology, 2005. 36(1): p. 75-82.

[28] Ahmed, S.A., M.M. El-Sayed, O.-k. Hassan, A. Nabiel, and A. Hossam, Studies on the Activity and Stability of Immobilized *Bacillus acidocaldarius* alpha-amylase. Aust. J. Basic Appl. Sci, 2008. 2(3): p. 466-474.

[29] Talekar, S. and S. Chavare, Optimization of immobilization of Î±-amylase in alginate gel and its comparative biochemical studies with free Î±-amylase. Recent Research in Science and Technology, 2012. 4(2).

[30] Dey, G., V. Nagpal, and R. Banerjee, Immobilization of α-amylase from *Bacillus circulans* GRS 313 on coconut fiber. Applied biochemistry and biotechnology, 2002. 102(1-6): p. 303-313.

[31] Bunch, P.K., F. Mat-Jan, N. Lee, and D.P. Clark, The *IdhA* gene encoding the fermentative lactate dehydrogenase of *Escherichia coli*. Microbiology, 1997. 143(1): p. 187-195.

[32] Westenberg, D.J., R.P. Gunsalus, B. Ackrell, H. Sices, and G. Cecchini, *Escherichia coli* fumarate reductase frdC and frdD mutants. Identification of amino acid residues involved in catalytic activity with quinones. Journal of Biological Chemistry, 1993. 268(2): p. 815-822.

[33] Chang, D.-E., S. Shin, J.-S. Rhee, and J.-G. Pan, Acetate metabolism in a pta mutant of *escherichia coli* w3110: Importance of maintaining acetyl coenzyme a flux for growth and survival. Journal of bacteriology, 1999. 181(21): p. 6656-6663.

[34] Castaño-Cerezo, S., J.M. Pastor, S. Renilla, V. Bernal, J.L. Iborra, and M. Cánovas, An insight into the role of phosphotransacetylase (pta) and the acetate/acetyl-CoA node in *Escherichia coli*. Microbial cell factories, 2009. 8(1): p. 54.

[35] Zhu, J. and K. Shimizu, Effect of a single-gene knockout on the metabolic regulation in *Escherichia coli* for D-lactate production under microaerobic condition. Metabolic engineering, 2005. 7(2): p. 104-115.

[36] Wu, H., Z.-m. Li, L. Zhou, and Q. Ye, Improved succinic acid production in the anaerobic culture of an *Escherichia coli* pflB ldhA double mutant as a result of enhanced anaplerotic activities in the preceding aerobic culture. Appl. Environ. Microbiol., 2007. 73(24): p. 7837-7843.

[37] Salgaonkar, M., S.S. Nadar, and V.K. Rathod, Combi-metal organic framework (Combi-MOF) of α-amylase and glucoamylase for one pot starch hydrolysis. International journal of biological macromolecules, 2018. 113: p. 464-475.

[38] Klapiszewski, Ł., J. Zdarta, and T. Jesionowski, Titania/lignin hybrid materials as a novel support for α-amylase immobilization: A comprehensive study. Colloids and Surfaces B: Biointerfaces, 2018. 162: p. 90-97.

[39] Dey, G., S. Palit, R. Banerjee, and B. Maiti, Purification and characterization of maltooligosaccharide-forming amylase from *Bacillus circulans* GRS 313. Journal of Industrial Microbiology and Biotechnology, 2002. 28(4): p. 193-200.

Chapter 4

Biohydrogen production from cheese whey powder by *Enterobacter asburiae*: Effect of operating conditions on hydrogen yield and chemometric study of the fermentative metabolites

Abstract

In this study, the response surface methodology (RSM) with a central composite design (CCD) was applied to evaluate the effect of temperature, initial pH and cheese whey powder concentration (CWP) on the hydrogen yield and hydrogen production rate by *E. asburiae*. Batch fermentations were performed in 120 cm^3 serological bottles with a working volume of 110 cm^3. The CWP concentration evaluated was in a range of 4.8-55.2 g dm^{-3}, initial pH in a range of 3.4-10.1 and temperatures of 4.8-55.2°C. The maximum hydrogen yield and production rate of 1.19 ± 0.01 mol mol^{-1} lactose and 9.34 ± 0.22 cm^3 dm^{-3} h^{-1}, respectively were achieved at the optimum conditions of 25.6°C, initial pH of 7.2 and 23.0 g dm^{-3} CWP. Moreover, a chemometric analysis was applied for the comparison and visualization of the effect of the different operational conditions on the distribution of the metabolites produced. According to the hierarchical clustering analysis (HCA), the production of acetic acid, formic acid and ethanol was stimulated mainly by low temperature conditions of 15°C, while the production of reduced compounds such as succinic acid, lactic acid and 2,3-butanediol was favored by 30°C, initial pH 6.8 and CWP concentrations ≥ 30 g dm^{-3}.

Keywords: Hydrogen; Dark fermentation; Agro-industrial wastes; RSM; Chemometrics.

Alvarez-Guzmán CL*, Cisneros-de la Cueva S*, Balderas-Hernández VE, Adam Smoliński, De Leon-Rodriguez A. Biohydrogen production from cheese whey powder by *Enterobacter asburiae*: Effect of operating conditions on hydrogen yield and chemometric study of the fermentative metabolites. Energy Reports. 2020;6:1170-1180. https://doi.org/10.1016/j.egyr.2020.04.038. **Equal contribution.*

1. Introduction

The growing energy demand has caused serious environmental problems; this has created the necessity for replacing fossil fuels with sustainable energy sources [1,2]. Hydrogen is now considered as one of the alternatives to fossil fuels. It is preferred over biogas or methane because it is not chemically bound to carbon, therefore the only product of its combustion is water [3,4]. Also, it has a high-energy yield of 122 kJ g^{-1}, which is almost three times higher than hydrocarbon fuels [5]. Although hydrogen has showed potential to be used for clean energy purposes, it is produced mostly by fossil fuel processing technologies; which are expensive and highly polluting due to the operating conditions [6]. Whereas in biological methods, hydrogen is produced by the metabolic transformation of a carbon source by a variety of microorganisms under anaerobic dark fermentation [7]. This process has the advantage of not requiring direct solar input, of accepting a variety of inexpensive substrates, and using a very simple reactor technology [8]. The application of cheap substrates on hydrogen production has been widely studied. Among a wide variety of economic carbon sources, cheese whey (CW), is a promising carbohydrate-rich substrate due to its nutritional characteristics which are beneficial for the hydrogen-producing bacteria [9]. This waste is the by-product obtained from cheese production which represents around 85-90% of the total volume of processed milk. It is estimated that 190 x 106 tons year-1 of CW are produced worldwide [10]. Typical CW mainly contains lactose (4.5-5.0% w v^{-1}), soluble proteins (0.6-1.0% w v^{-1}), lipids (0.4-0.5% w v^{-1}), and mineral salts (6-10% of dried extract) [11]. The low lactose content of CW requires processing large quantities of waste for H_2 gas production which represents an economic disadvantage [12]. On the contrary, cheese whey powder (CWP) is a concentrated and commercial form of CW. The use of CWP eliminates expensive ultrafiltration steps and has other considerable advantages over CW such as reduced volume, concentrated lactose content, long term stability and easy storage and transportation [13]. Several authors have reported the use of this substrate for hydrogen production by strict anaerobes such as *Clostridium saccharoperbutylacetonicum* (2.70 mol mol^{-1} lactose) [3], mixed cultures (1.8 mol

mol^{-1} lactose) [14] or facultative anaerobes such as *Escherichia coli* (1.78 mol mol-1 lactose) [15], or *E. aerogenes* (2.04 mol mol^{-1} lactose) [16]. Among the fermentative hydrogen producers; bacteria belonging to *Enterobacter* genus are attractive due to their high hydrogen evolution rate and because they have two routes to produce hydrogen known as the formate pathway and NADH pathway [17]. Even when *Enterobacter* is a genus widely studied for hydrogen production, to our knowledge, there is only one report addressing the use of a pure culture of *Enterobacter* with CW as substrate [16]. Therefore, the aim of the present study was to evaluate the combined effects of temperature, initial pH and CWP concentration on the hydrogen production by *E. asburiae* applying the RSM. In addition, a chemometric analysis of the experimental data concerning to the metabolites produced was applied with the aim to find and group various fermentation conditions which led to the different distribution of the metabolic products in each experimental set.

2. Materials and methods

2.1 Strain and culture

E. asburiae was cultured at 25°C in agar plates with growth medium containing in g dm^{-3}: 0.25 yeast extract (Difco), 2.75 Bacto-tryptone (Difco), and 20 lactose (Sigma). For batch fermentation experiments, CWP used was purchased from Land O' Lakes Inc. (Minnesota, USA) with a composition as follows: 75% (w w^{-1}) lactose, 14.5% (w w^{-1}) protein, 1.5% (w w^{-1}) lipids and 8.8% (w w^{-1}) mineral salts. Before its use CWP was pasteurized during 30 min at 65°C and chilled 20 min on ice.

2.2 Experimental design

A central composite design (CCD) 2^3 was applied to determine the effect of temperature (°C), initial pH and initial CWP concentration (g dm^{-3}) on the hydrogen yield and production rate by *E. asburiae*. The levels of the evaluated factors are listed in Table 11 and the design matrix with the corresponding hydrogen yield results are presented in Table 12. The empirical second order polynomial model

was applied (Eq. 4) to build surfaces graphs for the hydrogen yield model and to predict the optimum conditions:

$$Y = \beta_0 + \sum_{i=1}^{k} \beta_i X_i + \sum_{i=1}^{k} \beta_{ii} X_i^2 + \sum_{i=1}^{k-1} \sum_{j=2}^{k} \beta_{ij} X_i X_j \quad \text{(Eq. 4)}$$

Where Y is the predicted response, β_0 is the model intercept, β_i is the linear coefficient, β_{ii} is the interaction coefficient, β_{ij} is the interaction coefficient, whereas X_i X_j are independent variables [15]. The experimental design and the statistical analysis were performed with the Design Expert v7.0 software.

Table 11. Experimental range and levels of independent variables evaluated during hydrogen yield optimization.

Variable	Units	-α	-1	0	+1	+α
T	°C	4.8	15	30	45	55.2
pH	-	3.4	4.8	6.8	8.8	10.1
CW	g dm^{-3}	4.8	15	30	45	55.2

Table 12. Experimental conditions of the CCD and the corresponding hydrogen yield results.

Exp.	Temperature (°C)	pH (-)	CWP (g dm^{-3})	Lactose content (g dm^{-3})	H_2 yield (mol mol^{-1} lactose)	H_2 yield (mol mol^{-1} lactose) predicted	H_2 production rate (cm^3 dm^{-3} h^{-1})	H_2 production rate (cm^3 dm^{-3} h^{-1}) predicted
1	30	6.8	4.8	3.6	0.76	0.97	5.65	6.24
2	15	4.8	15	11.3	0.06	0.06	0.33	0.28
3	45	4.8	15	11.3	0	0.00	0	0.08
4	15	8.8	15	11.3	0.71	0.23	2.91	1.32
5	45	8.8	15	11.3	0	0.00	0	0.02
6	30	3.4	30	22.5	0	0.00	0	0
7	4.8	6.8	30	22.5	0	0.02	0	0.17
8	30	6.8	30	22.5	1.22	1.22	10.23	10.43
9	30	6.8	30	22.5	1.23	1.22	10.59	10.43
10	55.2	6.8	30	22.5	0	0	0	0
11	30	10.1	30	22.5	0	0.02	0	0.11
12	15	4.8	45	33.8	0.01	0.00	0.12	0.09
13	45	4.8	45	33.8	0	0.02	0	0.12
14	15	8.8	45	33.8	0.07	0.05	1.80	1.02
15	45	8.8	45	33.8	0.05	0.04	0.10	0.14
16	30	6.8	55.2	41.4	0.80	0.68	6.96	6.20

2.3 Batch fermentations

Pre-inocula of *E. asburiae* were grown in liquid medium containing 20 g dm^{-3} lactose, 0.25 g dm^{-3} yeast extract (Difco) and 2.75 g dm^{-3} Bacto-tryptone. Cells were harvested, washed and inoculated into 120 cm^3 serological bottles (Prisma, DF, Mex) containing 110 cm^3 of production medium with the corresponding CWP concentration according to Table 12. Production medium consisted in g dm^{-3} of:

0.25 yeast extract (Difco) and 2.75 Bacto-Tryptone (Difco) supplemented with 1 cm^3 dm^{-3} of trace elements solution with a composition in g dm^{-3}: 0.015 $FeCl_3 \cdot 4H_2O$, 0.00036 $Na_2MoO_4 \cdot 2H_2O$, 0.00024 $NiCl_2 \cdot H_2O$, 0.0007 $CoCl_2 \cdot 6H_2O$, 0.0002 $CuCl_2 \cdot 2H_2O$, 0.0002 Na_2SeO_3 and 0.01 $MgSO_4$. Cultures were started at an initial optical density at 600 nm wavelength ($O.D._{600nm}$) of 0.5. Initial pH was adjusted in each serological bottle according to the experimental design (Table 12). Silicon stoppers and screw caps were used to avoid gas leakage from the bottles.

2.4 Analytical methods

The volume of biogas produced was measured periodically by the acidic water (pH < 2) displacement method in an inverted burette connected to the serological bottles using a rubber tubing and a needle. The percentage of hydrogen in the gas was measured using a gas chromatograph (6890N, Agilent Technologies), equipped with a thermal conductivity detector and using an Agilent J&W HP-Plot Molesieve column (30 m x 0.32 mm i.d. 12 µm film thickness). Liquid samples of 1 cm^3 were taken, diluted and filtered using a 0.22 µm syringe filter. The final concentration of lactose, formic acid, and acetic acid were determined using a High-Performance Liquid Chromatograph (HPLC, Infinity LC 1220, Agilent Technologies) with a refraction index detector (Agilent Technologies) and a column Rezex ROA (Phenomenex, Torrance at 60°C, and 0.0025 M H_2SO_4 as mobile phase at 0.05 cm^3 min^{-1}. The final concentrations of ethanol and 2,3-butanediol were determined using a gas chromatograph (GC, 6890N, Agilent Technologies) with a flame ionization detector (Agilent Technologies). The capillary column HP-Innowax (30 m x 0.25 µm film thickness Agilent Technologies) was used to perform the analysis.

2.5 Data organization and methods of data exploration

The studied experimental data set was organized into matrix **X** (16 x 6), which rows represent 16 objects (experiments of hydrogen production under various conditions), whereas the columns correspond to the studied parameters

(metabolites produced in CWP fermentation), listed in Table 13. The studied data was centered and standardized before principal component analysis (PCA) [19–23], and hierarchical clustering analysis (HCA) [20,24–26] models were constructed. The PCA and HCA are the methods most often applied in data exploration. PCA allows reducing data dimensionality and visualization of the studied data by projection of objects and parameters on the space defined by the score and loading vectors [19–23]. It enables to decompose the data of a matrix **X** (m x n) into two matrices, **S** (m x fn) and **D** (n x fn), called score and loading matrices, respectively, where m and n denote the number of objects and parameters, respectively, whereas fn denotes the number of significant factors called the Principal Components (PCs). The hierarchical clustering analysis [20,24–26] allows investigating the similarities between studied objects in the parameter space, and between the parameters in the object space. The results of HCA are presented in the form of dendrograms differing in terms of the applied similarity measure between objects, as well as the way the similar objects are connected. The linkage methods include the single linkage, average linkage, complete linkage, centroid linkage and Wards linkage method [24,25]. To complement the analysis of HCA and to determine the relationships between objects in the parameters space and parameters in the objects space, a color map of the experimental data enabling a more in-depth interpretation of the data structure, and parallel tracing the similarities between studied objects and parameters was employed [26,27].

Table 13. Matrix **X** (16 x 16) of the metabolites formed during the fermentations by *E. asburiae* under different experimental conditions.

Objects	Parameters					
Experiment	**Lactic acid (g dm^{-3})**	**Succinic acid (g dm^{-3})**	**Formic acid (g dm^{-3})**	**Acetic acid (g dm^{-3})**	**2, 3-butanediol (g dm^{-3})**	**Ethanol (g dm^{-3})**
1	0.034	0.098	0.144	0.421	0.509	0.824
2	0.033	0.162	0.255	0.665	0.051	5.021
3	0.068	0.394	0.532	0.447	0.082	0.625
4	0.033	0.321	0.376	0.773	0.931	6.036
5	0.097	0.296	0.052	0.507	0.901	0.191
6	0.059	0.000	0.000	0.000	0.000	0.715
7	0.056	0.193	0.000	0.037	0.000	0.511
8	0.095	0.601	0.000	0.773	5.422	1.717
9	0.098	0.713	0.000	0.665	5.732	1.610
10	0.058	0.000	0.000	0.000	0.000	0.000
11	0.031	0.000	0.000	0.000	0.000	0.000
12	0.033	0.280	0.407	0.510	0.058	5.326
13	0.053	0.053	0.038	0.614	0.082	0.355
14	0.050	0.492	0.501	0.200	0.964	6.347
15	0.051	0.043	0.065	0.451	0.112	0.782
16	0.082	0.698	0.366	0.608	5.379	1.429

3. Results and discussion

3.1 Hydrogen yield under different operational conditions

The RSM was applied with the aid of a CCD in order to obtain the optimum combined effect of temperature, initial pH and CWP concentration on hydrogen yield by *E. asburiae*. In Table 12, the different experimental conditions evaluated and the respective hydrogen yield results are shown. According to the analysis of the Box-Cox plot, a data transformation was required to ensure that the model

meets the assumptions required for analysis of variance (ANOVA). Therefore, a Natural Log transformation was applied. The ANOVA of the optimization study (Table 14) showed that hydrogen yield was significantly affected ($p < 0.05$) by the quadratic terms of temperature and pH.

Table 14. ANOVA of the hydrogen yield obtained under different experimental conditions determined by the experimental design.

Source	Sum of Squares	Degrees freedom	Mean Square	*F*-value	*p*-value
Model	51.04	9	5.67	6.98	0.0140
T	3.27	1	3.27	4.03	0.0915
pH	1.96	1	1.96	2.41	0.1713
CWP	0.16	1	0.16	0.20	0.6683
T*pH	0.44	1	0.44	0.54	0.4884
T*CWP	2.97	1	2.97	3.66	0.1043
pH*CWP	0.025	1	0.025	0.031	0.8668
T^2	24.20	1	24.20	29.80	0.0016
pH^2	24.20	1	24.20	29.80	0.0016
CWP^2	0.19	1	0.19	0.24	0.6417
Residual	4.87	6	0.81		
Pure Error	1.084×10^{-4}	1	1.08×10^{-4}		
Cor Total	55.92	15			

As showed in Table 12, the highest hydrogen yield (1.23 ± 0.01 mol H_2 mol^{-1} lactose) was reached by the central points (Exp. 8 and 9) of the experimental design at 30°C, pH 6.8 and 30 g dm^{-3} of CWP. Experiments 1 and 16 with the axial points of CWP concentration, 30°C and initial pH 6.8, together with the experiment 4, showed hydrogen yields in a range of 0.71-0.80 mol mol^{-1} lactose. Moreover, lower yields in a range of 0.01-0.07 mol mol^{-1} lactose were obtained by experiments 2, 12 and 14 at 15°C along with experiment 15 at 45°C. On the other

hand, the pair of experiments 7 and 10 and 6 and 11 with the axial points of temperature and pH, respectively, showed no hydrogen production. The same was observed in experiments 3, 5 and 13 at 45°C.

The final second-order-polynomial in terms of the coded factors after the natural Log transformation is expressed as follows:

$$Ln\,(YH_2 + 0.01) = 0.21 - 178.57\,T + 0.38\,pH - 0.11\,CWP - 0.24\,T * pH + 0.61\,T * CWP + 0.056\,pH * CWP - 1.62\,T^2 - 1.62\,pH^2 - 0.14\,CWP^2 \quad \text{(Eq. 5)}$$

Which represents the hydrogen yield (YH_2) as a function of the evaluated variables in the experimental region. The value of the regression coefficient (R^2=0.91) revealed that the regression model was an accurate representation of the experimental data, which can explain 91.0% of the variability of the dependent variable. This model was used to construct the response surface and contour plots for hydrogen yield (Fig. 19). Fig. 19 A-B, shows the interaction of temperature and pH on hydrogen yield when the CWP concentration is fixed at 30 g dm^{-3}. It is possible to observe that the highest hydrogen yield is achieved at a small range of temperature and pH. When temperature and pH are raised from 15 to 30°C and 4.8 to 7, respectively, an increase in hydrogen yield is observed. However, a further increase to 35°C and pH 8 leads to a marked drop on hydrogen yield. In Fig. 19 C-F is easy to observe that increasing CWP concentration does not increase the hydrogen yield.

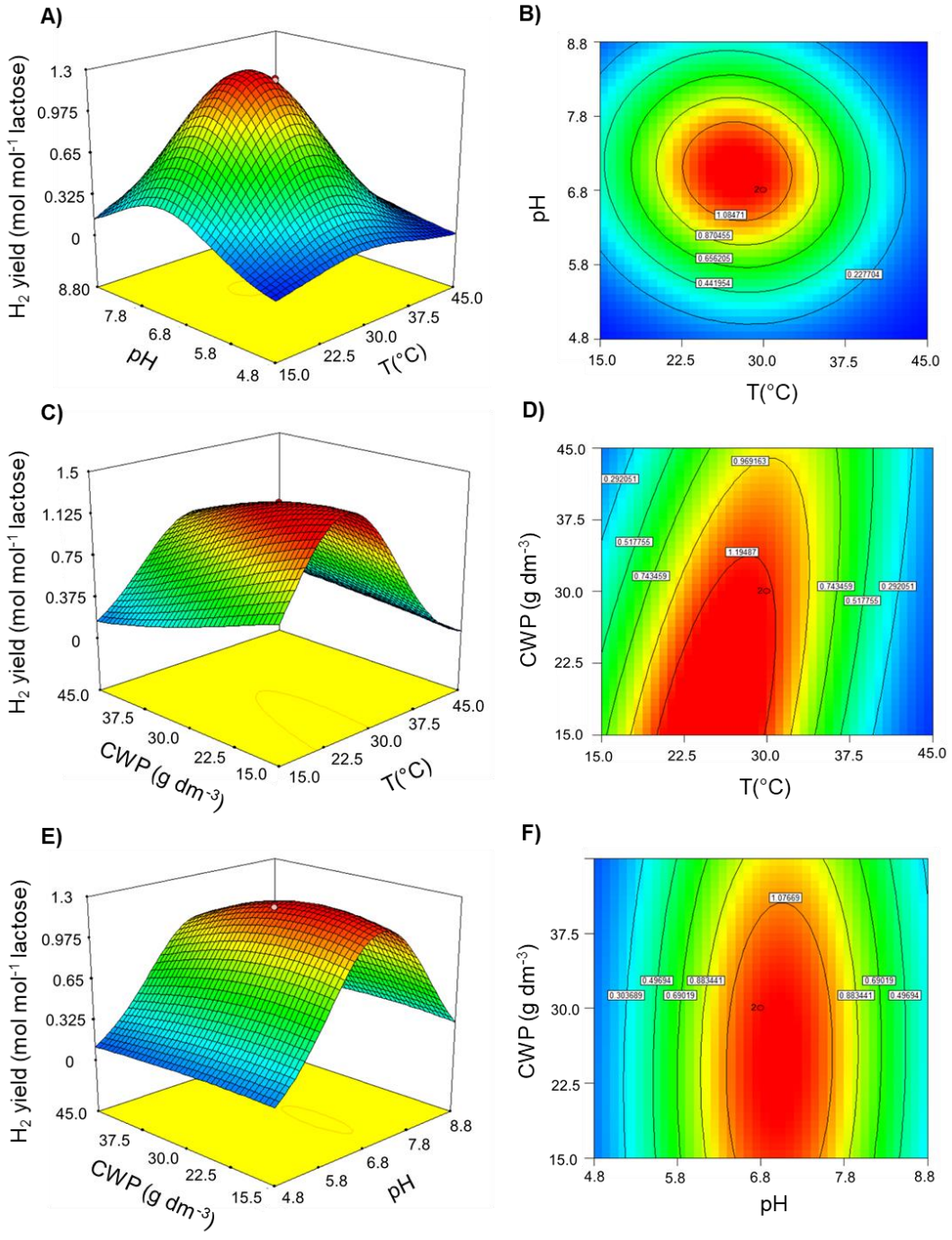

Figure 19. Different response surface and contour plots of the effects of temperature, initial pH and CWP concentration on hydrogen yield by *E. asburiae*. A-B) CWP concentration was fixed at 30 g dm^{-3}, C-D) initial pH was maintained at 6.8 and in E-F) temperature was kept at 30°C.

Fig. 19 C-D shows that the highest hydrogen yields are achieved at CWP concentrations in a range of 15 to 35 g dm^{-3} as long as temperature is maintained in a range of 22.5-30°C. The same effect is observed in Fig. 19 E-F, where initial pH must be maintained at slightly acidic to neutral conditions of 6.5-7.5. This effect can be attributed to a possible substrate inhibition at CWP concentrations above 15 g dm^{-3}. High substrate concentrations trigger the accumulation of organic acids that are inhibitory to hydrogen-producing bacteria. Although in this study, the analysis of soluble metabolites produced at each experimental condition showed that the organic acids are synthesized at a low extent compared to ethanol and 2,3-butanediol, being the alcohols, the most abundant liquid metabolites produced (Table 13). Another possible reason, could be the high osmolality caused by the highest CWP concentrations, resulting in growth inhibition and incomplete substrate conversion [28]. The pH is considered a key variable in dark fermentation processes, since it can directly affect the hydrogenase activity and metabolic pathways. The optimum pH range observed in this study is in agreement with the optimum range for hydrogen production using CW as reported by several authors. For instance, De Gioannis et al. [29] evaluated different pH values in the range of 5.5-8.5 using activated sludge and concluded that the optimum pH range for hydrogen production was between 6.5-7.5. Ferchichi et al. [3] evaluated the initial pH in a range of 5-10 and found that hydrogen yield peaked at an initial pH 6. At the same time, operating temperature also has a strong influence on fermentative hydrogen production. Wang and Wan [30] states that in an appropriate range, increasing culture temperature increases the ability of hydrogen-producing bacteria to evolve hydrogen during the fermentative process. It can be explained by the enhancement of the microbial metabolism, but an excessive temperature level affects the cell membrane integrity [31,32] which inactivates the microorganism and in turn hydrogen production. Several authors have reported different hydrogen yields which can be compared with the highest yield of 1.23 ± 0.01 mol mol^{-1} lactose achieved in this work. For instance, Rai et al. [16] evaluated the hydrogen production at 30°C by *E. aerogenes* MTCC 2822 using diluted raw CW at several lactose concentrations in a range of 5-40 g dm^{-3} at initial pH 6.8, achieving

hydrogen yields in a range of 0.77-2.04 mol mol^{-1} lactose. Vasmara and Marchetti [14] reported a hydrogen yield of 1.81 mol mol^{-1} lactose at 35°C, initial pH 8.0 and 51 g dm^{-3} lactose using scotta permate. Gioannis et al. [29] evaluated different pH set-up values in a range of 5.5-8.8 achieving different hydrogen yield values from 0.04-2.6 mol mol^{-1} lactose using anaerobic activated sludge. While Blanco et al. [33] reported a maximum hydrogen yield of 1.4 mol mol^{-1} lactose at 25°C with synthetic CW at an initial chemical oxygen demand (COD) of 24 g dm^{-3}. The yield achieved by *E. asburiae* is within the range reported by these authors. The theoretical hydrogen yield using lactose is 8 mol mol^{-1} lactose, however lower yields are achieved in practice. This stoichiometric yield is only attainable under near-equilibrium conditions, which implies very slow hydrogen rates and/or at very low hydrogen partial pressure (HPP) [34]. As HPP increases, hydrogen synthesis decreases and metabolic pathways shifts towards production of more reduced substrates, such as lactate and alcohols [34,35]. In this study, high substrate concentrations used may have provided high HPP which contributed to the low hydrogen yields achieved by the experiments with high level of CWP concentration (exp. 12, 13, 14, 15 and 16). At a metabolic level, low hydrogen yields indicate the presence of hydrogen competing pathways. In bacteria belonging to *Enterobacter* genus, hydrogen production is carried out through two ways, one is dependent of the cleavage of pyruvate into formate and Acetyl-CoA and the other one depends on the oxidation of NADH [17]. Therefore, the conversion of phosphoenol-pyruvate and pyruvate into reduced acids such as succinate and lactate, as well as alcohols such as ethanol and 2,3-butanediol, reduces significantly the hydrogen yield. In Table 13, the different soluble metabolites produced by *E. asburiae* at each experimental condition are shown. As noted, 2,3-butanediol and ethanol are the most abundant metabolites. Therefore, the hydrogen yield by *E. asburiae* was affected by the synthesis of these compounds. This could be further improved applying metabolic engineering over these competing pathways.

3.2 Hydrogen production rate under different operating conditions

Along with hydrogen yield, the rate of hydrogen production is another relevant variable to be evaluated in fermentative hydrogen production processes. Together, these two variables indicate the feasibility of the process. Thus, hydrogen production rate was also chosen as a response variable. Table 12 shows the different experimental conditions evaluated with the corresponding hydrogen production rate results. In the same way as with the hydrogen yield model, a natural Log transformation was applied to ensure that the model meets the assumptions required for ANOVA. The factors that significantly ($p < 0.05$) affected the hydrogen production rate were the linear and quadratic effect of temperature, and the quadratic effect of pH (Table 15).

Table 15. ANOVA of the hydrogen production rate obtained under different experimental conditions determined by the experimental design.

Source	Sum of Squares	Degrees freedom	Mean Square	*F*-value	*p*-value
Model	50.27	9	5.59	7.69	0.0110
T	4.43	1	4.43	6.10	0.0484
pH	1.62	1	1.62	2.24	0.1855
CWP	$3.83x10^{-4}$	1	$3.83x10^{-4}$	$5.27x10^{-4}$	0.9824
T*pH	1.40	1	1.40	1.93	0.2140
T*CWP	0.39	1	0.39	0.54	0.4888
pH*CWP	0.094	1	0.094	0.13	0.7317
T^2	24.68	1	24.68	33.99	0.0011
pH^2	24.68	1	24.68	33.99	0.0011
CWP^2	0.31	1	0.31	0.43	0.5375
Residual	4.36	6	0.73		
Pure Error	$5.86x10^{-4}$	1	$5.86x10^{-4}$		
Cor Total	54.63	15			

The highest hydrogen production rate (10.41 ± 0.25 cm^3 dm^{-3} h^{-1}) was achieved at the central points of the experimental design (Exp. 8 and 9) at 30°C, initial pH 6.8 and 30 g dm^{-3} CWP. While a decrease in the rates was observed in experiments 1 and 16 (5.65 and 6.96 cm^3 dm^{-3} h^{-1}, respectively) at the axial points of CWP concentration (4.8 and 55.2 g dm^{-3}), 30°C and initial pH 6.8. Lower rates in a range of 0.10-2.91 cm^3 dm^{-3} h^{-1} were obtained in experiments 12, 14 and 15 using 45 g dm^{-3} CWP and in experiments 2 and 4 at 15°C and 15 g dm^{-3} CWP. Whereas the absence of hydrogen production was observed in the experiments 7, 10, 6 and 11 with the axial points of temperature and pH, as well as for experiments 3, 5 and 13 at a high temperature of 45°C.

The final second-order-polynomial in terms of the coded factors after the natural Log transformation is expressed as follows:

$$Ln\,(HPR + 0.11) = 2.36 - 0.57\,T + 0.34\,pH - 0.0053\,CWP - 0.42\,T * pH + 0.22\,T * CWP + 0.11\,pH * CWP - 1.63\,T^2 - 1.63\,pH^2 - 0.18\,CWP^2 \quad \text{Eq. 6}$$

Eq. 6 represents the hydrogen production rate (*HPR*) as a function of the evaluated variables in the experimental region. The value of regression coefficient (R^2=0.92) revealed that the model was an accurate representation of the experimental data, which can explain 92% of the variability of the dependent variable. This model was used to construct the response surface and contour plots for hydrogen production rate (Fig. 20).

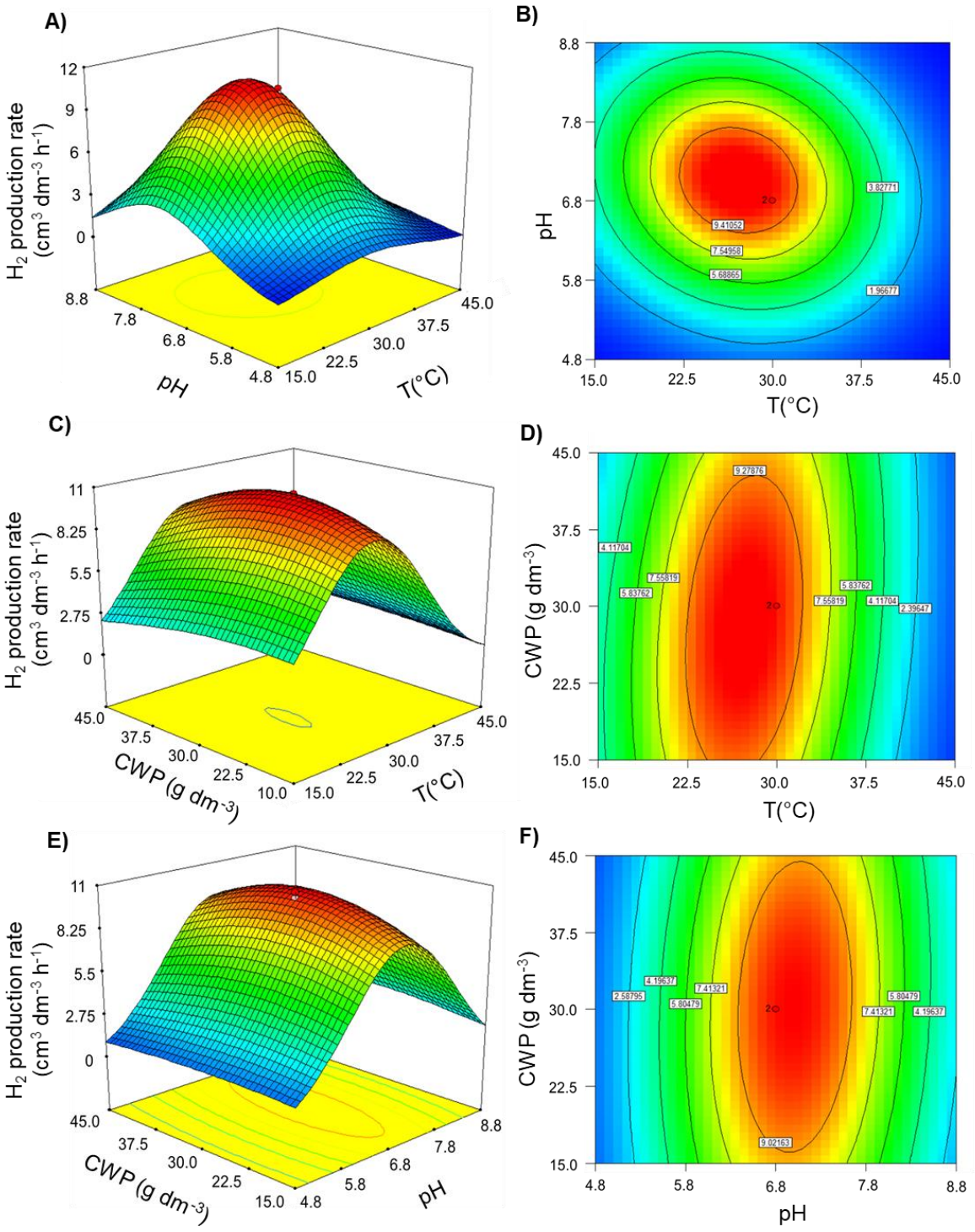

Figure 20. Different response surface and contour plots of the effects of temperature, initial pH and CWP concentration on hydrogen production rate by *E. asburiae*. A-B) CWP concentration was fixed at 30 g dm^{-3}, C-D) initial pH was maintained at 6.8 and in E-F) temperature was kept at 30°C.

As noted in Fig. 20, the effect of temperature, initial pH and CWP concentration followed the same trend as in the hydrogen yield model. Fig. 20 A-B shows that the highest production rate is achieved when temperature and pH are increased to 30°C and 7, respectively. Temperature has a direct effect on the reaction rate; an often-cited general rule states that a 10°C rise in temperature will double the rate of reactions [36]. Therefore, the increase from 15°C to 30°C resulted beneficial for the hydrogen production rate. However, when temperature is increased above 30°C a decline in the curve was observed. At higher temperatures than the optimum value, some essential enzymes and proteins associated with cell growth or hydrogen production (hydrogenases) may be inactivated (or denatured) [37]. As mentioned before, pH is another factor that influence the activity of the hydrogenases and the metabolic functions of bacteria. Low pH values give poor hydrogen production rates since these values have an initial inhibitory effect on bacteria causing longer lag phases [38]. Fig. 20 E-F shows that when initial pH increases to a range of 6.5-7, a maximum hydrogen production rate is achieved, moreover, it is evident that the increase of substrate concentration from 15 to 45 g dm^{-3} CWP shows no difference on hydrogen production rate under the optimum initial pH range. However, CWP concentrations below 15 g dm^{-3} or exceeding 45 g dm^{-3} lead to a fall in the production rate. According to Lu et al. [39], substrate concentration below the optimum value always leads to low hydrogen production rate, hydrogen content and biomass concentration, on the other hand, when substrate concentration is higher than its optimum value, hydrogen-producing microorganisms could overproduce volatile fatty acids and alcohols leading to decreased hydrogen production rates. In literature, different hydrogen production rates from CW are reported using different fermentation configurations, conditions and inocula. The maximum hydrogen production rate achieved in this work is within the range of the reported values in the literature. For instance, Kargi et al. [12] evaluated the hydrogen production from CWP by anaerobic sludge in batch serological bottles, where the highest hydrogen production of 3.46 cm^3 dm^{-3} h^{-1} was obtained at the thermophilic conditions of 55°C and pH 7, whereas in this study, the highest production rate of 10.59 cm^3 dm^{-3} h^{-1} was achieved. Ghimire et al. [40] evaluated

the co-fermentation of CW with buffalo manure as buffering agent in a semi-continuous reactor at 55°C and pH 4.8-5.0 reporting a production rate of 8.97 cm^3 dm^{-3} h^{-1}. Likewise, Lopes et al. [41] reported the co-fermentation of CW and crude glycerol in an expanded granular sludge bed at 30°C and pH 8.7-9.0 reaching a higher production rate of 42.5 cm^3 dm^{-3} h^{-1}. Perna et al. [42] observed a similar rate of 41.66 cm^{-3} dm^{-3} h^{-1} using an up-flow anaerobic packed bed reactor at 30°C and pH 5.6 with a mixed culture.

3.3 Optimization and validation of the optimum conditions

The simultaneous optimization of the two response variables evaluated in this study was carried out using the Design Expert v7.0 software. The maximum hydrogen yield and hydrogen production rate predicted by the model were 1.37 mol mol^{-1} lactose and 10.79 cm^3 dm^{-3} h^{-1}, respectively at the optimum conditions of 25.6°C, initial pH 7.2 and 23.0 g dm^{-3} CWP. The accuracy of the model was validated by performing an additional set of batch fermentations by triplicate under the optimum conditions (Fig. 21). The experimental results obtained for hydrogen yield and a hydrogen production rate were 1.19 ± 0.01 mol mol^{-1} lactose and 9.34 ± 0.22 cm^3 dm^{-3} h^{-1}, respectively, which are close to the values predicted by the model, indicating that RSM was a useful tool to optimize the response variables.

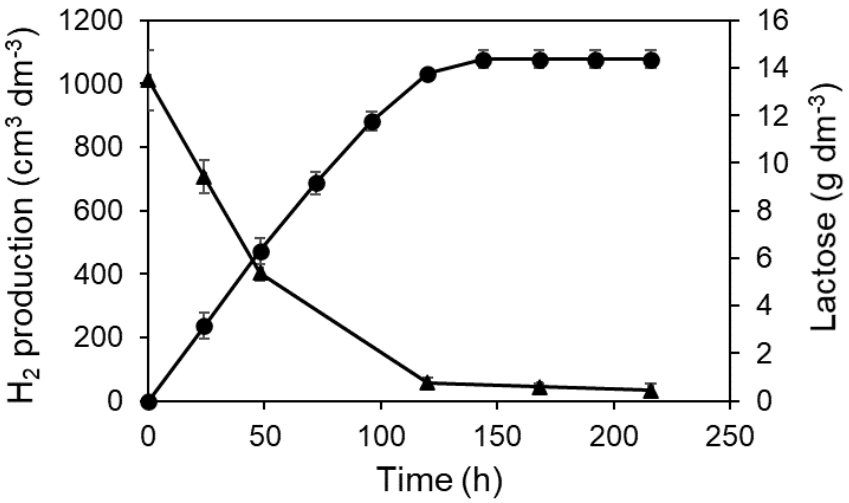

Figure 21. Hydrogen production (circles) and lactose consumption (triangles) kinetics by *E. asburiae* under the optimum conditions of 25.6°C, initial pH 7.2 and 23.0 g dm^{-3} CWP. The error bars indicate standard deviations.

3.2 Production of soluble metabolites

The main soluble metabolites produced in the different experimental conditions were succinic acid, lactic acid, formic acid, acetic acid, 2,3-butanediol and ethanol (Table 13). The distribution of these metabolic products was certainly influenced by the combined effect of the operating conditions. The RSM is an effective tool to evaluate simultaneously the effect of multiple factors on dark fermentation [30], however, the analysis of the data set can be improved by the application of chemometric tools such as HCA and PCA. These techniques allow an easy statistical and visual interpretation of complex data relationships frequently encountered in multivariate analysis, since they describe the similarities and differences between the set of variables [31]. Therefore, the production of the soluble metabolites was analyzed using these chemometric tools.

3.3.1 Chemometric analysis of the soluble metabolites produced during hydrogen production

3.2.1.1 PCA

The PCA model with four significant principal components (PCs) described 96.67% of the total data variance. Score plots and loading plots obtained as a result of the analysis are presented in Fig. 22 PC1, which described 47.66% of the total variance was constructed mainly due to the differences between the object 8 (30°C, pH 6.8 and 30 g dm^{-3} CWP) and all the remaining objects (Table 13). Moreover, along the PC1 the objects can be divided into three clusters and one non-grouped object 5 (45°C, pH 8.8 and 15 g dm^{-3} CWP). The first cluster was composed of objects 2, 4, 9 and 11. The second cluster was composed of the objects 1, 3, 6,10 and 12, while the third cluster was composed of objects 7, 8 and 13.

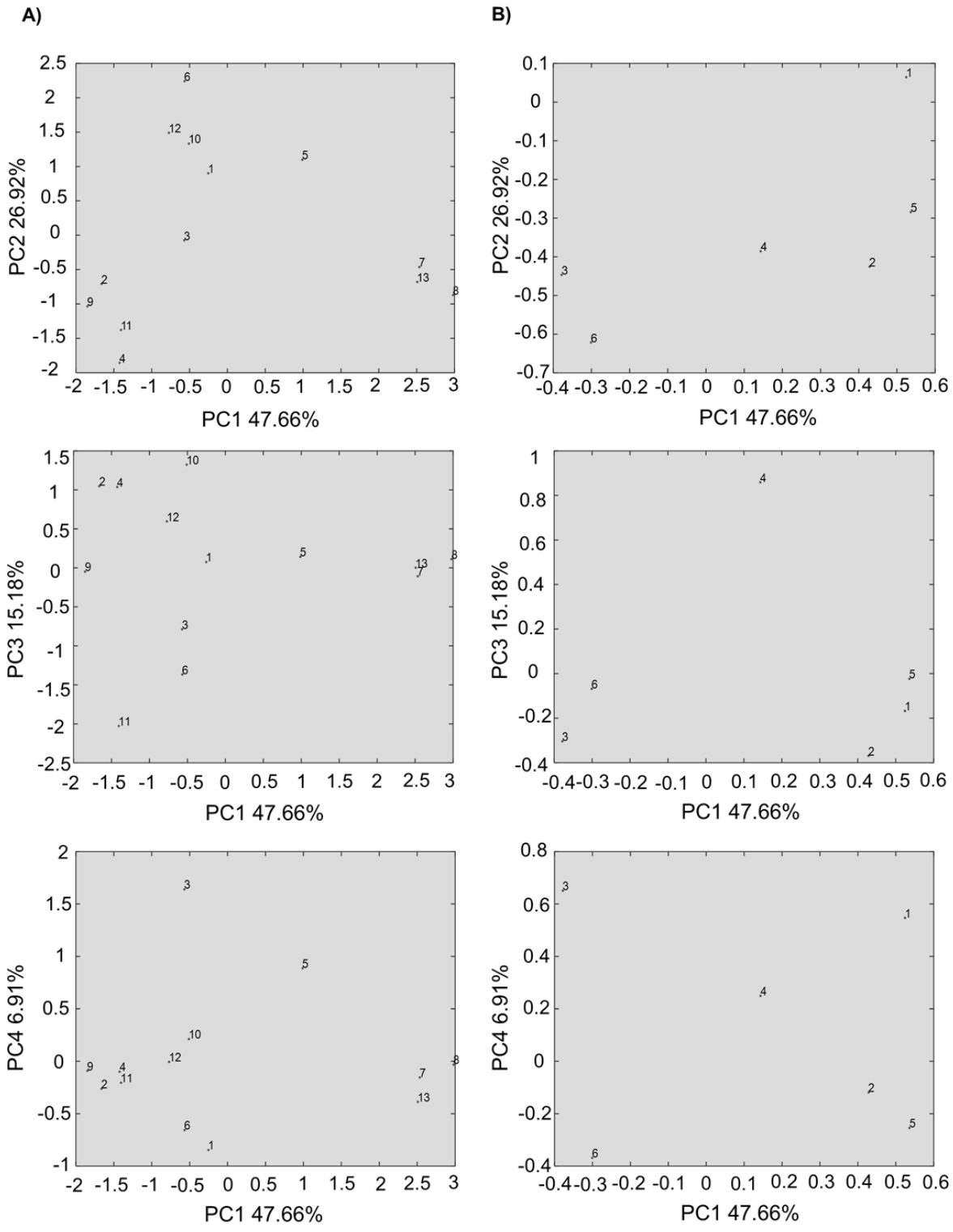

Figure 22. A) Score plots and B) loading plots of PCA for centered and standardized data set **X** (16 x 6).

Based on the interpretation of Fig. 22, it may be concluded that object 8 was characterized by relatively high concentration of lactic acid and 2,3-butanediol and the lowest concentration of formic acid. The objects included in the first cluster were characterized by relatively high concentrations of formic acid and 2,3-butanediol. The PC2, describing 26.92% of the total data variance was constructed due to the differences between the object 4, which was unique due to high concentration of ethanol and object 6 characterized by the lowest concentration of ethanol and high concentration of lactic acid. Moreover, along the PC2 it may be observed that objects 1, 5, 6, 10 and 12 were unique because of relatively high concentration of lactic acid and lower concentrations of all the remaining metabolites. The PC4, describing 6.91% of the total data variance was constructed because of the differences between object 3 and all the remaining objects. The object 3 differed from all the remaining objects in terms of the highest concentration of formic acid and low concentrations of 2,3-butanediol and ethanol. Although the metabolites were effectively segregated by PCA, their possible similarities were not greatly illustrated. Therefore, for a more in-depth analysis of the effect of temperature, pH and CWP concentration on the distribution of the metabolites, the HCA complemented with a visual display of the data was applied. HCA is a powerful chemometric tool used to discover the inherent grouping and distribution in the data set [31].

3.2.1.2 HCA

The dendrograms constructed with the application of the Ward's linkage method are presented in Fig. 23. The Euclidean distance was employed as the similarity measure.

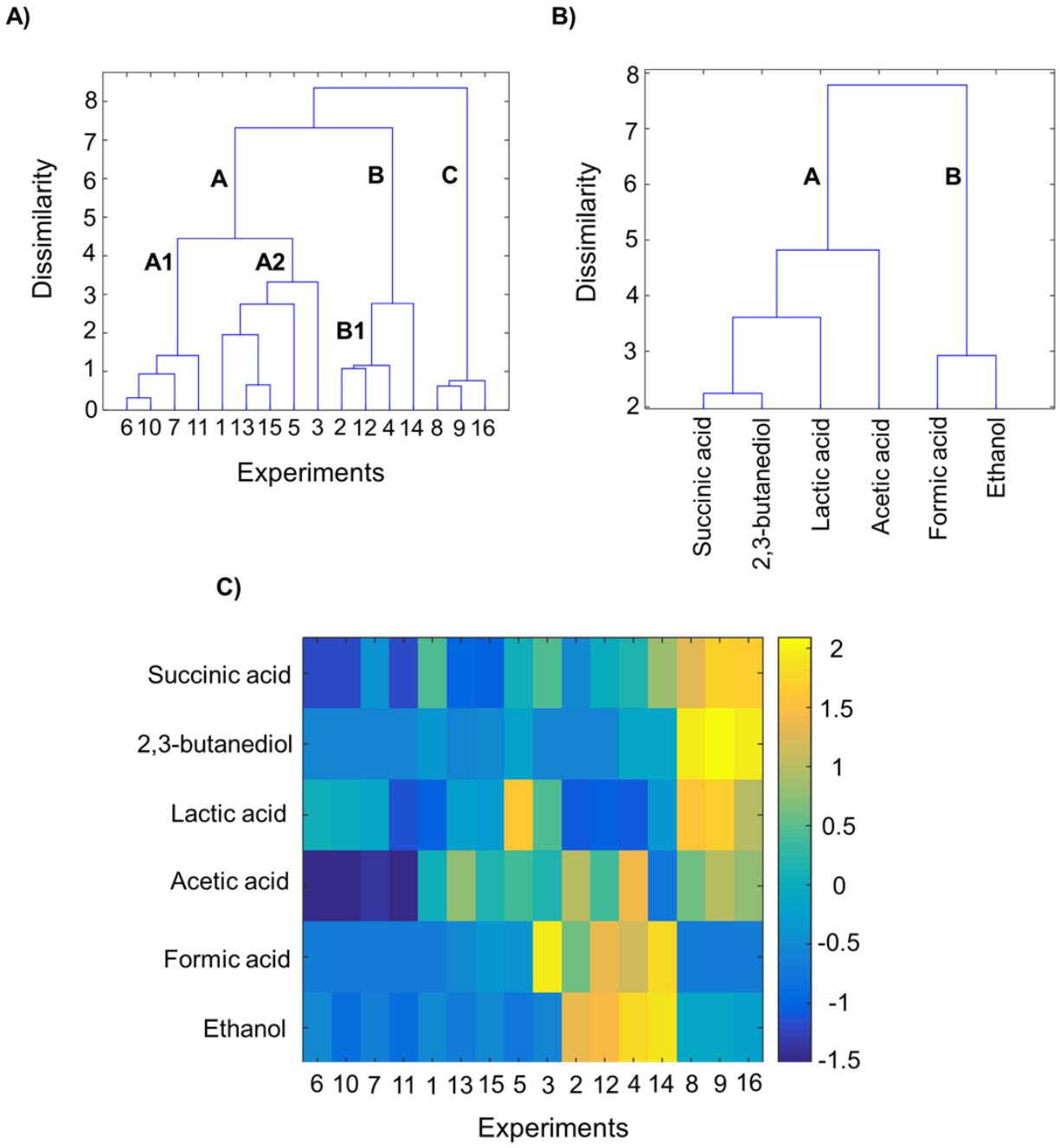

Figure 23. Dendrograms of A) studied objects (experiments of hydrogen production under various conditions), B) parameters (metabolites produced during CWP dark fermentation) in the objects space based on the Ward's linkage method and using the Euclidean distance as the similarity measure with C) the color map of the studied data sorted according to the Ward's linkage method.

The dendrogram presented in Fig. 21 A reveled three clusters: A, B and C of different experimental conditions.

- Cluster A composed of the objects 1, 3, 5, 6, 7, 10, 11, 13 and 15.
- Cluster B composed of the objects 2, 4, 12 and 14.
- Cluster C composed of the objects 8, 9 and 16.

Within the main clusters the following sub-clustering structures may be distinguished: two sub-clusters within cluster A (A1 and A2) and one sub-cluster within cluster B (B1):

- Sub-cluster A1 composed of the objects 6, 7, 10 and 11.
- Sub-cluster A2 composed of the objects 1, 3, 5, 16 and 15.
- Sub-cluster B1 composed of the objects 2, 4 and 12.

The dendrograms constructed for the metabolites produced during the fermentation under various operating conditions (Fig. 21 B) revealed two main classes:

- Class A containing parameters 1, 2, 4 and 5 (corresponding to lactic acid, succinic acid, acetic acid and 2,3-butanediol, respectively).
- Class B containing parameters 3, and 6 (corresponding to formic acid and ethanol, respectively).

The results obtained from the analysis of the dendrograms presented in Fig. 21 A-B shows the data structure but did not allow interpreting the observed patterns in terms of parameters. To solve this problem the color map of the studied data was employed (Fig. 21 C). A simultaneous analysis of the dendrograms of studied test of the experimental conditions in the parameters space with the color map of data allowed a more in-depth exploration of the relationships among the studied experiments.

In particularly, the objects grouped in cluster A differed from the remaining ones mainly in terms of low concentration of 2,3-butanediol and ethanol (parameters 5 and 6, respectively). The objects in sub-cluster A1 correspond to the axial points of temperature and pH (4.8 and 55.2°C and pH 3.4 and 10.1, respectively), which are

additional experiments at a α distance from the central point. These experiments allowed to estimate the curvature of the response surface; therefore, they constitute the lowest and the highest conditions of temperature and pH on the experimental design. While the four objects in sub-cluster A2 correspond to the experiments at temperature of 45°C. The absence of alcohol and the low production of the other metabolites can be attributed to the detrimental effect of the extreme conditions of these experiments. The difference between sub-clusters A1 and A2 is the higher concentration of acetic acid (parameter 4) in the latter. Also, within sub-cluster A2, the uniqueness of objects 3 and 5 was observed due to the high concentrations of lactic acid and formic acid.

Subsequently, Cluster B is composed by four objects, which were carried out at a low temperature of 15°C. The uniqueness of this cluster was related to high concentration of formic acid and acetic acid, as well as ethanol (parameters 3, 4 and 6), which indicates that these conditions were the most suitable for the formate hydrogen lyase complex activity, which is responsible for the breakdown of pyruvate into formate and acetyl-CoA [32]. On the other hand, the accumulation of formic acid suggests that the hydrogen evolving hydrogenases were partially inhibited during fermentation. Sub-cluster B1 was characterized by the highest concentrations of ethanol (parameter 6). In addition, within the cluster B, the uniqueness of object 4 was also observed caused by the highest concentration of acetic acid (parameter 4) among all objects.

Finally, cluster C, which is composed by three objects, is characterized by the highest concentrations of succinic acid and 2,3-butanediol (parameters 2 and 5) among all the studied objects. Also, it is characterized by a high concentration of lactic acid and low concentrations of formic acid and ethanol. This information suggests that the operating conditions of the objects in cluster C, stimulated the carbon flux through the first branches of the mixed acid pathway, where the involved reactions are used for the disposal of the reducing power generated by the catabolism of the lactose present in the CWP. Also, it indicates that most of the hydrogen produced on these conditions, was through the NADH pathway. As well,

the pH values of 6.8 in this cluster could have favored the synthesis of 2,3-butanediol, since it is known that the α-acetolactate synthase enzyme, which is one of the three key enzymes involved on 2,3-butanediol synthesis, has an optimum activity under slightly acidic conditions of 6 [33].

4 Conclusions

The RMS along with the PCA and HCA, allowed to identify in a more depth way the influence of key operating parameters such as temperature, initial pH and CWP concentration on hydrogen yield and soluble metabolites produced by *E. asburiae*. The RSM allowed estimating the optimum conditions for hydrogen yield and production rate (25.6°C, initial pH 7.2 and 23.0 g dm^{-3} CWP), as well as to identify the individual and conjugated effect of the factors on this response variable. According to the ANOVA of the model, only the quadratic terms of temperature and pH influenced hydrogen yield. While hydrogen production rate was affected by the linear and quadratic effect of temperature and the quadratic effect of pH. On the other hand, PCA and HCA allowed reducing the dimensionality of the data of the metabolites produced, thus allowing a better visualization and interpretation of the distribution of the organic acids and alcohols on response of each condition evaluated. The fact that CWP fermentation by *E. asburiae* produced mainly hydrogen and alcohols, could be exploited in later studies as a biorefinery concept.

5 Acknowledgments

The authors thank to CONACyT-Pro Nal 247498 and CONACyT Ciencias Básicas 281700. C.L. Alvarez-Guzmán thanks to CONACyT for her scholarship 330870.

6 References

[1] da Silva Veras T, Mozer TS, da Costa Rubim Messeder dos Santos D, da Silva César A. Hydrogen: Trends, production and characterization of the main process worldwide. Int J Hydrogen Energy 2017;42:2018–33.

https://doi.org/10.1016/j.ijhydene.2016.08.219.

[2] Lee DH. Econometric assessment of bioenergy development. Int J Hydrogen Energy 2017;42:27701–17. https://doi.org/10.1016/j.ijhydene.2017.08.055.

[3] Ferchichi M, Crabbe E, Gil GH, Hintz W, Almadidy A. Influence of initial pH on hydrogen production from cheese whey. J Biotechnol 2005;120:402–9. https://doi.org/10.1016/j.jbiotec.2005.05.017.

[4] Azbar N, Dökgoz FTÇ, Peker Z. Optimization of basal medium for fermentative hydrogen production from cheese whey wastewater. Int J Green Energy 2009;6:371–80. https://doi.org/10.1080/15435070903107049.

[5] Rosales-Colunga LM, Razo-Flores E, Ordoñez LG, Alatriste-Mondragón F, De León-Rodríguez A. Hydrogen production by *Escherichia coli* Δ*hycA* Δ*lacI* using cheese whey as substrate. Int J Hydrogen Energy 2010;35:491–9. https://doi.org/10.1016/j.ijhydene.2009.10.097.

[6] Holladay JD, Hu J, King DL, Wang Y. An overview of hydrogen production technologies. Catal Today 2009;139:244–60. https://doi.org/10.1016/j.cattod.2008.08.039.

[7] Mohan SV, Chandrasekhar K, Chiranjeevi P, Babu PS. Biohydrogen Production from Wastewater. Biohydrogen, 2013, p. 223–57. https://doi.org/10.1016/B978-0-444-59555-3.00010-6.

[8] Bao M, Su H, Tan T. Biohydrogen production by dark fermentation of starch using mixed bacterial cultures of *Bacillus* sp and *Brevumdimonas* sp. Energy and Fuels 2012;26:5872–8. https://doi.org/10.1021/ef300666m.

[9] Prazeres AR, Carvalho F, Rivas J. Cheese whey management: A review. J Environ Manage 2012;110:48–68. https://doi.org/10.1016/j.jenvman.2012.05.018.

[10] Ryan MP, Walsh G. The biotechnological potential of whey. Rev Environ Sci Biotechnol 2016;15:479–98. https://doi.org/10.1007/s11157-016-9402-1.

[11] Zhou X, Hua X, Huang L, Xu Y. Bio-utilization of cheese manufacturing wastes (cheese whey powder) for bioethanol and specific product (galactonic acid) production via a two-step bioprocess. Bioresour Technol 2019;272:70–6. https://doi.org/10.1016/j.biortech.2018.10.001.

[12] Kargi F, Eren NS, Ozmihci S. Bio-hydrogen production from cheese whey powder (CWP) solution: Comparison of thermophilic and mesophilic dark fermentations. Int J Hydrogen Energy 2012;37:8338–42. https://doi.org/10.1016/j.ijhydene.2012.02.162.

[13] Kargi F, Ozmihci S. Utilization of cheese whey powder (CWP) for ethanol fermentations: Effects of operating parameters. Enzyme Microb Technol 2006;38:711–8. https://doi.org/10.1016/j.enzmictec.2005.11.006.

[14] Vasmara C, Marchetti R. Initial pH influences in-batch hydrogen production from scotta permeate. Int J Hydrogen Energy 2017;42:14400–8. https://doi.org/10.1016/j.ijhydene.2017.04.067.

[15] Manuel Rosales-Colunga L, Donaxí Alvarado-Cuevas Z, Razo-Flores E, De León Rodríguez A, Rosales-Colunga LM, Alvarado-Cuevas ZD, et al. Maximizing Hydrogen Production and Substrate Consumption by *Escherichia coli* WDHL in Cheese Whey Fermentation. Appl Biochem Biotechnol 2013;171:704–15. https://doi.org/10.1007/s12010-013-0394-9.

[16] Rai PK, Singh SP, Asthana RK. Biohydrogen production from cheese whey wastewater in a two-step anaerobic process. Appl Biochem Biotechnol 2012;167:1540–9. https://doi.org/10.1007/s12010-011-9488-4.

[17] Lu Y, Zhao H, Zhang C, Lai Q, Wu X, Xing XH. Expression of NAD+-dependent formate dehydrogenase in *Enterobacter aerogenes* and its involvement in anaerobic metabolism and H2 production. Biotechnol Lett 2009;31:1525–30. https://doi.org/10.1007/s10529-009-0036-z.

[18] Gunst RF, Myers RH, Montgomery DC. Response Surface Methodology: Process and Product Optimization Using Designed Experiments. Technometrics 1996;38:285. https://doi.org/10.2307/1270613.

[19] Djaković Sekulić T, Božin B, Smoliński A. Chemometric study of biological activities of 10 aromatic Lamiaceae species' essential oils. J Chemom 2016;30:188–96. https://doi.org/10.1002/cem.2786.

[20] Howaniec N, Smoliński A, Cempa-Balewicz M. Experimental study on application of high temperature reactor excess heat in the process of coal and biomass co-gasification to hydrogen-rich gas. Energy 2015;84:455–61. https://doi.org/10.1016/j.energy.2015.03.011.

[21] Jolliffe I. Principal component analysis. Series: Springer Series in Statistics. Springer New York, NY 2002;29:487.

[22] Smoliński A. Coal char reactivity as a fuel selection criterion for coal-based hydrogen-rich gas production in the process of steam gasification. Energy Convers. Manag., vol. 52, 2011, p. 37–45. https://doi.org/10.1016/j.enconman.2010.06.027.

[23] Wold S, Esbensen K, Geladi P. Principal Component Analysis. Chemom Intell Lab Syst 1987;2:37–52. https://doi.org/10.1016/0169-7439(87)80084-9.

[24] Gentle JE, Kaufman L, Rousseuw PJ. Finding Groups in Data: An Introduction to Cluster Analysis. Biometrics 1991;47:788. https://doi.org/10.2307/2532178.

[25] Milligan GW, Romesburg HC. Cluster Analysis for Researchers. J Mark Res 1985;22:224. https://doi.org/10.2307/3151374.

[26] Smoliński A. Gas chromatography as a tool for determining coal chars reactivity in the process of steam gasification. Acta Chromatogr 2008;20:349–65. https://doi.org/10.1556/AChrom.20.2008.3.4.

[27] Smoliński A. Analysis of the Impact of Physicochemical Parameters Characterizing Coal Mine Waste on the Initialization of Self-Ignition Process with Application of Cluster Analysis. J Sustain Min 2014;13:36–40. https://doi.org/10.7424/jsm140306.

[28] Ciranna A, Ferrari R, Santala V, Karp M. Inhibitory effects of substrate and

soluble end products on biohydrogen production of the alkalithermophile Caloramator celer: Kinetic, metabolic and transcription analyses. Int J Hydrogen Energy 2014;39:6391–401. https://doi.org/10.1016/j.ijhydene.2014.02.047.

[29] De Gioannis G, Friargiu M, Massi E, Muntoni A, Polettini A, Pomi R, et al. Biohydrogen production from dark fermentation of cheese whey: Influence of pH. Int J Hydrogen Energy 2014;39:20930–41. https://doi.org/10.1016/j.ijhydene.2014.10.046.

[30] Wang J, Wan W. Factors influencing fermentative hydrogen production: A review. Int J Hydrogen Energy 2009;34:799–811. https://doi.org/10.1016/j.ijhydene.2008.11.015.

[31] Infantes D, González Del Campo A, Villaseñor J, Fernández FJ. Influence of pH, temperature and volatile fatty acids on hydrogen production by acidogenic fermentation. Int J Hydrogen Energy 2011;36:15595–601. https://doi.org/10.1016/j.ijhydene.2011.09.061.

[32] Raso J, Barbosa-Cánovas G V. Nonthermal Preservation of Foods Using Combined Processing Techniques. Crit Rev Food Sci Nutr 2003;43:265–85. https://doi.org/10.1080/10408690390826527.

[33] Blanco VMC, Oliveira GHD, Zaiat M. Dark fermentative biohydrogen production from synthetic cheese whey in an anaerobic structured-bed reactor: Performance evaluation and kinetic modeling. Renew Energy 2019;139:1310–9. https://doi.org/10.1016/j.renene.2019.03.029.

[34] Nath K, Das D. Improvement of fermentative hydrogen production: Various approaches. Appl Microbiol Biotechnol 2004;65:520–9. https://doi.org/10.1007/s00253-004-1644-0.

[35] Hallenbeck PC, Benemann JR. Biological hydrogen production; Fundamentals and limiting processes. Int. J. Hydrogen Energy, vol. 27, Pergamon; 2002, p. 1185–93. https://doi.org/10.1016/S0360-3199(02)00131-3.

[36] Slowinski E, Wolsey W, Masterton W. Chemical Principles in the Laboratory.

2004.

[37] Lee KS, Lin PJ, Chang JS. Temperature effects on biohydrogen production in a granular sludge bed induced by activated carbon carriers. Int J Hydrogen Energy 2006;31:465–72. https://doi.org/10.1016/j.ijhydene.2005.04.024.

[38] Skonieczny MT, Yargeau V. Biohydrogen production from wastewater by Clostridium beijerinckii: Effect of pH and substrate concentration. Int J Hydrogen Energy 2009;34:3288–94. https://doi.org/10.1016/j.ijhydene.2009.01.044.

[39] Lu C, Zhang Z, Zhou X, Hu J, Ge X, Xia C, et al. Effect of substrate concentration on hydrogen production by photo-fermentation in the pilot-scale baffled bioreactor. Bioresour Technol 2018;247:1173–6. https://doi.org/10.1016/j.biortech.2017.07.122.

[40] Ghimire A, Luongo V, Frunzo L, Pirozzi F, Lens PNL, Esposito G. Continuous biohydrogen production by thermophilic dark fermentation of cheese whey: Use of buffalo manure as buffering agent. Int J Hydrogen Energy 2017;42:4861–9. https://doi.org/10.1016/j.ijhydene.2016.11.185.

[41] Lopes HJS, Ramos LR, Silva EL. Co-Fermentation of Cheese Whey and Crude Glycerol in EGSB Reactor as a Strategy to Enhance Continuous Hydrogen and Propionic Acid Production. Appl Biochem Biotechnol 2017;183:712–28. https://doi.org/10.1007/s12010-017-2459-7.

[42] Perna V, Castelló E, Wenzel J, Zampol C, Fontes Lima DM, Borzacconi L, et al. Hydrogen production in an upflow anaerobic packed bed reactor used to treat cheese whey. Int J Hydrogen Energy 2013;38:54–62. https://doi.org/10.1016/j.ijhydene.2012.10.022.

[43] Wang J, Wan W. Optimization of fermentative hydrogen production process by response surface methodology. Int J Hydrogen Energy 2008;33:6976–84. https://doi.org/10.1016/j.ijhydene.2008.08.051.

[44] Upadhyay R, Sehwag S, Niwas Mishra H. Chemometric approach to develop frying stable sunflower oil blends stabilized with oleoresin rosemary and

ascorbyl palmitate. Food Chem 2017;218:496–504. https://doi.org/10.1016/j.foodchem.2016.09.105.

[45] Ji X, Huang H, Ouyang P. Microbial 2, 3-butanediol production: a-state-of-the-art review. Biotechnol Adv 2011;29:351–64. https://doi.org/https://doi.org/10.1016/j.biotechadv.2011.01.007.

[46] Celińska E, Grajek W. Biotechnological production of 2,3-butanediol-Current state and prospects. Biotechnol Adv 2009;27:715–25. https://doi.org/10.1016/j.biotechadv.2009.05.002.

Conclusions

The psychrophilic N92 and GA0F bacteria have the potential to be used in biofuel production processes using simple or complex substrates, since the yields achieved at room temperature conditions in the respective studies are comparable to those reported for mesophilic and thermophilic microorganisms. Moreover, the expression of an α-amylase enzyme on the cellular surface of *E. coli* strains WDHA and WDHFP by the AIDA system has shown to be an efficient approach to produce valuable products from starch which is one of the most abundant components of agroindustrial residues. Also, the use of the response surface methodology along with the application of chemometric tools such as PCA and HCA allow to identify the optimum conditions for hydrogen production as well as the relationship between the different operating conditions evaluated and the distribution of the soluble metabolites produced by *E. asburiae*.